MUD DYNAMICS IN A TIDAL CHANNEL: THE IMPACT OF OPENING SALT PONDS ON CHANNEL DEEPENING

CARLOS REY

MSc Thesis WSE-HECEPD-15.08

MUD DYNAMICS IN A TIDAL CHANNEL: THE IMPACT OF OPENING SALT PONDS ON CHANNEL DEEPENING

Master of Science Thesis
by
CARLOS REY

Supervisors
Prof. Dano Roelvink

Mentors
Dr. Mick van der Wegen
Ir.Fernanda Achete

Examination committee
Prof. Dano Roelvink
Dr. Mick van der Wegen
Dr. Thijs van Kessel

This research is done for the partial fulfilment of requirements for the Master of Science degree at the UNESCO-IHE Institute for Water Education, Delft, the Netherlands

Delft
March 2015

Abstract

This research was carried out at Alviso Complex, located at the Southern side of South Bay San Francisco U.S., during large wetland restoration project. The opening of the salt ponds caused a dramatic change, in terms of, hydrodynamics, sediment transport and remobilization of contaminated sediments (mercury). The contaminated sediments entered and deposited in the South bay at Alviso Slough, which was caused by historical gold mining. It is important to understand the dynamic of the sediment transport along the Alviso Slough and the east salt ponds (A6, A5, A7 and A8). A numerical model was developed, based on D-FLOW FM and DELWAQ (Delft 3D water quality package). The model was calibrated and validated which provided an excellent tool to evaluate the dynamics of the study area. With numerical modelling it is possible to analyze the most important events that dominated the sediment transport. Events such as: spring - neap tidal cycle, high and low river discharge and evolution of the bathymetry due to opening of salt pond (wetland restoration project). The sediment dynamics evaluation identified the patterns of erosion and deposition of the study area, and also the sediment direction through the Slough and openings.

Keywords: Sediment dynamics, hydrodynamics, flexible mesh, Alviso Complex, wetland restoration.

Acknowledgements

Firstly, I would like to thank to Unesco IHE Institute, the Coastal Engineering and Port Development department and United States Geological Services (USGS) to make me part of this research project.
Since the first day, that I started to work in this project, I always counted with the supported and advice of Dr. Mick van der Wegen and MSc. Fernanda Achete. I really appreciate all your help, guidance, incredible advices and kindness.

I would like to thank to Prof. Dano Roelvink the supervisor of this research, to provide me well guidance and ideas that clarified this research process. Also to Gregory Shellenbarger from USGS, I would like to thank you for all helped provided.

None of this it would be possible without the supported of my family, especially, to my Mom and Dad. Also, I would like express my gratitude to Sandra, for all supported and motivation. Finally, to all the colleagues of CEPD program and friends that fully help me directly or indirectly during this research, especially to: Ruchira, Lerika and Md. Salauddin.

Table of Contents

List of Figures

List of Tables

Abbreviations

USGS	United States Geological Service
SF	San Francisco
SSC	Suspended Solids Concentration
m/s	meter per second
cms	cubic meter per second
mg/l	milligrams per litter
MDU	Master Definition Unstructured
WL	Water level
FM	Flexible mesh
ALV	Alviso

CHAPTER 1

Introduction

This chapter introduces the problem description of this research, as well as the state of art and importance of this study.

1.1. PROBLEM DESCRIPTION

Throughout history, human activities have inflicted increased pressure on estuaries. Interventions such as dike construction, land reclamation (roads, airports, ports and others) have impacted estuarine water quality, hydro and morphodynamics. Human activities contribute to the coastal ‘squeeze theory’ (Doody, 2004), which refers to decreasing the coastal environment from both the land and the sea, thus ‘squeezing’ the coastal zone from its natural resources.

The area under investigation is located in Southern part of San Francisco Bay, the South Bay, California, United States. The focus is placed on the tidal wetlands of this region. Tidal wetlands are the boundaries of an estuary, which are periodically inundated by tides. Therefore, they include all habitats within the *“tidal frame”*. The tidal frame refers to the elevation range between the lowest low water level and highest high water level. Habitats included in these areas are intertidal mudflats, regularly inundated tidal marsh plain, tidal channels within the mars, and infrequently inundated wetland-upland transition zones at the edge of the upland (Williams and Faber, 2004).

Since 2003, the largest tidal wetland restoration project on the west coast of United States took place in South Bay, (http://southbayrestoration.org/). The main goal of this project is to restore 6000 hectares of industrial salt ponds to a rich mosaic of tidal wetlands, and other habitats.

Restoration of the South Bay salt ponds provided opportunities to reverse impact trends, by improving the health of San Francisco Bay (http://southbayrestoration.org/). Restoration also contributes to improving the ecological value to this area. Many more reason can be added to realize the importance of restoration. Hence, nowadays restoration is finally a priority in many of the region's natural resource management plans (Montalto and Steenhuis, 2004).

From the tidal frame mentioned above, this study will focus on the intertidal channel to evaluate erosion and deposition patterns due to salt ponds opening. Furthermore, the influence of contaminated sediments will also be investigated (focussed on mercury). The mercury source is historical mercury mine located upstream of the catchment. The Mercury adhered to cohesive sediment enters South bay, mainly via Alviso Slough which is one of the most contaminated waterways (Marvin-DiPasquale and Cox, 2007).

As a consequence of salt ponds opening, recent research have found trends of mercury in biota (Josh T. Ackeman, 2013), due to scour in Alviso slough, that exposed the contaminated sediment. This remobilization of mercury compromise the project and further salt ponds restoration.

For all mentioned above, the objective of the current research is to investigate sediment dynamics and mercury remobilization in Alviso Slough after the salt pond opening for marsh restoration.

1.2. RESEARCH QUESTION

In order to accomplish the objective mentioned above, the following research question will be guided this research.

- How are the sediment transport dynamics in Alviso Slough, due to salt pond opening restoration?
- What is the relationship between future mercury mobilization and potential scouring in Alviso Slough?
- What are the effects of different opening scenarios at Pond A8 in Alviso Slough?
- Is this investigation applicable in further planning salt pond restoration in San Francisco Bay?

1.3. RESEARCH METHODOLOGY

1.3.1. Literature review

The literature review covers various topics including the historical events and developments in the area. Also, previous studies related with wetland restoration. The knowledge of previous experiences and the fact of understand historical processes at the study area; enable to have a clear objectives to be investigated and a good methodology to achieve this research.

1.3.2. Numerical Modelling

The entire data gathering used to set up the numerical model, it was based on, the information under control of national agencies or institutes of United States (U.S.), such as, United States Geological Survey (USGS) and National Oceanography and Atmospheric Administration (NOAA), who are in control of gathering and processing data publish on the web.

The study was based on numerical model that provide a better understanding of the sediment dynamics in the area. The software D Flow Flexible Mesh (D FLOW FM) and the Water Quality and Ecology (DELWAQ) a module of Delft 3D package was used in this research. A 3D model was developed and calibrated. The model was also validated to further assess such issues, according with the data available.

1.3.3. Evaluation of scenarios and results

With a validated model, a few scenarios will be evaluated the impact and the behaviour of the fine sediments dynamics of the area. These scenarios are based on historical events and also further predictions. These scenarios consider the project at hand: Salt Pond restoration.

The scenarios results provided the tool to understand the sediment dynamic at Alviso Slough, in addition, to identify the impact of salt pond opening due to erosion at Alviso Slough. Besides, enable to identify the most influences events that might impact the sediment transport in the area, such as, runoff and spring-neap tidal cycle.

CHAPTER 2

LITERATURE REVIEW

South San Francisco Bay (South Bay) is both a geographically and hydrodynamically complex system, with fresh water tributary inflows, tidal currents, and wind stress on the water surface interacting with complex bathymetry (Walters, 1982). In general, the width of the Bay ranges from less than 2 km near the Dumbarton Bridge to more than 20 km north of the San Mateo Bridge. The mean depth of the Bay is less than 4 m, with a channel depth of 10 to 15 m. The intertidal areas contain a network of small branching channels that effectively drain these areas at low water, leaving exposed extensive mudflats (Williams and Faber, 2004).

The research area of this work is Alviso complex at the Southern of San Francisco Bay, California, (Foxgrover, 2007). This area receives fresh water tributaries, Coyote creek, Alviso Slough and Guadalupe Slough. The area experiences mixed, semi diurnal tide and it is primarily sediment composed of mud (Jaffe and Foxgrover, 2006). The **Figure 2-1** bellow described a series of maps, locating the area from the overall picture till the detailed location of the Alviso Complex.

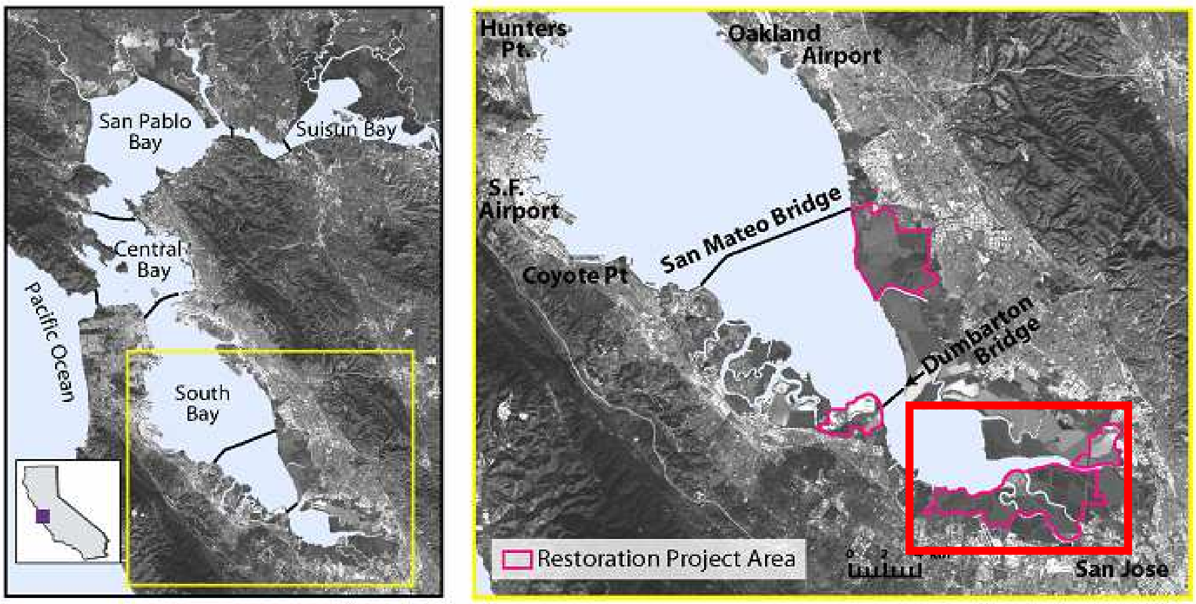

Figure 2-1. Location of study area. San Francisco Bay (top - left). South bay (top - right), and Alviso Complex, red frame denoting the area (bottom). Source. (Foxgrover, 2007) and www.southbayrestoration.org/maps/

Over the past 150 years, San Francisco Bay Estuary has been suffering with the most significant anthropogenic changes, resulting in over 85% of fringing tidal wetlands and the contamination of the estuarine food web with mercury (Korschgen, 1992). These impacts are particularly pronounced in the South Bay, which was historically fringed with extensive tidal marshes and which receives drainage from New Almaden, the largest historic mercury (Hg) mining area in North America. (Josh Ackerman, 2010).

One of the largest tidal wetlands restoration projects has place in south of San Francisco Bay, improving the health of the area and the ecological value (Williams and Faber, 2004). This kind of project provides many functions in the area, for instance, supplying a foraging habitat to hundreds of thousands of shore birds each year (Stenzel, et al., 2002).

First of all, over 45 tidal marsh restoration projects have been conducted around the Bay since 1970's. Those projects have been implemented by a variety of different entities, with widely different planning approaches and designs. Unfortunately, monitoring of long-term evolution and performance of these *"experimental"* or first generation restoration sites was rarely carried out (Williams and Faber, 2004). However, at the begging of 1990's a long term monitoring and a lot of efforts to study the area was implemented.

As mentioned in the problem description, this research is focusing in sediment transport dynamics due to salt ponds opening in Alviso Slough. These effects basically related with sediment transport, as a consequence or remobilization of mercury. Based on literature review related with this issue, the following studies are describing below.

One of these studies was the investigation of the historical bathymetry due to patterns of deposition and erosion in the south bay. In summary, this study found the sediment system changes from 1956 to 2005 but also additional research is needed to fully understand the causes of these changes and to predict future changes and their effects on restoration of the South San Francisco Bay salt ponds.(Jaffe and Foxgrover, 2006).

Besides the understanding of the sediment system of the area, one of the biggest issue is the contamination of mercury in the south bay and special focus at the restoration project on going, where unknown behaviour of this tendency in short and long term is a threat to the area and the project itself. However, studies have been carried out monitoring the mercury among the area within the process of restoration since 2006 by Marvin-DiPasquale and Cox (2007) and the last document that combined all information about this issue, it is the using biosentinels to monitor effects of wetland restoration for the South Bay Salt Pond Restoration Project (Josh T. Ackeman, 2013)

This last project highlights the effects of the wetland restoration actions on mercury and resulting mercury concentration in animals. As a consequence of the restored Ponds A8 /A7 / A5 complex, as well as Alviso Slough after the pond A8 notch was opened. The uncertainties become a big awareness for managers for short term biota impacts and long term tendency for mercury dynamics.

In terms of sediment dynamic in the area a few studies have been developed. In which, the most recent study done by Gregory G. Shellenbarger (2014) emphasizes the research to identify the major transport direction and dynamics for sediment and quantify the flux in Alviso Slough measuring by an instrument package deployed at beginning of 2010 in the Thalweg of Alviso Slough (USGS station #11169750). For measures of around 2 years and 2 months, it was concluded that, "storms and associated runoff, greatly influence sediment flux. Strong spring tides promote upstream sediment flux and weak neap tides have only a small net flux. During neap tides, stratification likely suppresses sediment transport during weaker flood and ebb tides".

Moreover research have been done in the area such as; a focus study of dynamics of sediment accumulation in Pond A21 at the island ponds (Callaway, et al., 2009), in which, Pond A21 was breached into two locations along the Coyote Creek. The aim of this study was to quantify sedimentation rates within Pond A21. Effects on existing mudflats and tidal marshes surrounding Pond A21 and Coyote Creek were also examined. It was found that the breaches at Pond A21 appear to have no significant impacts on adjacent marshes. On the other hand, there were differences in sediment dynamics for the mudflat stations along Coyote Creek that were closest to the two breaches at Pond A21, indicating that some local dynamics may be affecting adjacent mudflat stations. Hence of these results it was found that, as more salt ponds are opened to tidal action within particular local regions of the South Bay. Ultimately, it would be very useful to evaluate regional patterns of both sedimentation rates within ponds and effects on existing adjacent mudflats before and after breaching. This was possible due more salt ponds being open to tidal action within local regions of the South Bay.

In general, all the studies mentioned above followed one main approach. The developments were based on monitoring or measurements in situ for short term. Through this one can only obtain a short term understanding. For long term understanding, further additional research is recommended.

On the other hand, based on the description of the area, done by Philip Williams & Associates (2005) other sediment transport models have been complied of the San Francisco South Bay, for another approache and purpose. Some of those models are: (H. T. Harvey & Associates, et al.) and (McDonald and Cheng, 1996) developed a one-dimensional model for the Bay based on the work of Krone (1962). (Moffatt & Nichol Engineers, 2005b) coupled the two-dimensional RMA model with SED-2D in order to perform hydraulic scour analysis of the proposed replacement span of the Bay Bridge. (Bricker, 2003) coupled TRIM3D with SWAN in order to compare erosion and deposition patterns in the South Bay with earlier modelling work performed by (Inagaki, 2000). Ultimately, the USGS developed a sediment box model based on (Uncles and Peterson, 1995) salinity model, in order to develop a sediment budget for the South Bay (Shellenbarger, et al., 2004).

From all this models coupled none of them had approached to the problem address in this report. For this reason, further investigations become a good opportunity to give a better understanding in uncertainties, such as: of sediment dynamic in this kind of habitats, hydrological links, and restoration processes.

Abroad of this subject, the interest to restoring degraded tidal rivers and salt marshes for the human impact over the last century, it happens all around the world. All this projects has a main goal to increase biological productivity, improve water quality, and provide recreational uses that benefit the ecosystems and human society. (MacBroom, 2000). Some examples are: the restored of Scheldt estuary in between of The Netherlands and Belgium cause by nature during a severe storm in 1990, a dike was breached in the brackish part of the Scheldt estuary and returned tidal influence to the Sieperda polder. In the 10 years since the dike breach, the former polder has changed into a brackish tidal marsh (Eertman, et al., 2002). From this restored area this region has taken the advantage of giving and ecological value with an advantage of water management in terms of safety by flood and resilience or restoring other natural dynamics.

Other examples about restoration projects and their challenge include: Snohomish River, Washington (Yang and Wang, 2012) where an accurate modelling was needed on the post - process to improve efficiency in the drainage. Montalto and Steenhuis (2004) have experienced in restoring areas in New York and New Jersey. They found links between hydrology and restoration of tidal marshes depended on accurately determining hydrologic factors and how their interdependencies are incorporate into design. Furthermore, Le Havre - Port 2000 with the restoration of Seine estuarine (Scherrer, 2006) where the Le Havre Port and the state of France willing to improve the ecological interest of this ecosystem.

Studies show that great effort has been put into understanding ecosystem characteristics and processes. Even though many studies have been carried out, a full understanding of the processes occurring are still lacking. This has become a challenge for restoration projects and approaches to restoration of the South bay. However, this study will contribute to solving some uncertainties within the restoration project of Alviso Slough and will form part of documentation contributing to understanding this complex ecosystem concerning the estuaries and tidal marshes.

CHAPTER 3

STUDY AREA

3.1. DOMAIN AREA

The study area is located at the Southern part of San Francisco Bay. The **Figure 3-1** showed how the bay is surrounded and occupied by human developments, such as: cities, marinas, industry, infrastructure and others. Alviso complex is not an exception of system squeeze.

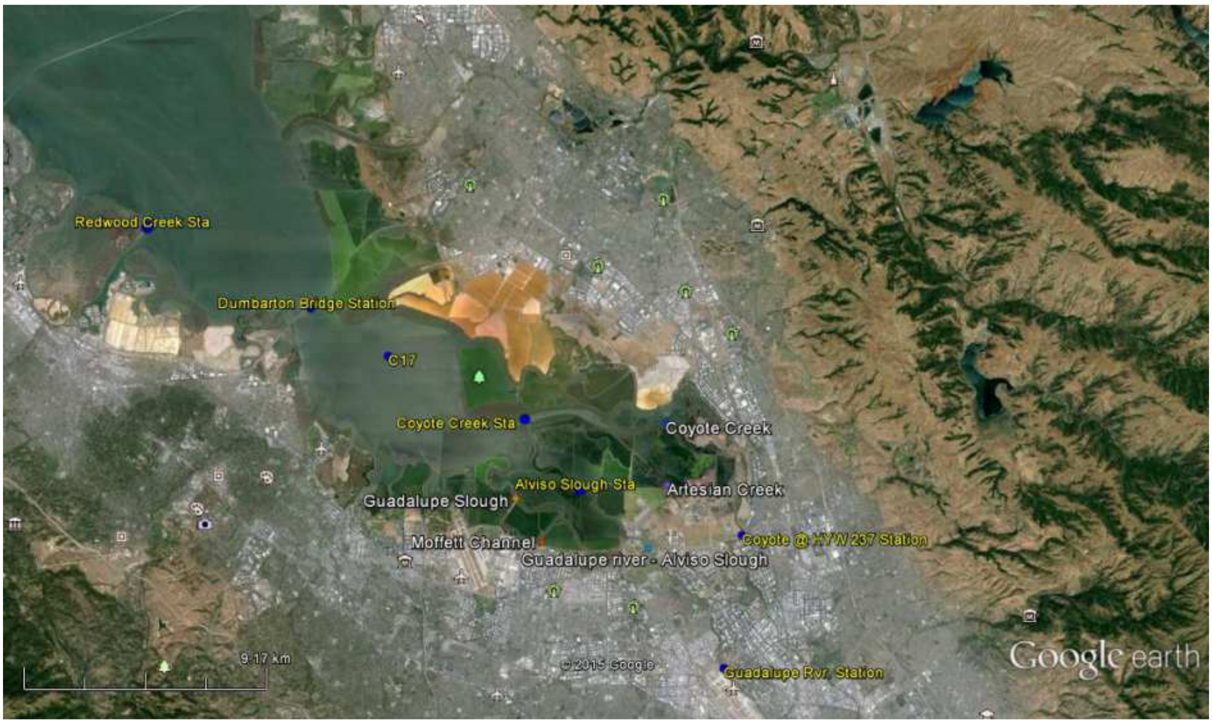

Figure 3-1. South San Francisco Bay and Gather Stations.

Figure 3-2. Alviso Complex Area. Source: South Bay Salt Pond Restoration

Alviso complex: it is surrounded at the north with Freemont and the Cargill Salt Pond at the south with Sunnyvale, San Jose and Santa Clara, at the east side with Milpitas and the west side Dumbarton bridge, Palo Alto Baylands Nature Preserve and Redwood city. Alviso complex area is approximately 3238 Ha (8000 acres), consisting of 21 ponds as shown **Error! Reference source not found.**. However, the domain area of study it does not included the area of ponds A1 and A3N and A3W at the western side. Due to study the sediment dynamic of Alviso Slough and the impact of salt ponds opening surrounded the slough.

3.1.1. Tides

The tide in the area is classified as mixed semidiurnal, with two high and two low levels every day. Moreover, the tidal wave propagating from Goden Gate (Alameda) through the enclosed shape of the south bay is distorted in amplitude and phase (Figure 3-3). The gather stations mentioned in Figure 3-3 are located along the south bay from seaward to landward (Figure 3-1).

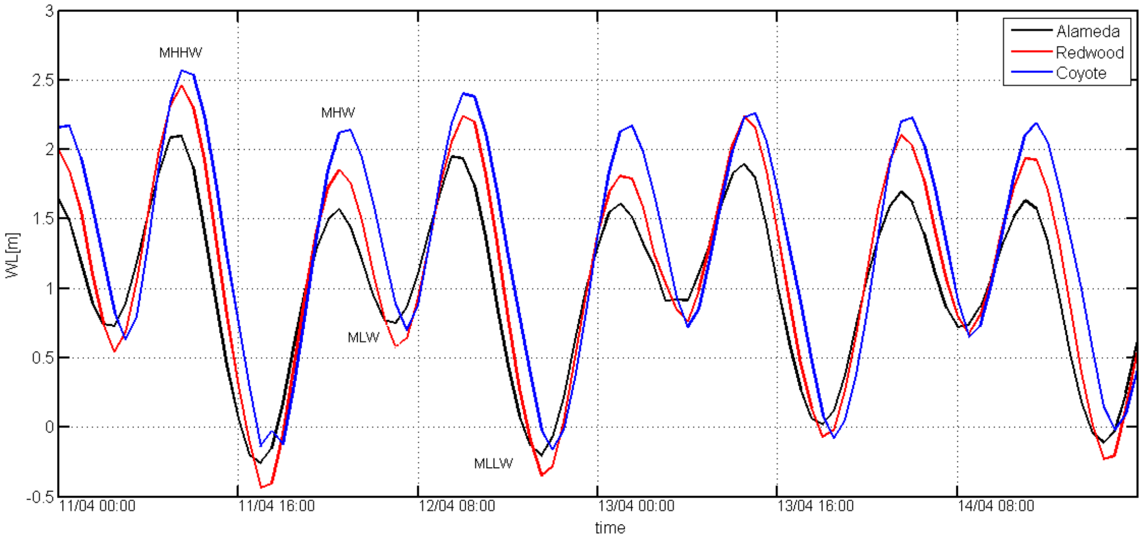

Figure 3-3. Tidal variations at the South Bay

The tides exhibit strong spring-neap variability, where the spring tides occurring approximately every two weeks during and largest tidal cycle (Figure 3-4). "The tides also vary on an annual cycle, with the strongest spring tides occurring in May/June and November/December, and the weakest neap tides occurring in March/April and September/October " (Philip Williams & Associates, 2005).

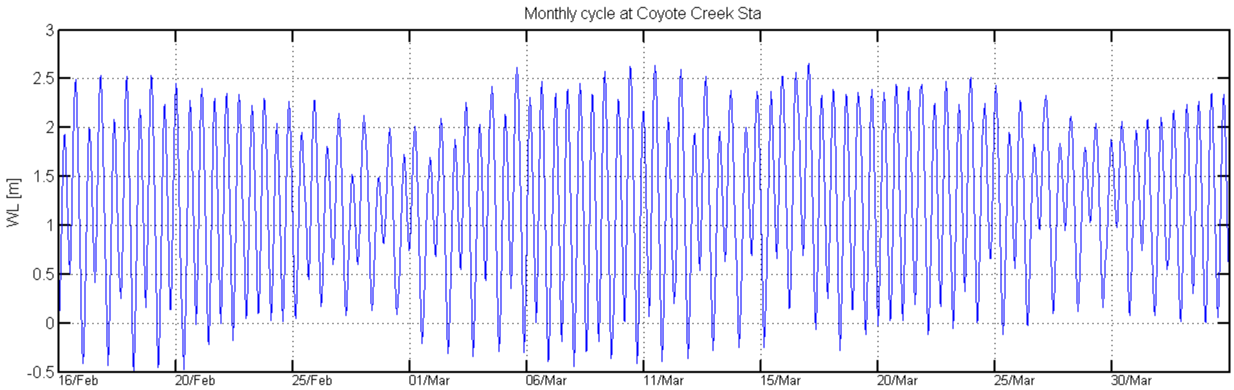

Figure 3-4. Typically Monthly Tidal Cycle at Coyote Creek Station.

3.1.2. Tributary inflows

The main fresh water tributaries discharging in the area include, Guadalupe River that ends as Alviso Slough, Coyote Creek, Artesian Slough, Moffet Channel, Mud slough and Calabazas Creek. Guadalupe River and Coyote Creek behave as Mediterranean climate Rivers, presenting high peak discharge related with storms in winter and low discharges at summer (Figure 3-5).

Guadalupe River and Coyote Creek are the most influences tributaries in the study area. On the other hand, the other tributaries include: the Artesian slough that receives the San Jose municipal wastewater treatment plant discharges with an average of 2.6 m^3/s (60 mgd). Besides it is a tributary of Coyote Creek. Additionally, the Moffet channel receives the Sunnyvale municipal water treatment plant discharges approximately 1.30 m^3/s (29.5 mgd) into Moffett Channel (Board, 2009). Finally Mud Slough which is connect with Coyote creek receives a minimal of fresh water during all seasons (Life Science, 2003).

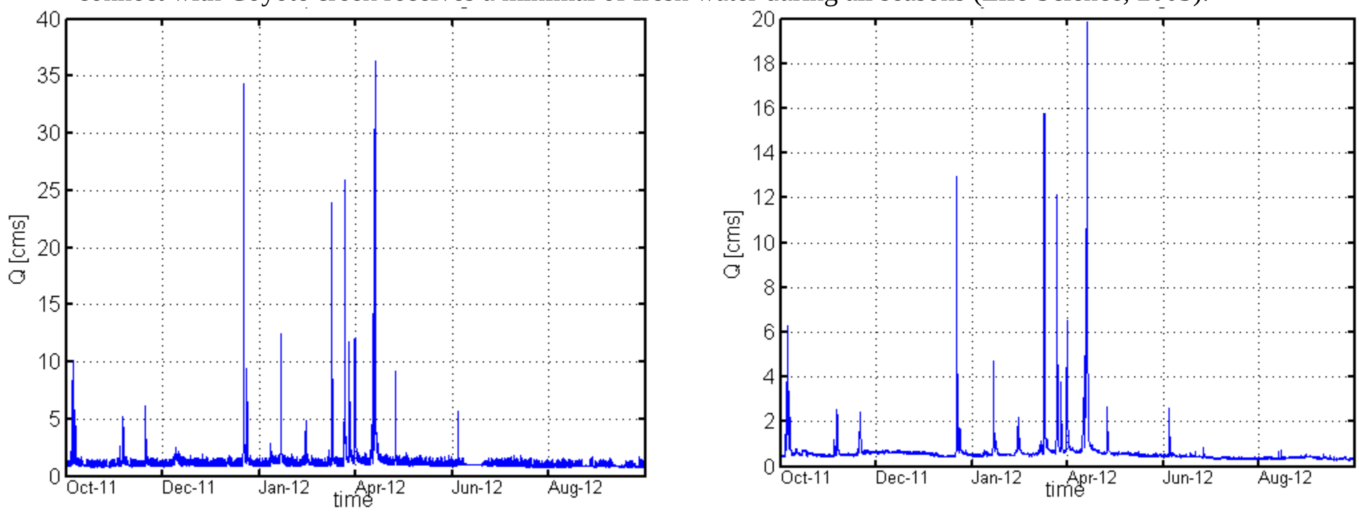

Figure 3-5. Guadalupe river discharge - USGS 11169025, b) Coyote Creek discharge - USGS 11172175.

Figure 3-5 showed the runoff mentioned above during winter. Those events occurred in short time period the whole peak during 1-3 days maximum. Also this high peak, frequently occurred during March/April. During the rest of the hydrological year, there is a constant behaviour, which stayed quite the same discharging 1.5 m^3/s at Guadalupe river and 0.5 m^3/s at Coyote Creek.

3.1.3. Salinity

Salinity in South Bay depends basically under three factors: Central Bay Salinity and the exchange between South Bay and Central Bay, the fresh water input to South Bay tributaries, and the evaporation. In General, this area is vertical well mixed, due to the fact, of low fresh water input through the year. However, Alviso and Coyote can present vertical variations of salinity and density stratification, governed by high flows. (Life Science, 2003).

No salinity data is available for the area, so the data used as boundary condition was taken from the station C17 or M17, which was used in literature such as, Moffatt & Nichol Engineers (2005b) and Philip Williams & Associates (2005). Figure 3-1 showed salinity behaviour through the year, in which, from the beginning of the year until July there was a general decreasing, from 25 to 15 parts per thousand (ppt), and rose again from July to the end of the year. Where, July is lowest drop or point of inflexion. This variation is mainly driven by seasonal variation from San Francisco delta (Philip Williams & Associates, 2005).

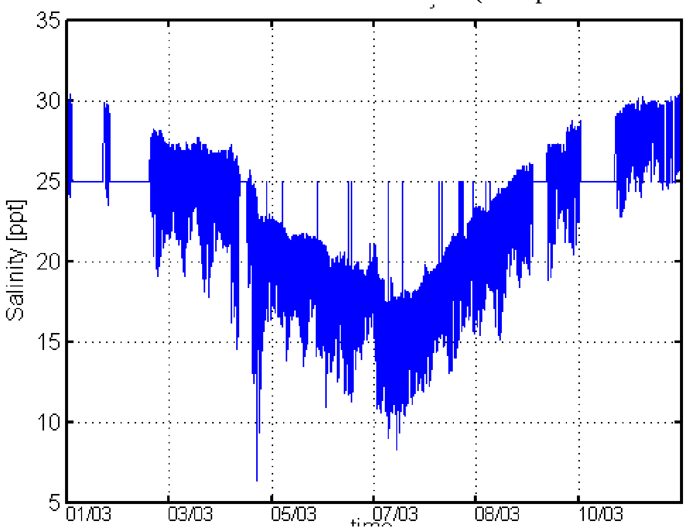

Figure 3-6. C17 Sta.- Salinity.

3.1.4. Temperature

The temperature variation through the year was showed in Figure 3-7. Due to seasonal variation, there was a rose trend from January until July, and from there a slightly dropped till the end of year. Although, the fluctuation of salinity showed at Dumbarton bridge plot, represented the influences due to tidal cycle and high runoff that flowing from San Francisco Delta, through the Central Bay and ends into the South Bay. For those descriptions, this parameter was also considered important due to vertical stratification.

The data available for temperature at the study area, corresponded to the main fresh water tributaries and gather station at Dumbarton Bridge (Figure 3-1). At the station of Guadalupe River and Coyote Creek correspond to a daily available data. Although, at Dumbarton bridge correspond to 15 minutes time series. The three stations also represented to measures near bottom temperature.

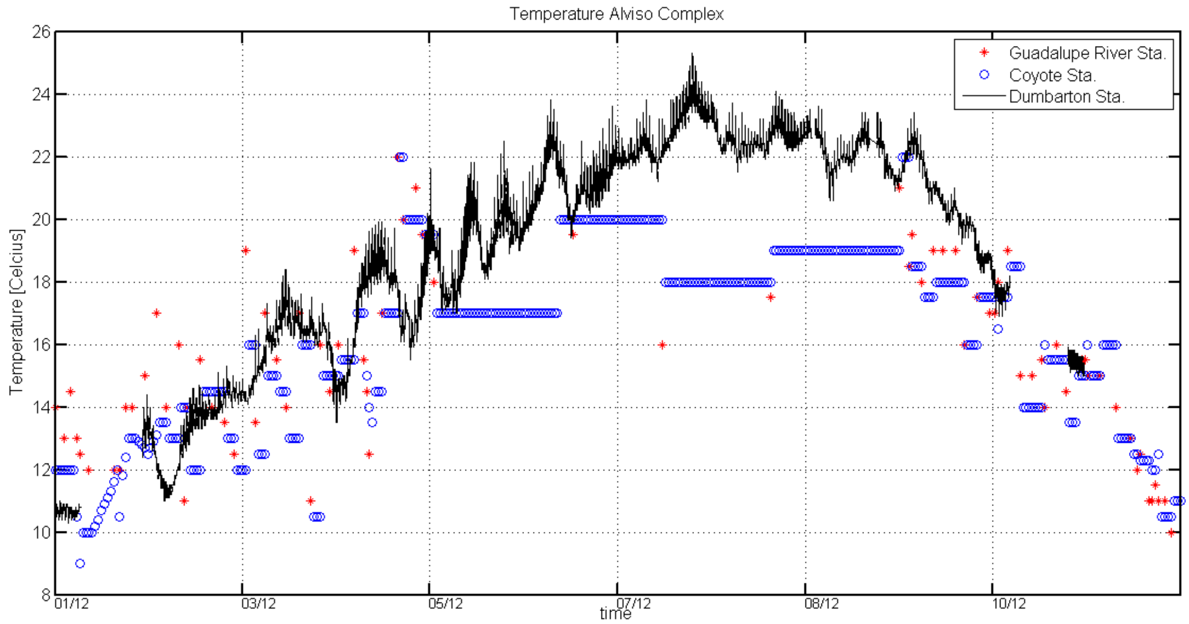

Figure 3-7. Temperature of Alviso Complex Boundaries 2012.

3.1.5. Sediment regional setting

For this study it is highly relevant the sediments characterization. The area evolution was directly influences by the sediment transport and processes of sedimentation and erosion. Processes that have been shaped the area through tidal cycle, fresh water inflows, seasonal variation and climate change. Regardless, the human activities, that had transformed the ecosystem to industrial salinas (salt ponds), urban areas, agricultural and also the historical contamination from gold mining at New Almaden through Guadalupe river (Figure 3-1).

As a first approximation of the sediment characteristic, the USGS (2004) describes the most of salt ponds area composed of a sand, silt and clay. Within, material percentages around: sand 38%, silt 36% and clay 26 %. For the slough and creeks, the contain percentages varying compare with the salt ponds, on average, 13% sand, 54% silt and 33% clay.

Additionally, the survey made by Marvin-DiPasquale and Cox (2007), detailed describes of bed composition at Alviso Slough and is the base characterisation of the sediment for this research.

Figure 3-8. Sediment sampling at Alviso Slough, Source: (Marvin-DiPasquale and Cox, 2007).

Figure 3-8 showed the layout of sampling where the bore hold core took place. Focusing along the Alviso Slough, in which was taken samples from right marshes, bottom channel and left marshes. As a matter of example set deep core were presented in **Figure 3-9**.

Regarding, the sediments core description, most of the samples showed a constant distribution of material with a predominance of clay and clayey silt. The following figures described some of the single sediment core section, with information such as, whole core section photograph and dominant lithology (Marvin-DiPasquale and Cox, 2007).

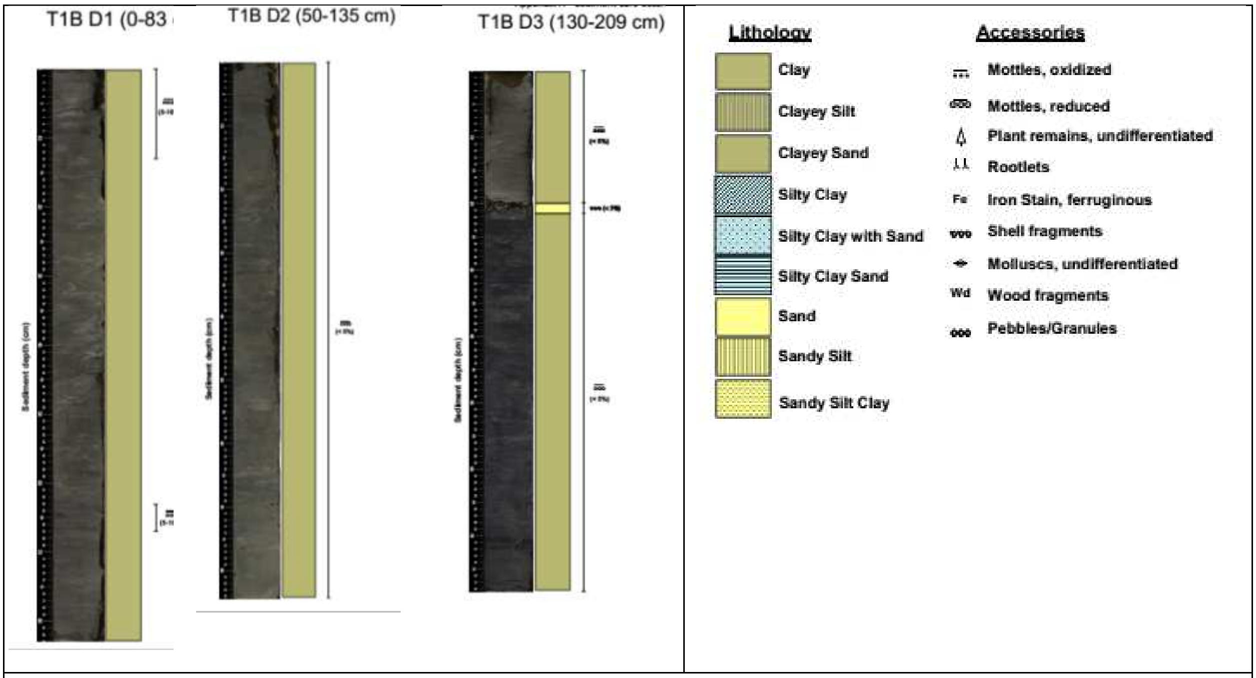

Figure 3-9. Single core section at the Alviso's slough bottom (T1B) and Single core section at the Alviso's slough left marsh (T1C). Source: (Marvin-DiPasquale and Cox, 2007).

Also from this deep core samples which fairly represented the area sampling by Marvin-DiPasquale and Cox (2007) it can be distinguished the material uniformity and the lack of layering of other material. As well as, confirmed the first survey by the USGS (2004), where the predominant materials were the clay and clayey silt. Besides, the following table summarized the main parameters used for this study taken from Marvin-DiPasquale and Cox (2007) and Josh T. Ackeman (2013), which provided also material uniformity due to lower standard deviation of bulk density.

Table 3-1 Summary statistics for Bed composition at Alviso Slough. Source: (Marvin-DiPasquale and Cox, 2007).

Statistic parameters	Grain size (%<63 μm)	Bulk Density (g/cm^3)	Porosity (ml/cm^3)
Mean	93.9	1.4	0.71
Std. Dev.	17.4	0.1	0.08
Minimum	7.6	1.2	0.31
Maximum	103.8	1.9	0.77
Total N	140	140	140

In terms of mercury composition, also in the report of Marvin-DiPasquale and Cox (2007), detailed describes the total mercury concentration and reactive mercury and methylmercury. Where, from the survey approximately all samples shown a constant concentration along the depth profile Figure 3-10, In addition, the sampling concentration stayed quite constant comparing bottom samples with marshes.

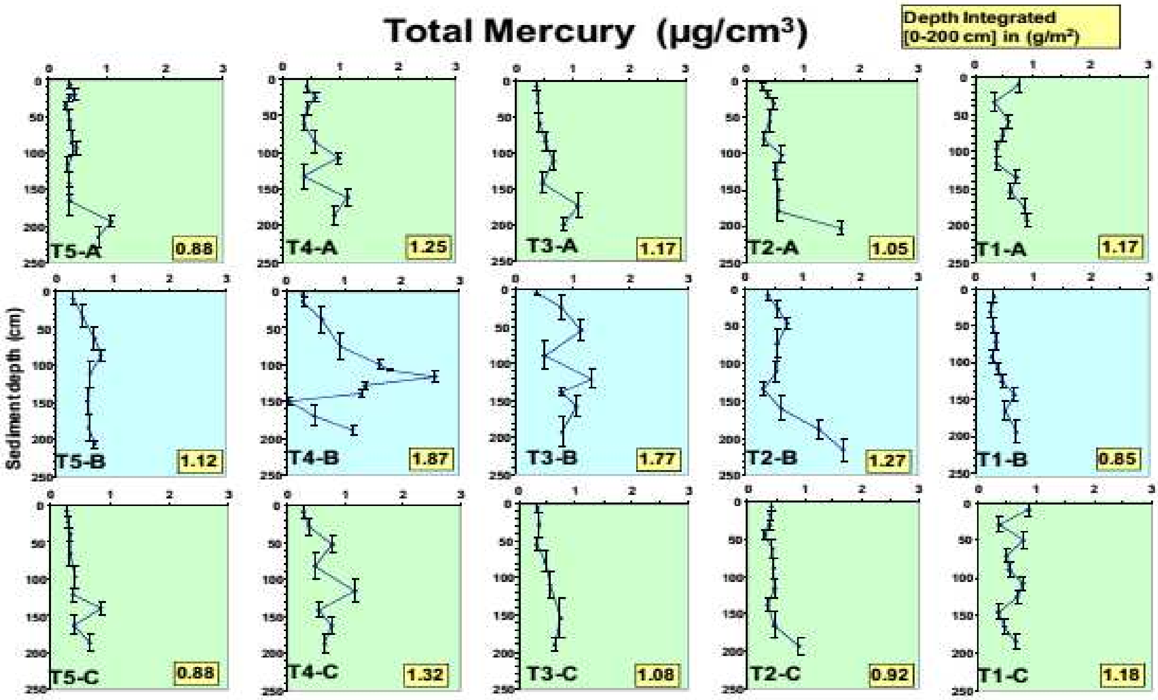

Figure 3-10. Total mercury concentration of depth profile sampling. Source: (Marvin-DiPasquale and Cox, 2007)

In addition to the bed composition, the characterization of the surface water sediment parameters was carried out by the report "The South Bay Mercury Project" of Josh T. Ackeman (2013).

Table 3-2 Mean results for sediments parameters of water surface at Alviso Complex. Source: (Josh T. Ackeman, 2013).

Location & Date	Grain size (%<63 µm)	Bulk Density (g/cm^3)	Total Suspended Solids (mg/L)
Ponds 2010	77.3	1.21	328.7
Ponds 2011	81.7	1.10	112.8
Upstream Alviso Slough 2010	88.3	1.24	30
Upstream Alviso Slough 2011	73.4	1.31	35.1
Alviso Slough 2010	95.3	1.18	87.7
Alviso Slough 2011	89.2	1.24	182.5

Note: The specific ponds are A5, A6, A7 and A8.

From Table 3-1 and Table 3-2 it can be conclude the bulk density in the area both, ponds and tidal channel, kept same value with lower variance. However, in Table 3-2 provided a slightly difference in terms of total suspended solids concentration (SSC), where towards upstream Alviso slough the SSC was lower compare measures upon Alviso Slough and ponds. Although, the available data for suspended sediment concentration in stations, such as: Guadalupe River, Coyote Highway 237, Dumbarton Bridge and Alviso Slough. These data provided additional information to characterize the area, also used as boundary condition.

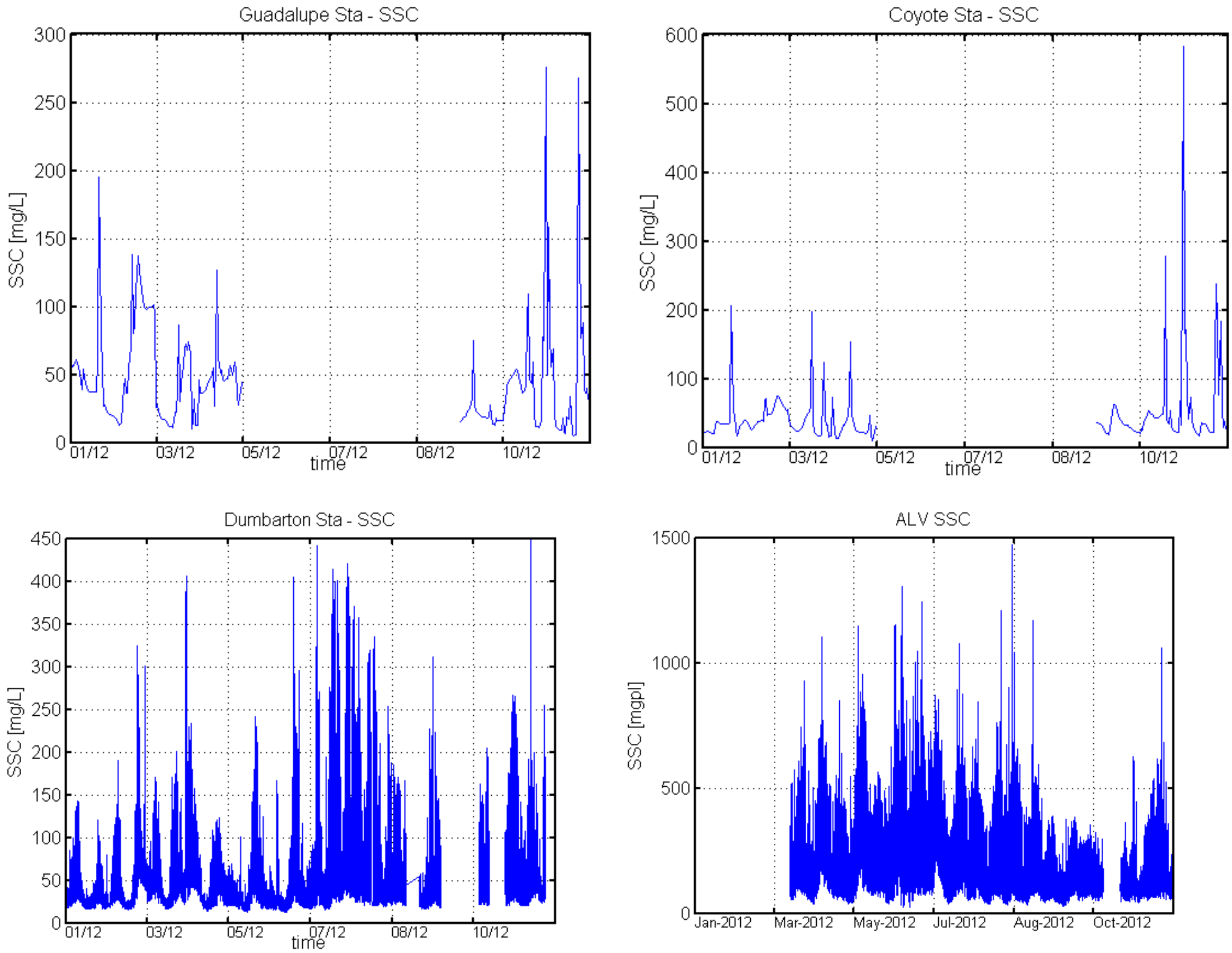

Figure 3-11. a)Suspended Sediments Concentration [mg/l] - USGS 11169025(top left), b) Coyote @HYW 237 Sta. Suspended Sediments Concentration [mg/l] - USGS 11170725 (top right), c) Dumbarton Bridge Sta. Suspended Sediments Concentration [mg/l] (bottom left) and d) Alviso Slough Sta. Suspended Sediments Concentration [mg/l] (bottom right)

Figure 3-11 showed the differences of SSC from upstream sources towards the bay. Where, tributaries located upstream of Alviso Complex (Figure 3-1) showed low SSC values compares with station at Alviso and Dumbarton bridge. Also, the upstream station behaved according with runoff events. Meanwhile, at Dumbarton bridge and even at Alviso Slough can be clearly identify the influences of spring - neap cycle.

3.1.6. Bathymetry

The base bathymetry for this research was accomplished from a merging between USGS aerial Light Detection and Ranging (LIDAR) collected in 2010 (June to November) and the bathymetry survey base line in 2010 collected by the USGS (Figure 3-12). The result was a detailed high-resolution digital elevation model (DEM) of the study area.(Foxgrover, et al., 2014).

Besides the merging DEM of 2010, there is available a detailed bathymetric of Alviso Slough, Coyote Creek and Guadalupe Slough, listed from, October 2011, February 2012, April 2012 and October 2012.

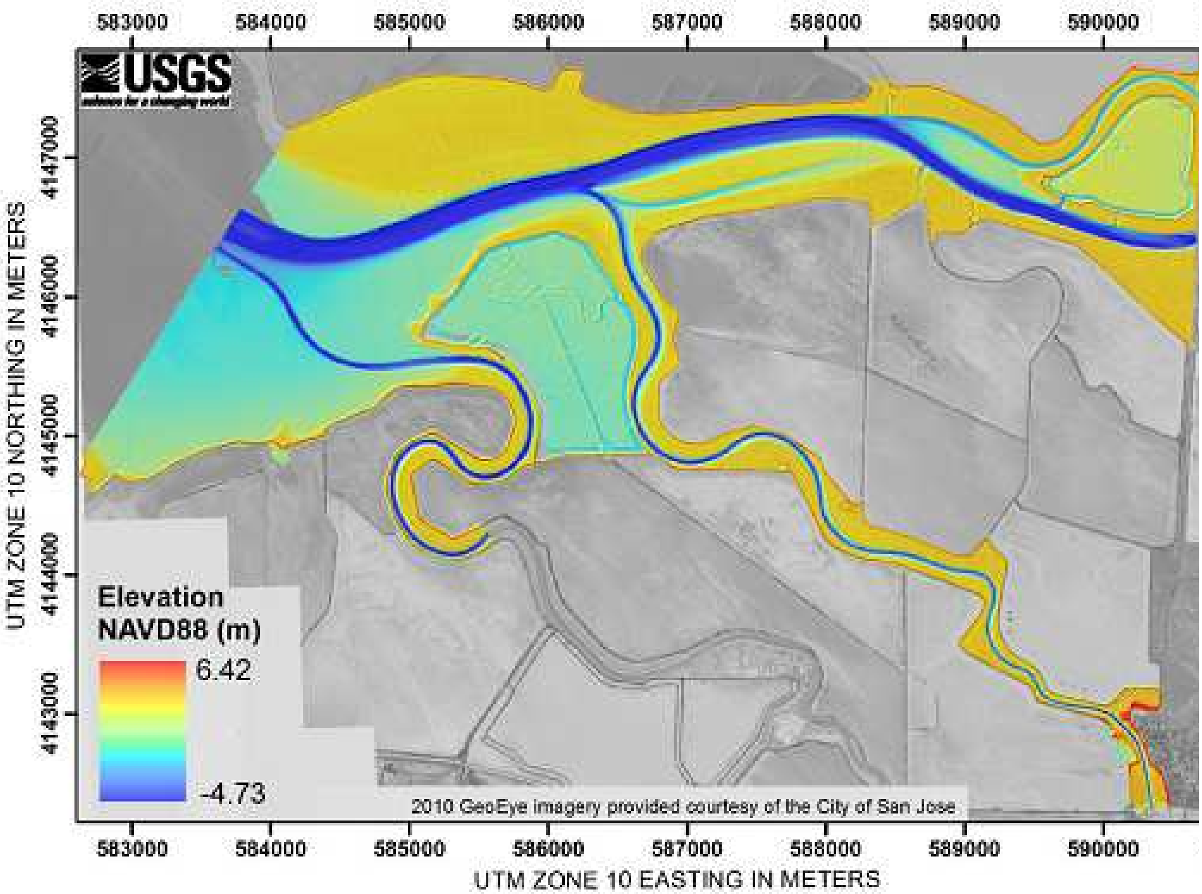

Figure 3-12. Coyote Cree, Alviso Slough, Guadalupe Slough and Salt pond A6, 2010 bathymetric/topographic. Source: (Foxgrover, Finlayson, Jaffe and Fregoso, 2014).

It is important to highlight the horizontal and vertical datum conversions, due to the lack of certainty of converting datum at this area. For instance, conversion between NAVD88 and MLLW varied from 17 cm near Dumbarton Bridge, 20 cm where Guadalupe Slough and Coyote Creek meets. These differences also have an impact at the moment of convert the data water levels.

Additionally, the evolution of the area took place along the time frame bathymetry survey (2010 to 2012). Along this time frame, the area has changed due to salt ponds management. As a consequence, opening at the salt ponds and changed in bed levels both channels and salt ponds. The following Figure 3-13 showed a whole picture of this evolution.

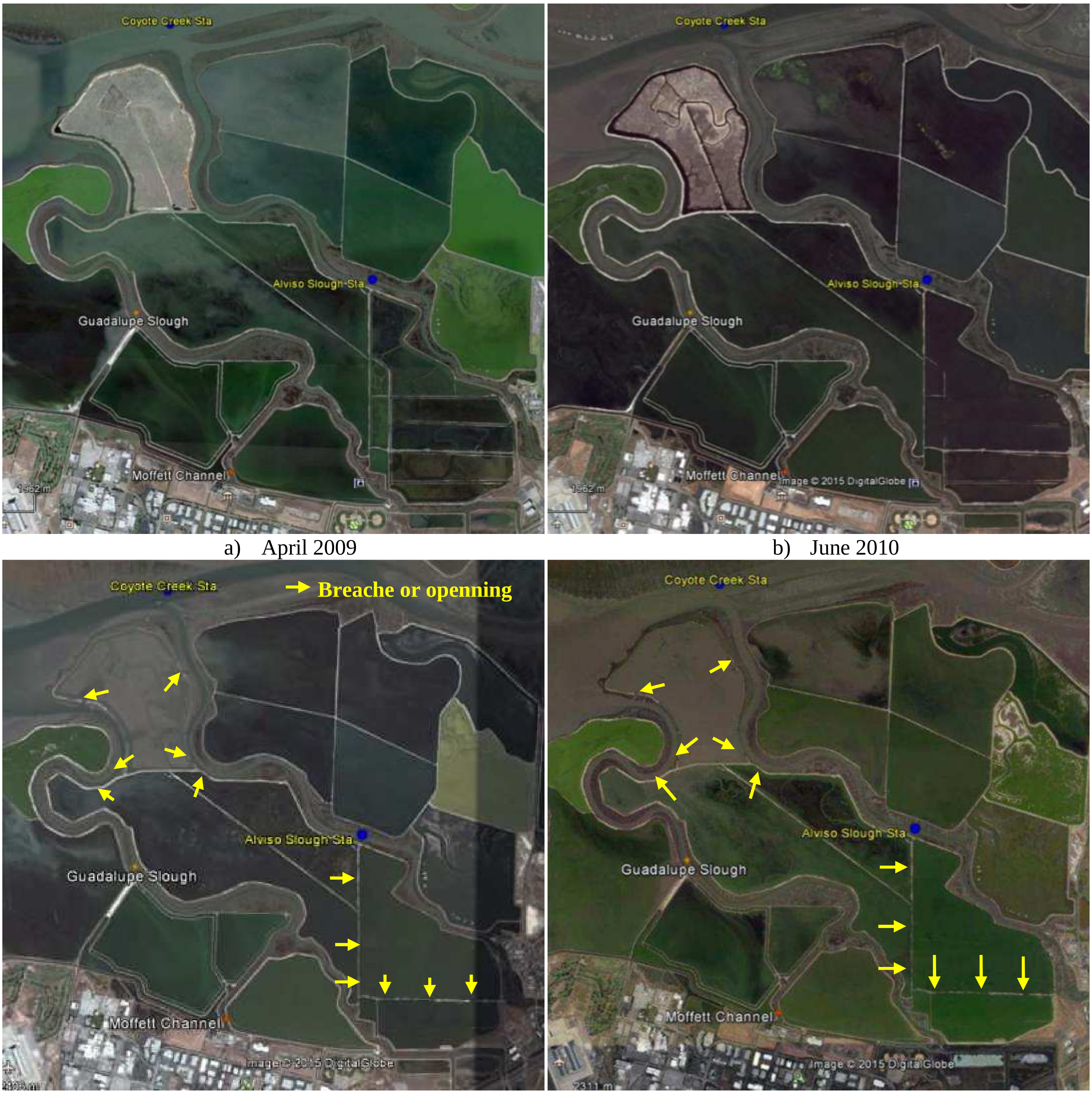

a) April 2009 b) June 2010

c) September 2011 d) June 2010

Figure 3-13. Evolution of bathymetry at Alviso Complex.

Taking into account this evolution of the area, the bathymetry used to set up the numerical model must agreed with the tidal frame and setting up of the model, in order to increase accuracy of the model. However, the study counted with an overall bathymetry from 2010, and updated bathymetry along 2011 and 2012 among the main channels. Nevertheless, the numerical model was set up with, the overall bathymetry updating within the main channels bathymetry, according with the time frame of modelling.

3.2. DATA SOURCES

Listing the overall data used for this research the following table summarize the information compiled and used to set up the numerical model.

Table 3-3 List of Data

PARAMETER	STATION OR AREA	TIME	SOURCE
Water Levels	1.Alameda 2.Redwood, 3.Coyote Creek	1997-2015 1997-2015 2011 -2015	http://tidesandcurrents.noaa.gov/stations.html
Discharge	1.Alviso Slough, 2.Guadalupe River, 3.Coyote HWY 237	2012-2014 2007-2015 2007-2015	http://waterdata.usgs.gov/ca/nwis/
Water Depths	1.Alviso Slough	2012-2014	http://waterdata.usgs.gov/ca/nwis/5
Suspended sediment concentration	1.Alviso Slough 2.Dumbarton Bridge 3.Coyote HWY 237 4.Guadalupe River	2012-2014 2007-2011 2007-2015 2007-2015	http://waterdata.usgs.gov/ca/nwis/
Temperature	1.Alviso Slough 2.Coyote HWY 237 3.Dumbarton Bridge	2012-2014 2003-2004 2013-2015	http://waterdata.usgs.gov/ca/nwis/
Salinity	1.Alviso Slough 2.C17	2012-2014 2003-2004	http://waterdata.usgs.gov/ca/nwis/
Bathymetry	Alviso Complex	2010 February 2012 April 2012 October 2012	http://www.southbayrestoration.org/documents/technical/, (Foxgrover, et al., 2014)

CHAPTER 4 NUMERICAL MODEL

NUMERICAL MODEL

The methodology used to develop this research was based on the generation of a numerical model, that provided the tool to evaluate the sediment dynamic at Alviso Slough due to potential scouring. To assess this methodology the following steps represented on figure below were approached.

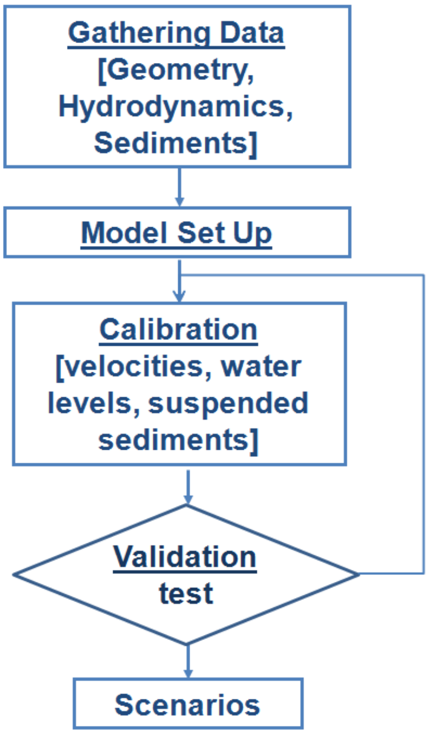

Figure 4-1. Methodology diagram

For the numerical model, was used D-Flow Flexible Mesh (D-FLOW FM) as the core of hydrodynamic simulation. Besides, the simulation of sediment transport DELFT 3D D- WAQ was used. The following chapters will explained the steps mentioned on Figure 4-1.

4.1. D FLOW FM SET UP

D-Flow Flexible Mesh (D-Flow FM) is a 1D-2D-3D hydrodynamic simulation package that runs on flexible meshes, developed by Deltares (Deltares, 2014). The reason to choose this software was the adaptable flexibility to areas like South Bay of San Francisco. The geometry of this location, created a complex environment with the difficulty to set up a model through rectangular grid. Hence, D-Flow FM generates a comfortable and trustable mesh for the systems.

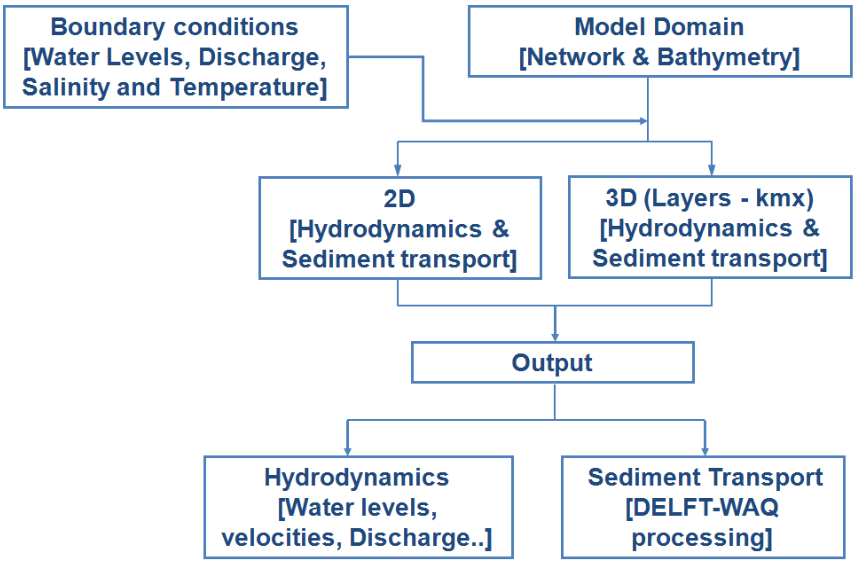

Figure 4-2. Modelling methodology diagram

As follows, it will describe the methodology to set up the numerical model of Alviso Complex regarding the hydrodynamic simulation.

4.1.1. Domain and Network

The domain contain the main fresh water tributaries that influence the Alviso Complex area, and the seaward side downwards Dumbarton Bridge nearby Stevens Creek and Pond M2 (**Error! Reference source not found.**). Once the domain was defined, the network generation was the next step. In which, it is very important stage at the moment to set up the model. As better is defined the network an accurate and reliable outcomes you will get. For that reason a methodology was develop to generate the network. The detailed proceeded can be found at appendix D-FLOW - FM detailed set up and remarks.

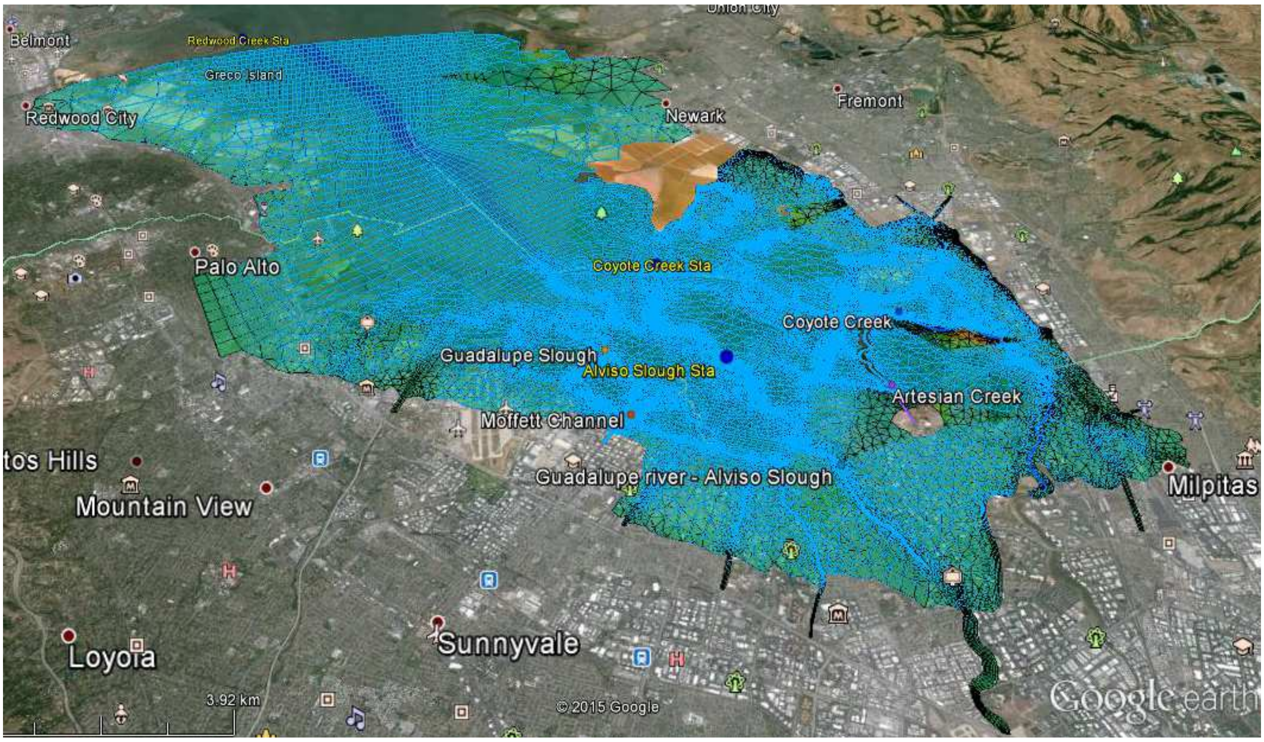

Figure 4-3. Unstructured mesh of Alviso Complex.

4.1.2. Boundaries

The boundaries defined for the model are listing in **Table 4-1**:

Table 4-1 Boundaries

BOUNDARIES	DESCRIPTION	2D	3D
SEAWARD	Water levels (Coyote Creek Sta.)	X	X
	Salinity (C17 Sta.)	X	X
	Temperature (Dumbarton Bridge Sta.)		X
	SSC (Dumbarton Bridge)	X	X
ALVISO	Discharge (Guadalupe River Sta.)	X	X
	SSC (Guadalupe River Sta.)	X	X
	Temperature (Guadalupe River Sta.)		X
COYOTE	Discharge (Coyote @ HWY 237 Sta.)	X	X
	SSC (Coyote @ HWY 237 Sta.)	X	X
	Temperature (Coyote @ HWY 237 Sta.)		X
MOFFET CHANNEL	Constant discharge	X	X
ARTESIAN SLOUGH	Constant discharge	X	X

The boundaries were set up according with the model to compute either 3D or 2D as described **Table 4-1**. However, the reason to include a larger domain it was to get the whole prospect and impact that might affect the study area. Therefore, the network extension at upstream tributaries, such as: Guadalupe River (Named in Figure 4-4 as Alviso) and Coyote Creek. As mentioned in previous chapter, the main boundaries that influences the area both hydrodynamic and sediment transport were set up, as Figure 4-4 shown.

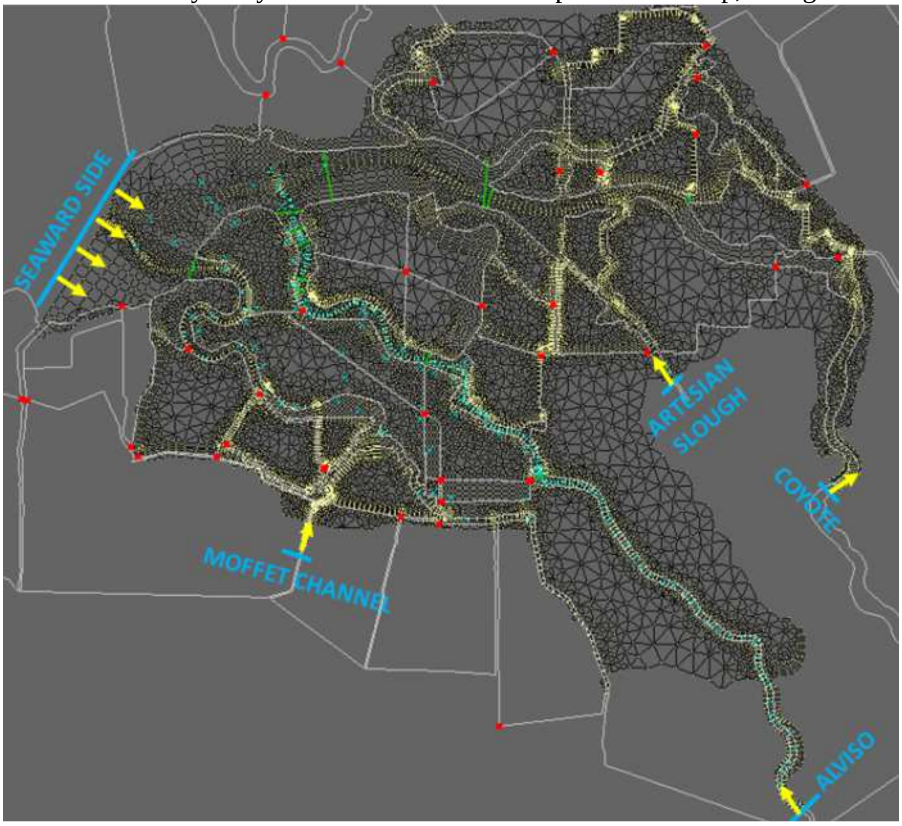

Figure 4-4. Boundaries set up at the domain.

Finally to set up the D-Flow FM model, it is recommended the following remarks:

- The initial water level: this value should be assign according with the water level boundary. In order, to reduce the spin time. If the water level boundary started with high water levels the initial water level should be less than zero (0) and vice versa with lower water level values.
- The model can be set up as 2D model, in which, kmx is established by zero (0). Kmx is the parameter that defined the maximum number of vertical layers. O n the other hand, 3D model is defined by kmx up to 1.
- The friction coefficient it depends of a range of variables, such as: bed composition, vegetation, channel geometry and shape of the system. Although, this subject it will discussed in detailed in calibration and validation chapter.
- The default time zone is GMT. This time should be in accordance with the time series data given included at the boundary.
- It is recommended to use seconds as time unit. Nevertheless, the boundary time series should be set up in minutes.
- All cross sections should be drawing in the same direction, whether upstream or downstream direction. In order to dismiss confusion with the outcome. Although, further comparison with data available.

- The MapInterval it is recommended to set up by day or 12 hours, otherwise the output (*.map) will be a bigger size.
- It is recommended to use a time window, in which, it is include, a complete tidal cycle, dry periods and high runoff. In order, to evaluate the hydrodynamic computations. Normally, this time window is approximately two to three months (February to May, winter season). Also, it is recommended to evaluate the hydrodynamic computations during dry periods (summer season) and a complete spring - neap tides.
- Parameters such as, salinity and temperature take around 5 days to spin up. This initial spin up time should be taking for hydrodynamic computations.

4.2. Delft 3D - WAQ

Once the hydrodynamic simulation is accomplished, the sediment transport is modelling by Delft 3D - WAQ (DELWAQ) using the outcome of D-Flow - FM. DELWAQ is a 3-dimensional water quality model framework. It solves the advection diffusion reaction equation on a predefined computational grid and for a wide range of model substances. (Deltares, 2011).

4.2.1. Time frame

The time set up is for default given by D-Flow-FM time frame. However, the time step should be adjust, in order to avoid errors at the moment of running the model. For this research the values used for time step are: 2D model 10 minutes and 2 minutes for 3D model.

4.2.2. Bed composition

For this study case, it was defined one layer S1 as the bed composition. Regardless, the soil uniformity, composed by clay and clayey silt, classified as mud bed composition. The vertical bed layer (S1) of soil was defined by two materials: one that has been deposited by historically process (IM2) and other material from the sources, seaward and upstream or landward (IM1). Figure 4-5 provided a sketch that illustrate how was set up the numerical model. Thus, identifying patterns of erosion and deposition, due to historical contaminated fine sediments and sediments transported by the river and the bay. This layer was initially set up with two meters (2m) thickness of dry matter available corresponding to 2.6 e10 ^{6} [gDM].

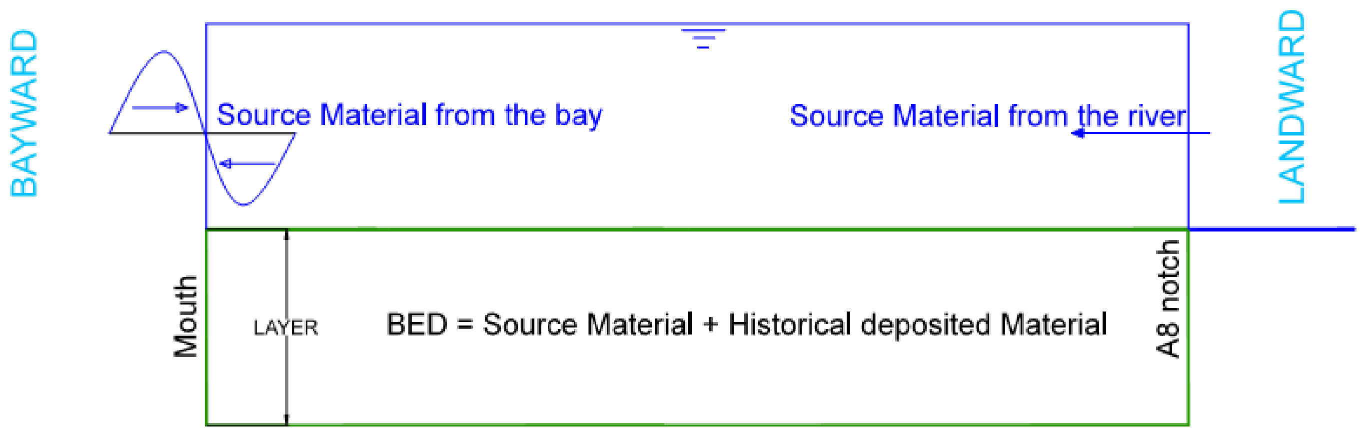

Figure 4-5. Bed composition sketch.

The reason to defined one layer model with uniform thickness, it is related with the description of the regional bed compositions of the area. Where, from studies by Marvin-DiPasquale and Cox (2007) and

USGS (2004) can be defined and uniform mud material both vertical and horizontal bed composition, specifically at the study area.

4.2.3. Initial Condition of water column

The initial condition of this model was divided by initial suspended sediment concentration of column water and the initial bed layer thickness.

The water column SSC was based on the information given by previous chapter 3.1.5. Setting up as follow: from the tributary fresh water the SSC was of 30 mg/l,, and from the seaward side of 150 mg/l. Those values correspond to the average of the SSC information at the location near by the boundaries in consideration.

4.2.4. Boundaries

The boundaries included in this model, consisting of the suspended sediment concentration (SSC) according with the data. The discharges boundaries are coupling with D-Flow FM hydrodynamics output. Additionally, there was not included SSC at Moffet Channel and Artesian Slough, because there is not record about it and also the discharge are very low.

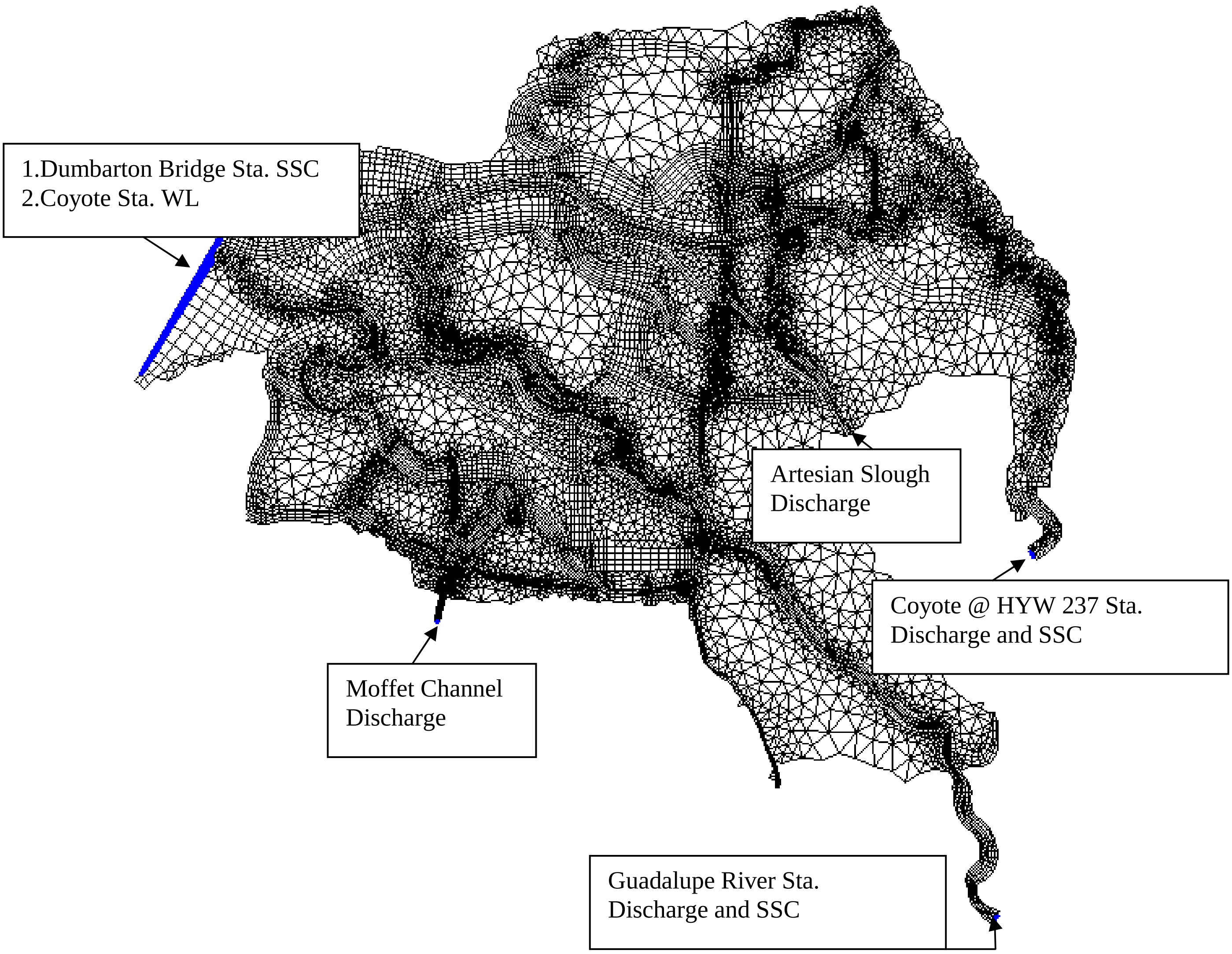

Figure 4-6. Boundaries defined in DELWAQ.

4.2.5. Process Parameters

From the material is on the system both the bed and suspended solids. It is classified as fine grained (cohesive) sediments. Thus, process like suspension, sedimentation and erosion. Most of those process are based on Krone (1962) and Partheniades (1962) concept. Each of those mentioned processes are related with parameters to be setting up in the model. Those parameters are calculating based on the information of sediments both bed composition and suspended sediments in column water.

Sedimentation is directly related with settling velocity. That occurs when the actual shear stress is lower than the user-defined critical shear stress for sedimentation. (Deltares, 2011).

The settling velocity was calculated as follows:

Firstly, acknowledge the grain size along the study is approximately 90% of (%<63 μm) fairly classified as mud. Besides, the study of Ganju (2011) described the relation between the floc size and density in San Francisco. In which, it was classifying the bay material between 20 to 80 microns. Based on this classification, the mud velocity can varied theoretically form 0.001 to 1 mm/s according with Stokes law (Figure 4-7). However, the falling velocity due to other factor, such as, salinity, ph, turbulence, organic matter might increase. From Ganju (2011) settling velocity has been found between 0.1 - 0.25 mm/s for South San Francisco Bay (Identified with a red frame in Figure 4-7).

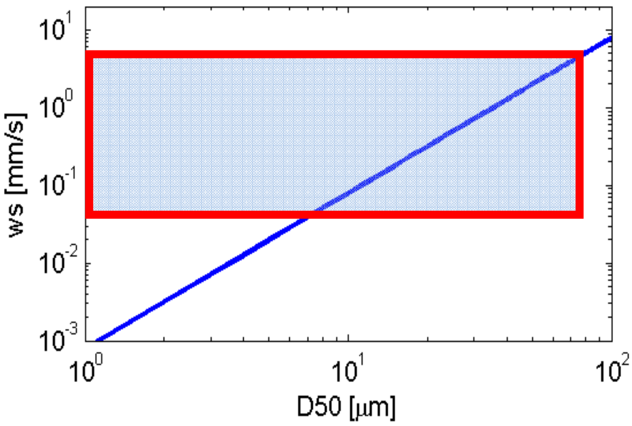

Figure 4-7. Single particle velocity of mud (Stokes law).

The critical shear stress which is related with processes, as settling and resuspension can be calculated from Figure 4-8. Where, based on many experiments the bed critical shear stress has been performed to determine the bed critical shear stress and the initiation of motion for natural beds composition (Sand, clay and silt). Figure 4-8 shows the relation between the grain size and the bed critical shear stress. Herein, the cohesive effects and binding effects for lower densities become an important parameter (Rijn, 2007). All those experiments to fine bed sediments estuaries are quite realistic and provided a tool to calculate a preliminary value to study area. In which, for a bulk density (1 - 1.3 g/cm^3) and a grain size lower 63 μm the approximate values are range between 0.05 and 0.45 N/m^2:

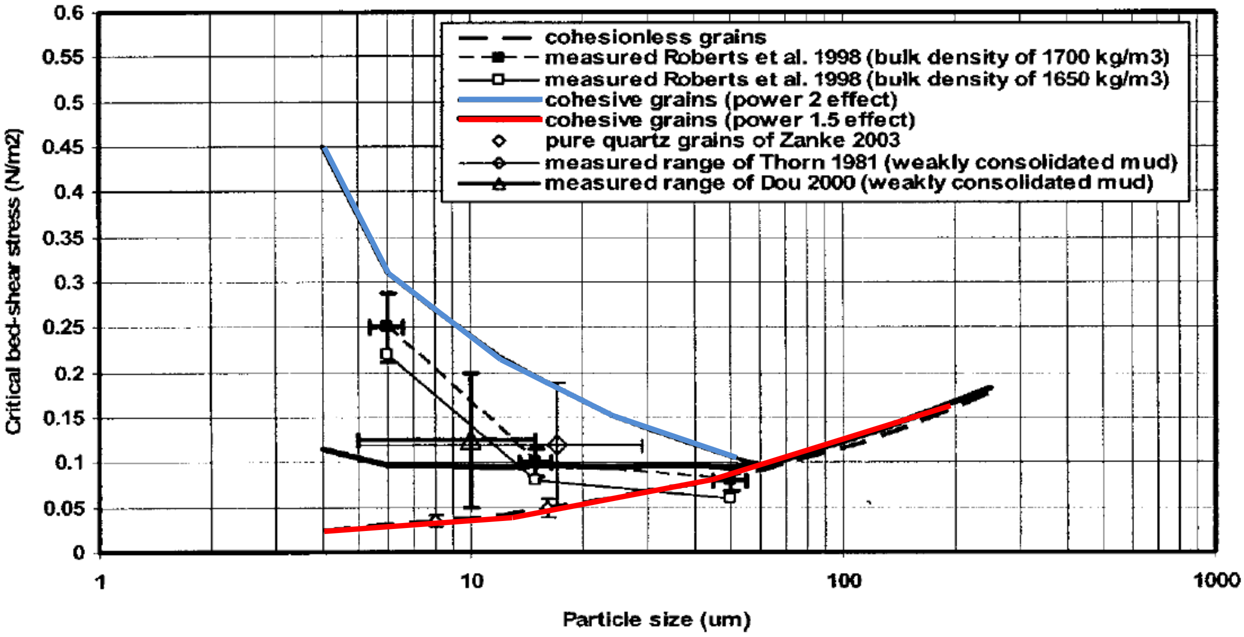

Figure 4-8. Critical bed shear stress. Source: (Rijn, 2007)

The rate suspension was assumed based on previous experience in the area and sediment characteristics. The value is approximately 1 $*10^{-5}$ kg m^{-2} s^{-1} and 2 $*10^{-5}$ kg m^{-2} s^{-1} defined by Manning and Schoellhamer (2013). From the same study, in order to validate the calculations above, taking into the uncertainty and difficult to quantify the precise parameters value, the model parameters are:

- Settling velocity: 0.10 - 0.25 mm s^{-1}.
- Erosion rate: 2 $*10^{-5}$ kg m^{-2} s^{-1}.
- Bed critical shear stresses: 0.1 - 1.0 N m^{-2}.

Finally, all the values calculated and assumed in this stage of setting up. However, the model was evaluated by the calibrating criterion. Thus, the calibration and validation chapter provided a sensitivity analysis, to enhance the model for a good performance of future scenarios and management of Alviso Complex due to opening the salt pond.

CHAPTER 5

CALIBRATION AND VALIDATION

Calibration of a model implies adjusting the model to represent measured data. Validation of the model implies simulation and comparison using another known situation, without adjusting the model any further. Calibration alone is not a sufficient guarantee of reliability. Both calibration and validation stress the need to in-situ data. Alviso Slough station (USGS 11169750) operated by USGS is the data source for calibration and validation of the present work

5.1. D-FLOW - FM CALIBRATION

The first calibration stage is described below explaining the methodology used to calibrate the hydrodynamics model for 3D model of 10 vertical layers.

Once the model was set up (Chapter 4), the calibration the calibration was carried out. The calibration periods were base on management operations of the salt pond A8 (pond A8) in Alviso Slough (Table 5-1) and data availability. Alviso Slough station data goes from March 2012 until current date,for most of the hydrodynamic parameters, such as: water depths, discharge, velocities suspended solids concentration, salinity and temperature. "The station consists of a near-bottom sonde (0.46m above bottom) and upward looking acoustic Doppler current profiler to profile the velocity" (Gregory G. Shellenbarger, 2014). The calibration period is from March to May of 2012. This period consist of high and low river discharges, spring - neap tidal cycle and A8 pond closed. The reason to choose this period aim to cover most of the main sediment transport forcing.

Table 5-1 History of pond management at A8.

OPENED	June 2011	June 2012	June 2013	March 2014	September 2014
CLOSED	December 2011	December 2012	December 2013	September 2014	On date
Notch opened	5 feet (1 of 8 gates)	15 feet (3 of 8 gates)	15 feet (3 of 8 gates)	15 feet (3 of 8 gates)	25 feet (5 gates)

One of the difficulties of the calibrating the numerical model was the constructing the bathymetry and achieving the same bathymetrical patterns. Between 2010 and 2012 severe changes in bathymetry occurred, due to opening of the ponds. These changes cannot be taking into account accurately, because the recorded bathymetry only covers the mouth at Alviso and Guadalupe Slough and along Alviso Slough until the notch of A8. Nevertheless, this was taken into account, while calibrating the model checking levees alignments.

For a proper calibration a series of parameters needed to be adjusted. The first parameter was the friction coefficient, guide by G. Arcement (1989). Taking into account, bed composition, variation of cross sections, meandering, vegetation and flood plains. The friction factor can be assigned to a range of values depending on the system characteristics. Alviso Slough complex presents muddy channels which has characteristic friction coefficient varying from 0.01-0.015 (manning coefficient) and vegetated tidal flats with coefficients 0.01 to 0.05.

The distribution of the friction coefficient was range between, 0.012 and 0.035 (manning coefficient). Where, 0.012 corresponds to mud bed composition with lower amount of vegetation at the flood plain and area surrounded the channels. Values of 0.035 corresponded to moderate vegetation with mud bed composition. To evaluate the sensitivity of the model due to friction parameter, 6 models were developed (Table 5-2).

Table 5-2 D-FLOW FM models and friction coefficient variation.

Model	Friction Factor
R001	0.014
R002	0.026
R003	0.032
R004	0.030
R005	0.012 - 0.020
R006	0.014 - 0.035

The models r005 and r006 were set up with spatial friction distribution. Where the channels and slough has the lowest friction factor and the areas surrounded the highest friction factors (Figure 5-1).

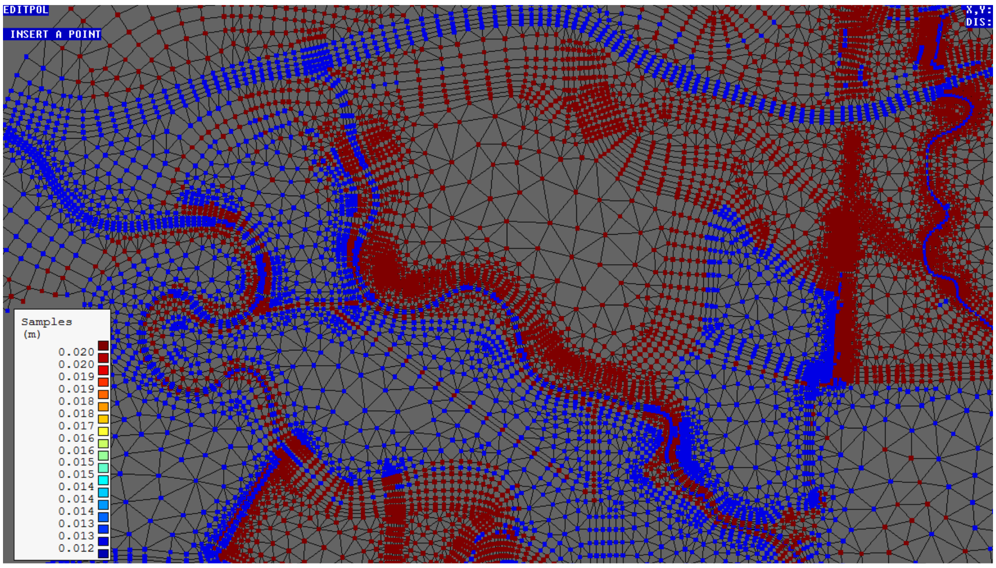

Figure 5-1. Samples friction coefficient setting up at D-FLOW-FM

First parameters evaluated were the water depths, velocities and discharge. Figure 5-2 shows a zoom out of the entire simulation period. In general, all models evaluated (Table 5-2) in terms of phasing behave quite well. However, the differences occurred in amplitude variation, in all the three parameters evaluated. Herein, as roughness the model (up to 0.03) lower the amplitude for all parameters.

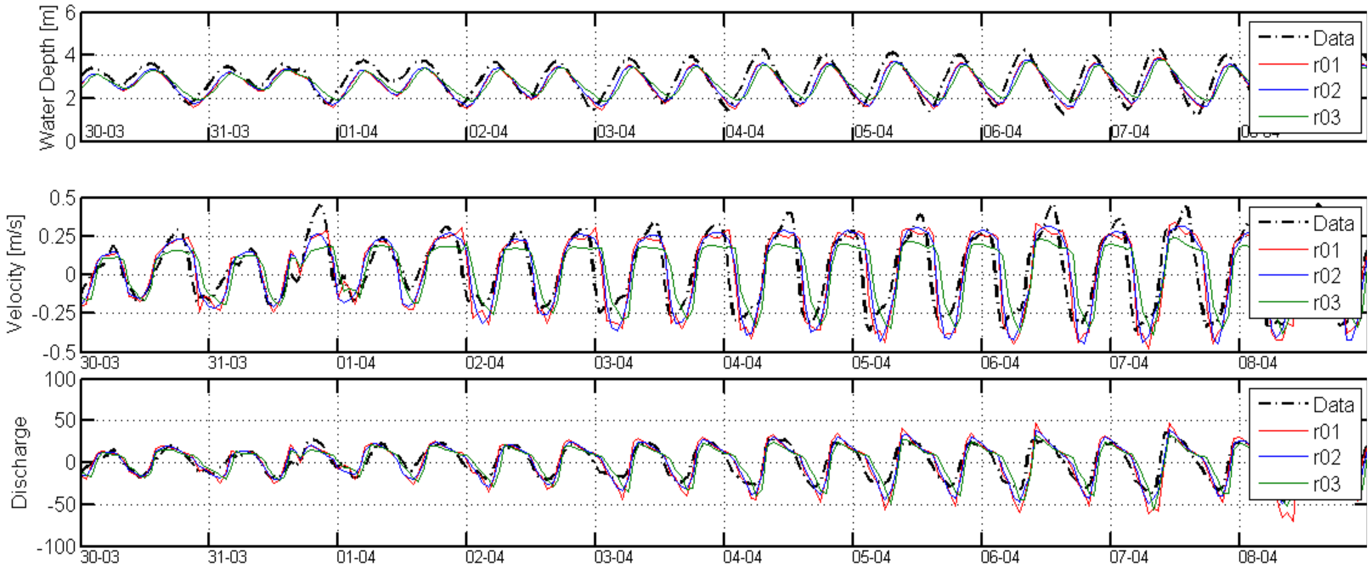

Figure 5-2. Water depth (Top), velocity (middle), discharge (bottom). Data Vs. Models r01, r02, r03. End of March until begin of April 2012.

In terms of the water depth, the model has good match in phasing and lowers levels. However, at high water levels, either of the models reached this up for two reasons: first, the Alviso Slough station does not have a fixed datum references, and due changes in bathymetry.

Nevertheless, the model agrees with velocities and discharge data. Some differences were found corresponding to lower friction coefficient, less than 0.020. In which, the amplitude of discharge and velocities during spring tide, increased significantly compare with friction coefficient up to 0.020 Moreover, spatial varying friction coefficient presents similar behaviour than fixed friction coefficient.

Figure 5-2. Water depth (Top), velocity (middle), discharge (bottom). Data Vs. Models r01, r02, r03. End of March until begin of April 2012. also provides hydrodynamic information of the slough. In which, the highest velocities occurred during lower and higher water levels, also the oscillation from peak to peak, where the velocities are zero occurred at slack tide. The same behaviour occurred to discharge.

Therefore to further evaluation and to define the best model setting, discharge output was analyzed and processed using the summary diagrams. This output (discharge) was considered highly important, because, it provides an overall model performance involving the velocities and the geometry. It is also gives an indication of the sediment transport. Before, moving forward, an explanation of the summary diagrams will be described on chapter below.

5.1.1. Summary diagrams

Summary diagrams are useful tools to evaluate the sensitivity/accuracy of complex models. The diagrams used for this analysis were: the target diagram and normalised target diagram (Jolliff K, et al., 2009).

The target diagram provides the relationship between Bias (Eq. 5.1) and the total Root-Mean Square Difference (RMSD′, Eq. 5.2), defined in a Cartesian plot, wherein as close to the centre, better the model efficiency it is.

$$B = \bar{m} - \bar{r} \tag{5.1}$$

In which:

$B = bias$

$\bar{m} = model\ mean$

$\bar{r} = data\ mean$

$m = model\ field$

$r = data\ field$

$\sigma_m = model\ \ standard\ deviation$

$\sigma_r = data\ standard\ deviation$

$$RMSD' = \left(\frac{1}{N}\sum_{n=1}^{N} [(m_n - \bar{m}) - (r_n - \bar{r})]^2\right)^{0.5} \tag{5.2}$$

The normalised target diagram allows a better way to identify and clarify the performance of the model. In which the linear correlation coefficient (R) is defined by:

$$R = \frac{\left(\frac{1}{N}\sum_{n=1}^{N} [(m_n - \bar{m})(r_n - \bar{r})]^2\right)}{\sigma_m \sigma_r} \tag{5.3}$$

The normalized standard deviation is defined as:

$$\sigma_* = \frac{\sigma_m}{\sigma_r} \tag{5.4}$$

Finally the normalised bias and RMSD are defined as:

$$B_* = \frac{\bar{m} - \bar{r}}{\sigma_r} \tag{5.5}$$

$$RMSD^{*\prime} = \sqrt{1.0 + \sigma *^2 - 2\sigma * R} \tag{5.6}$$

The first analysis using the summary diagram evaluates discharge of all models related in Table 5-2. From Figure 5-3 the best model are r02 and r05 presenting the lowest standard deviation. On the other hand, the normalised target diagram provided even better overview of model efficiency. In which, normalized total RMSD (RMSD*') is related as a predictor of how well the model is performed. (Jolliff K, et al., 2009). In other words, as closer the output to 1, better the performance of the model will be. For this case, r02 and r05 were the best model performance.

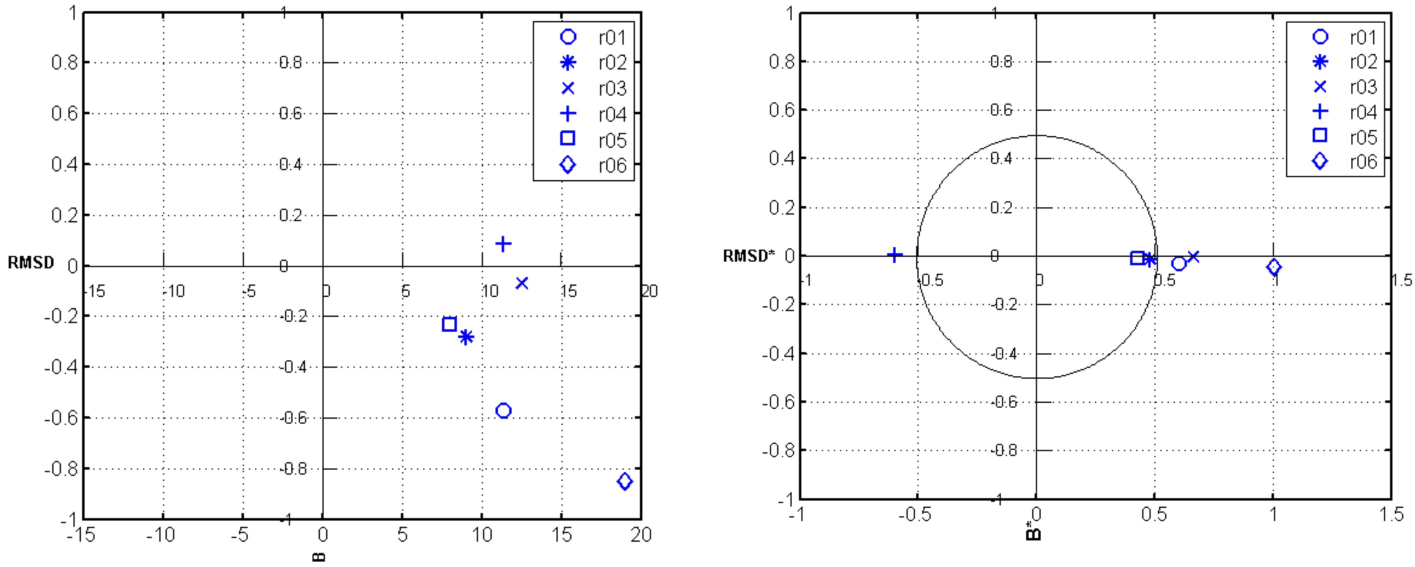

Figure 5-3. Discharge summary diagrams. Target diagram (left) and normalised target diagram (right).

The filter approach is related with the process of remove unwanted information. For this case, it was remove the tides component, in such a way, to distinguish other components that might affected the discharge. Figure 5-4 shows the filtered discharge for model r02 and r05.

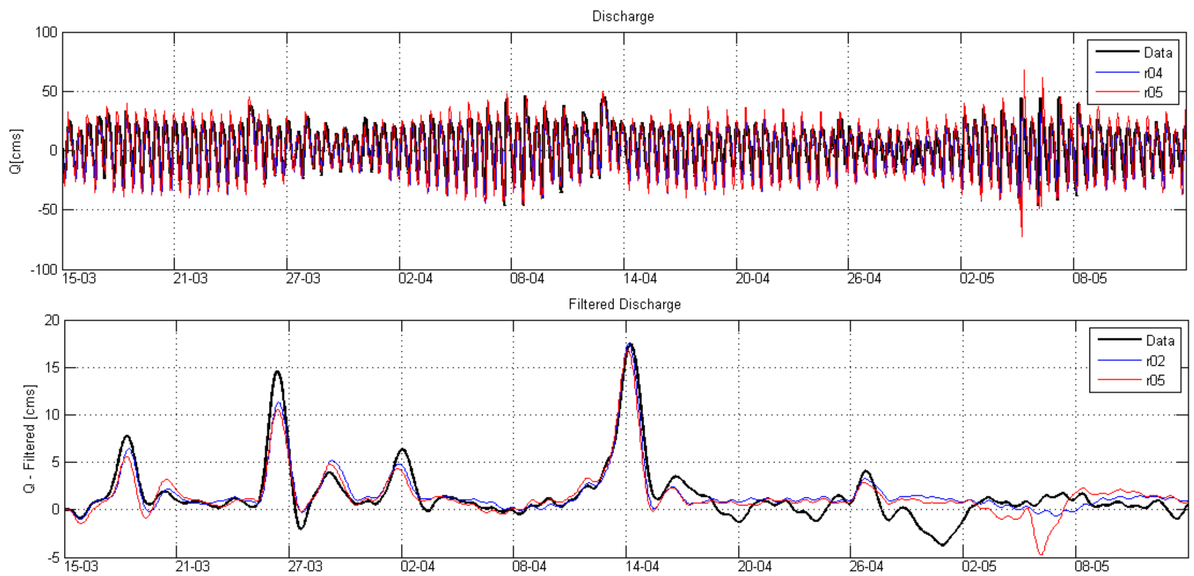

Figure 5-4. Filtered discharge models.

Figure 5-4 provides a clearer idea of the best model performance, r02 with 0.026 friction coefficient. Also provides interesting information of how the discharge had been impacted by storm events. These impacts are directly related with the peak on Figure 5-4.

The 3D model considers temperature and salinity to obtain a better understanding of the area in terms of vertical stratification, that might influence the sediment transport in the Slough.

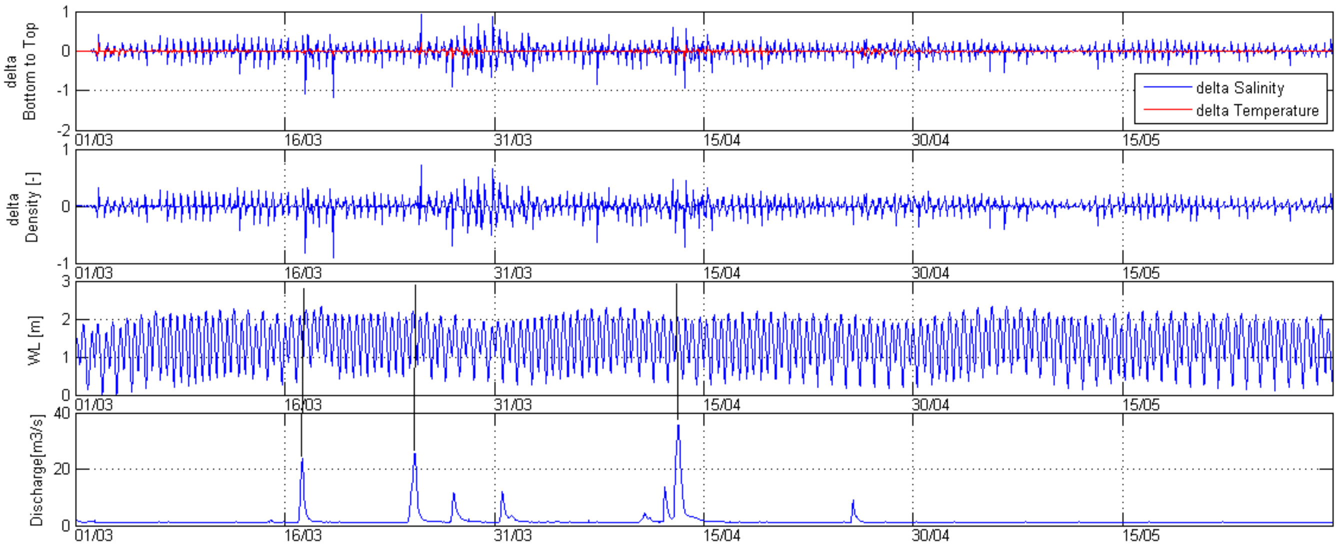

Figure 5-5. Stratification at Alviso Slough Station. Plots from top to bottom. 1. Differences of Bottom to top of salinity and temperature, 2. Delta density, 3. Water levels and 4. Discharge at Guadalupe river station.

Figure 5-5 showed the importance to identify the factor of parameters that might affected the Alviso Slough dynamics. One of them, took place with density driven current related with density variation and the influence of inflow of fresh water through the Slough. As Figure 5-5 showed, the highest differences of both density and salinity and temperature variation. Moreover, the variability was not higher enough to allow vertical stratification.

Nevertheless, there is not a big vertical stratification. Figure 5-5 also provided that salinity was a major impact compare with temperature due to density stratification. Additionally, during lower river discharge, the Slough presented very low density variation. In conclusion, the Slough can be classified as well mixed, where bay waters do not allow that fresh water reach at least, up to Alviso Slough station.

5.2. SEDIMENT TRANSPORT CALIBRATION

The second phase the suspended sediment transport calibration. This part was based on the sensitivity analysis of process parameter such as: falling velocity, critical shear stress and erosion rate (Krone, 1962) and (Partheniades, 1962). These are parameters of Krone-Partheniades formulation for fine sediment erosion and deposition.

The model performance was compared with suspended sediments concentration (SSC) measurements at Alviso Slough. The numerical model runs listed below described the SSC values calculated for each model. As well as, hydrodynamic model, it was used a 3D model of 10 vertical layers.

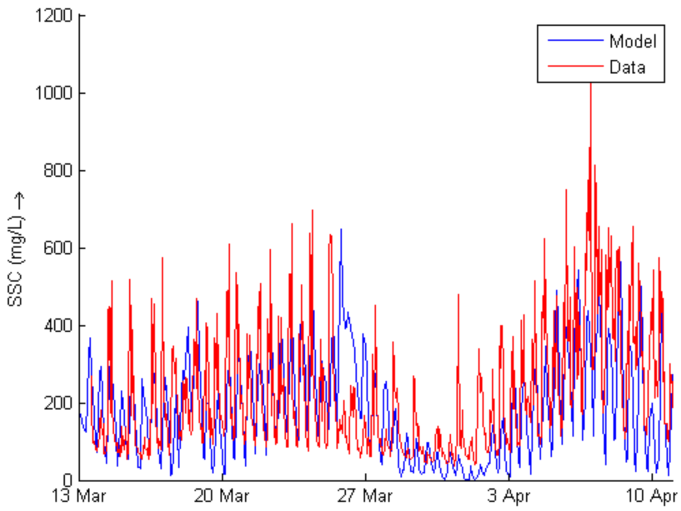

Figure 5-6. SSC at Alviso Slough Station. Erosion rate 2 *10-5 kg/m2 s, falling velocity 0.04 mm/s and critical shear stress 0.08 N/m2.

The first parameter to evaluate the sensitivity of the model was the erosion rate, starting with a value of 2 $*10^{-5}$ kg/m^2 s (Figure 5-6). To ensure good values for falling velocity and critical shear stress, it was necessary lower values from data (out of record mentioned in chapter 4.2.5) for a suitable performance when comparing the prototype data versus model calculations. This is how the first value for erosion rate 1 $*10^{-5}$ kg m^{-2} s^{-1} was determined (Figure 5-6).

Table 5-3 DELWAQ models.

Model	PROCESS PARAMETES				
	Falling velocity IM1* mm/s	Falling velocity IM2** mm/s	Erosion rate. kg/m2/s	Critical Tao IM1 N/m2	Critical Tao IM2 N/m2
r001	0.17	0.17	0.00001	0.2	0.2
r002	0.06	0.06	0.00001	0.2	0.2
r003	0.12	0.12	0.00001	0.1	0.1
r004	0.06	0.06	0.00001	0.15	0.15
r005	0.23	0.23	0.00001	0.15	0.15
r006	0.12	0.12	0.00001	0.2	0.2
r007	0.12	0.12	0.00001	0.15	0.15
r008	0.12	0.12	0.00001	0.2	0.2
r009	0.06	0.12	0.00001	0.2	0.15
r010	0.06	0.09	0.00001	0.2	0.18
r011	0.46	0.46	0.00001	0.15	0.15
r012	0.35	0.35	0.00001	0.2	0.2

**IM1 corresponds to set up material as source material.*
**IM2 corresponds to set up material as deposited material.*

The sensitivity analysis was based on a range of the falling velocity ranging between 0.05 to 0.50 mm/s and 0.10 to 0.20 N/m^2 explained in previous chapter. The analysis aims to cover the percentiles of the parameter ranges (0%, 25%, 50%, 75% and 100%). However, in the case of calibrating the critical shear stress, the range is quite small, even though significance variation was observed in the model. Therefore, maximum, minimum and 50% percentile values were used when calibrating the model.

The results of the numerical model runs are described in Figure 5-7. Appendix B provided in detailed each model against data plot. Figure 5-7 showed the high variability of the outputs and the complexity to evaluate the modelling efficiency or sensitivity of the parameters. It can be distinguished that in general all models has a good phase agreement.

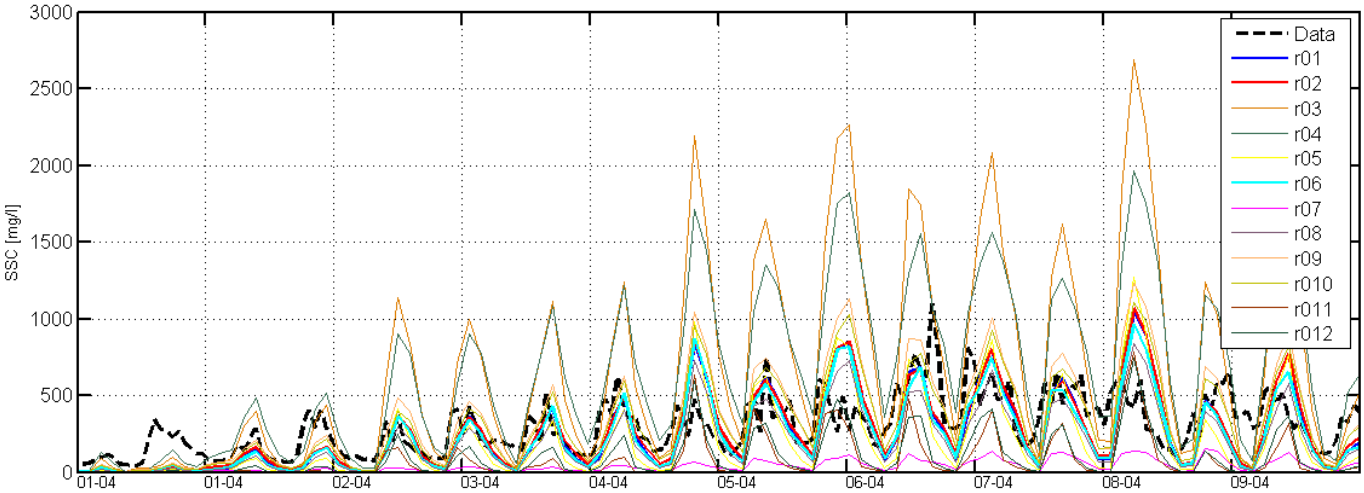

Figure 5-7. Suspended solids concentration, Model vs Data at Alviso Slough Sta.

To identify which parameters suited the model best, the summary diagrams, provided an excellent tool to analyse the model performance (Figure 5-8). In target diagram the lowest standard deviation and the lowest error, evaluating by Bias, it was performed by runs 01, 02, 06 and 08. On the other hand, as additional tool the normalised diagram allowed to identify the optimal runs performance. The runs 01, 02 and 06 achieved a good correlation.

Figure 5-8 shows that with lower values of critical shear stress (0.1 - 0.15 N/m^2), there was a bad performance, due to high variability in SSC amplitude. Low shear stress combined with low velocity, runs r03 and r04 (lower than 0.012 mm/s), increases even more the variability. On the other hand, with high velocities, up to 0.3 and critical shear stress of 0.2 N/m^2, the model performed out of target, decreasing amplitude of SSC.

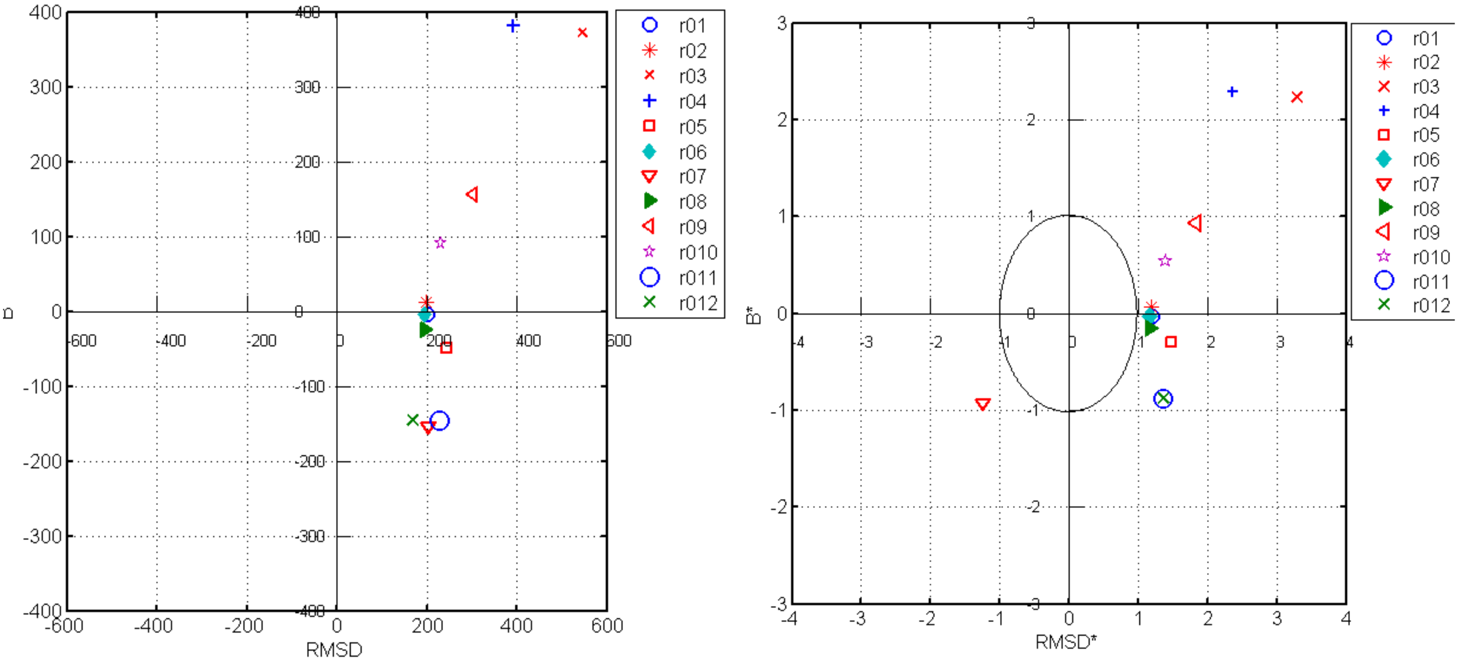

Figure 5-8. Summary diagrams of SSC calibration model.

Nevertheless, none of the runs reached the optimal performance. The cumulative sediment flux was calculated and compared with Alviso Slough station, in order to evaluate the model in a longer timescale and provides the sediment direction at Alviso Slough station (Figure 5-9). The run 02 achieved the best correlation.

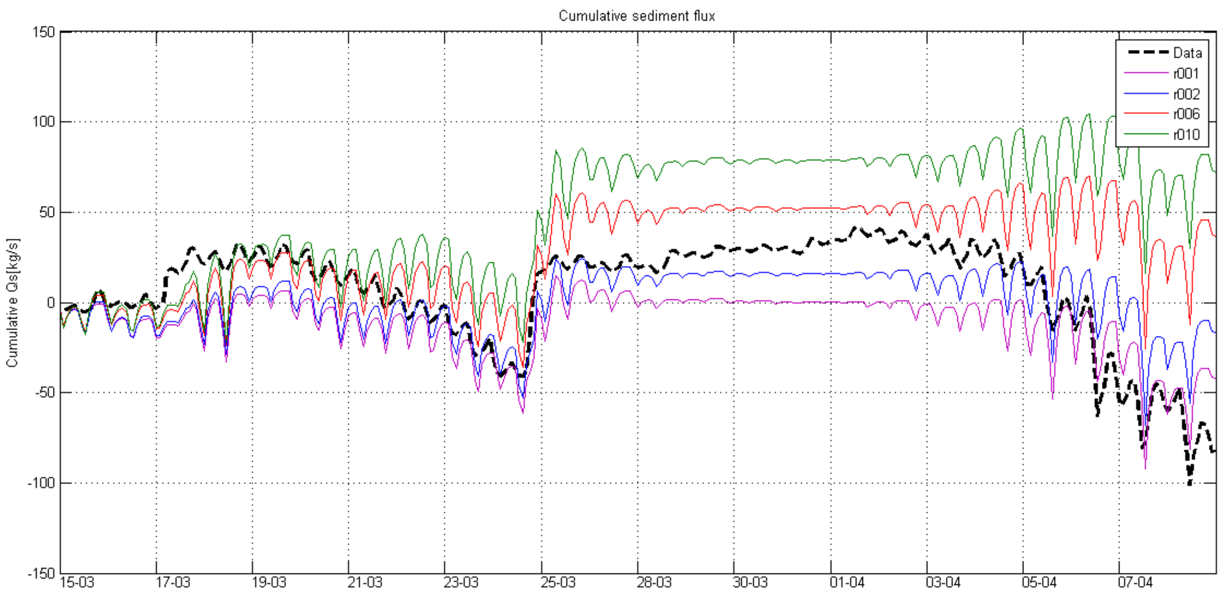

Figure 5-9. Cumulative sediment flux at Alviso Slough Sta.

Where the positive values correspond to export sediments towards the bay (bayward) and negative values corresponds to import sediments towards upstream (landward).

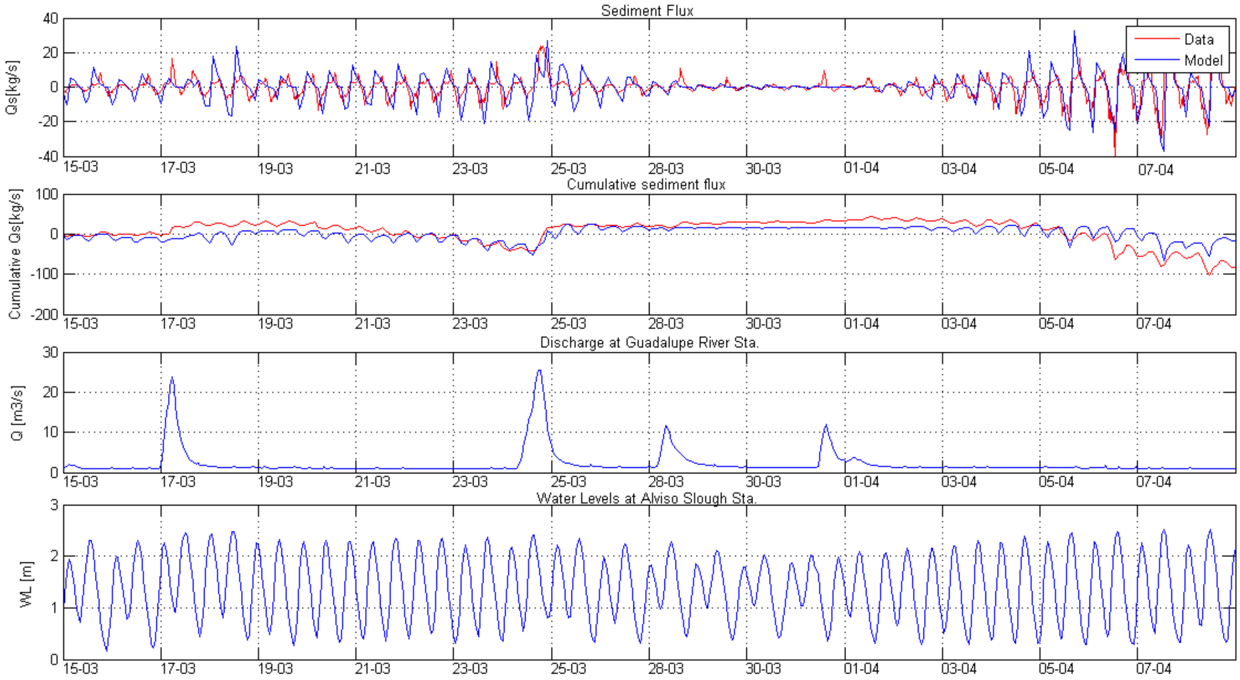

Figure 5-10. Sediment flux of r002 at Alviso Slough Station. From top to bottom: 1. Sediment flux, 2. cumulative time series sediment flux, 3.river discharge at Guadalupe river station and water levels at Alviso slough.

Figure 5-10 provided detailed information in terms of impact due to sediment transport. Where, the sediment flux in Alviso Slough it is tidal dominated, due to the oscillation along the time series. It can be distinguish the difference between the tidal cycles. During spring tide more sediment is transported then during neap tide. High peak discharge direct impact changing the sediment direction from importing to exporting.

Finally, the most suitable numerical model was r02, which presents: erosion rate 1 $*10^{-5}$ kg/m^2 s, falling velocity 0.06 mm/s and critical shear stress 0.2 N/m^2.

5.3. VALIDATION

The validation was carried out for August 2012 which indicates post salt opening of A8 notch. Due to available data at Alviso Slough Station, the time series used for validation occurred in August to end of September. The following method was used for validation.

A 3D model was set up to evaluate the hydrodynamics using D-FLOW -FM, after which the second phase of validation was carried out by making use of DELWAQ to evaluate the sediment transport. The best fit friction coefficient (0.026) was applied to this model including temperature and salinity boundaries.

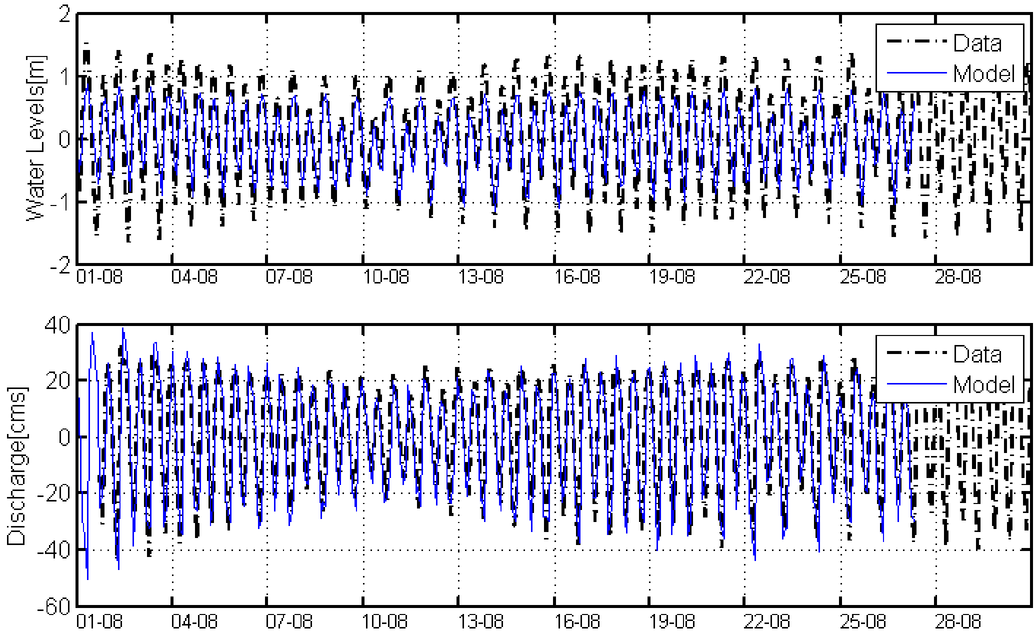

Figure 5-11. Water levels (top), and discharge (bottom). 3D model time series of August 2012.

Figure 5-11 shows a good agreement for both water levels and discharge the model between the model and data. Analysing phasing and amplitude of both parameters, in general the match is quite good. In terms of water levels, the high water levels are underestimated as previously calibration chapter. Despite the fact, a good agreement can be distinguished comparing the discharges.

D-FLOW FM and DELWAQ models were set up for validation purposes making use of the calibrated parameters. The model are in phase with data, however the model overestimated SSC amplitude (Figure 5-12)

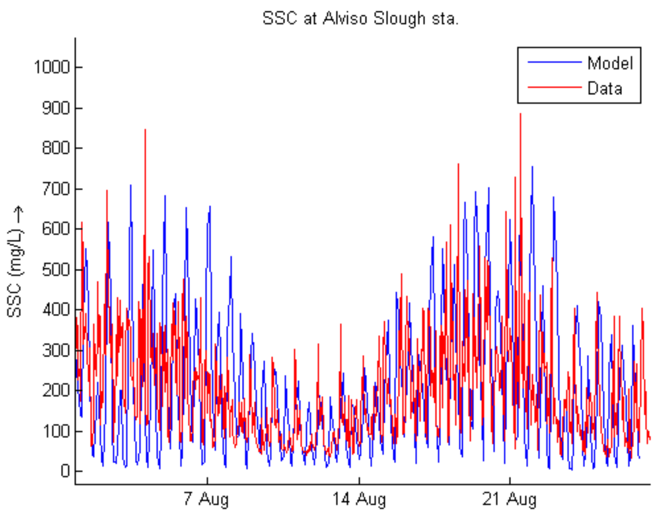

Figure 5-12. SSC validation at Alviso Slough.

In addition, sediment flux and cumulative sediment transport was calculated. Figure 5-13 shows a good agreement between the data and the model calculations.

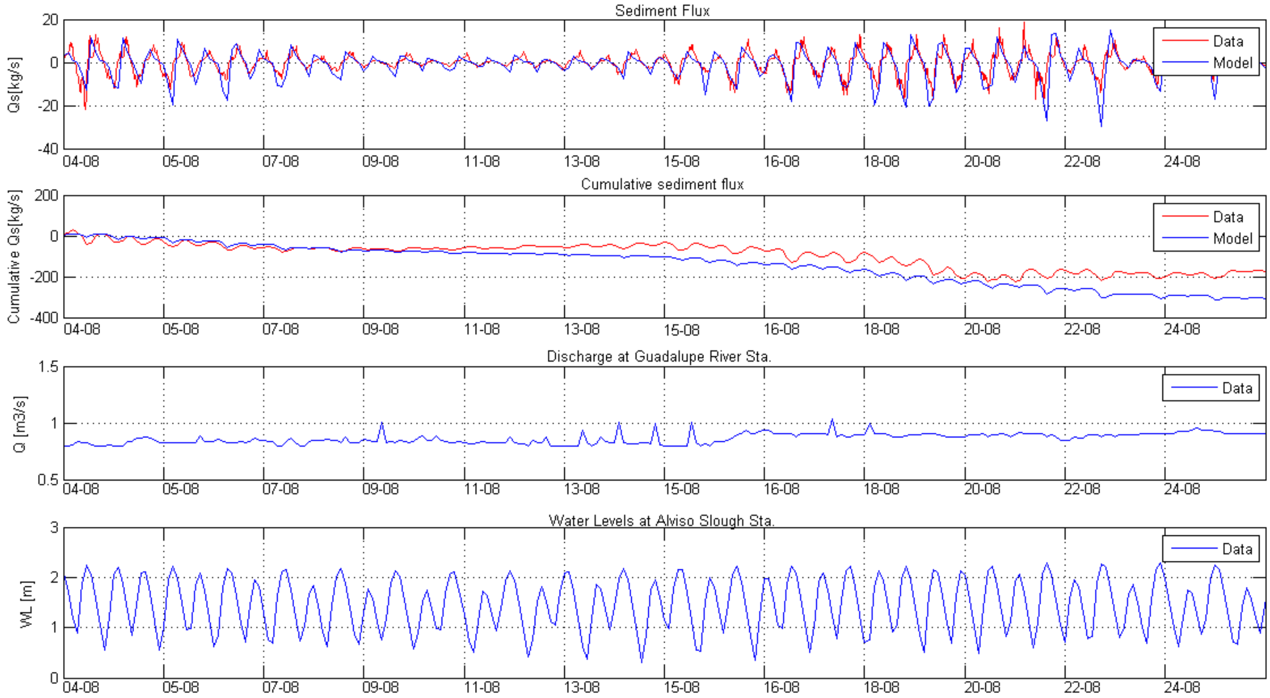

Figure 5-13. Sediment flux at Alviso Slough Station of August 2012. From top to bottom: 1. Sediment flux, cumulative time series sediment flux, river discharge at Guadalupe river station and water levels at Alviso slough.

Figure 5-13 also shows that tidal forcing governs the sediment transport. During spring tide, the sediment flux increases and during neap tide, the sediment flux variability is small. Alviso Slough station transport integrated over the spring-neap tidal cycle show sediment import, similar to the observed in the calibration phase during los river discharge.

CHAPTER 6

SCENARIOS EVALUATION

In previous chapter was described the best fit model and the parameters that lead to the most accurate result. The scenarios used to evaluate the sediment dynamics at Alviso Slough comply the following restrictions.

1. 2 months time frame including dry periods and high run off, which describes the Mediterranean climate, characteristic of the study area.
2. 3D runs with 10 vertical layers set up.
3. The parameters used were defined in the calibration.
4. The scenarios include a entire spring - neap tidal cycle .
5. Finally, two kind of bathymetry set up scenarios were used making used of 2010 bathymetry and October 2012 bathymetry. This was done to define two bathymetry set up scenarios which would enable one to understand the sediment dynamic, before the salt ponds management and also after the opening.

Table 6-1 Scenarios description.

Scenario	Bathymetry	Boundaries	Openings
1	2010	2010	Closed Notch
2	2010	2010	A8 Notch - 5 m (Around 15 ft)
3	2012	Average (2011-2014)	A8 Notch - 5 m (Around. 15 ft)
4	2012	Average (2011-2014)	A8 Notch - 15 m (Around 40 ft)
5	2012	Average (2011-2014)	A8 Notch - 15 m (Around 40 ft) and open breach at Pond A7

The aforementioned methodology was used to describe and understand the sediments dynamics of each scenario. The sediment flux was calculated on cross sections along the Alviso Slough, considering breaches and intakes Figure 6-1.

Figure 6-1. Alviso Slough and cross sections.

The sediment dynamics also was evaluated during spring and neap tides, dry periods and high river runoff events. Where, for each section it was calculated the cumulative sediment flux, during the following events:

- Dry periods or lower discharge and neap tidal cycle.
- Dry periods and spring tidal cycle.
- High flow discharges and neap tidal cycle.
- High flow discharges and spring tidal cycle.

All the cumulative sediment flux sections along the tidal channel for each scenario are included at appendix C.

6.1. Scenario 1

The first scenario took place before any influences of salt ponds management. Thus, the bathymetry and data of 2010 was used. The analysis of this scenario includes the same events mentioned before, as follows:

Where the events set up, as follows:

1. Spring tide and high flow river discharge.
2. Neap tide and high flow river discharge.
3. Neap tide and low flow river discharge.
4. Spring tide and low flow river discharge.

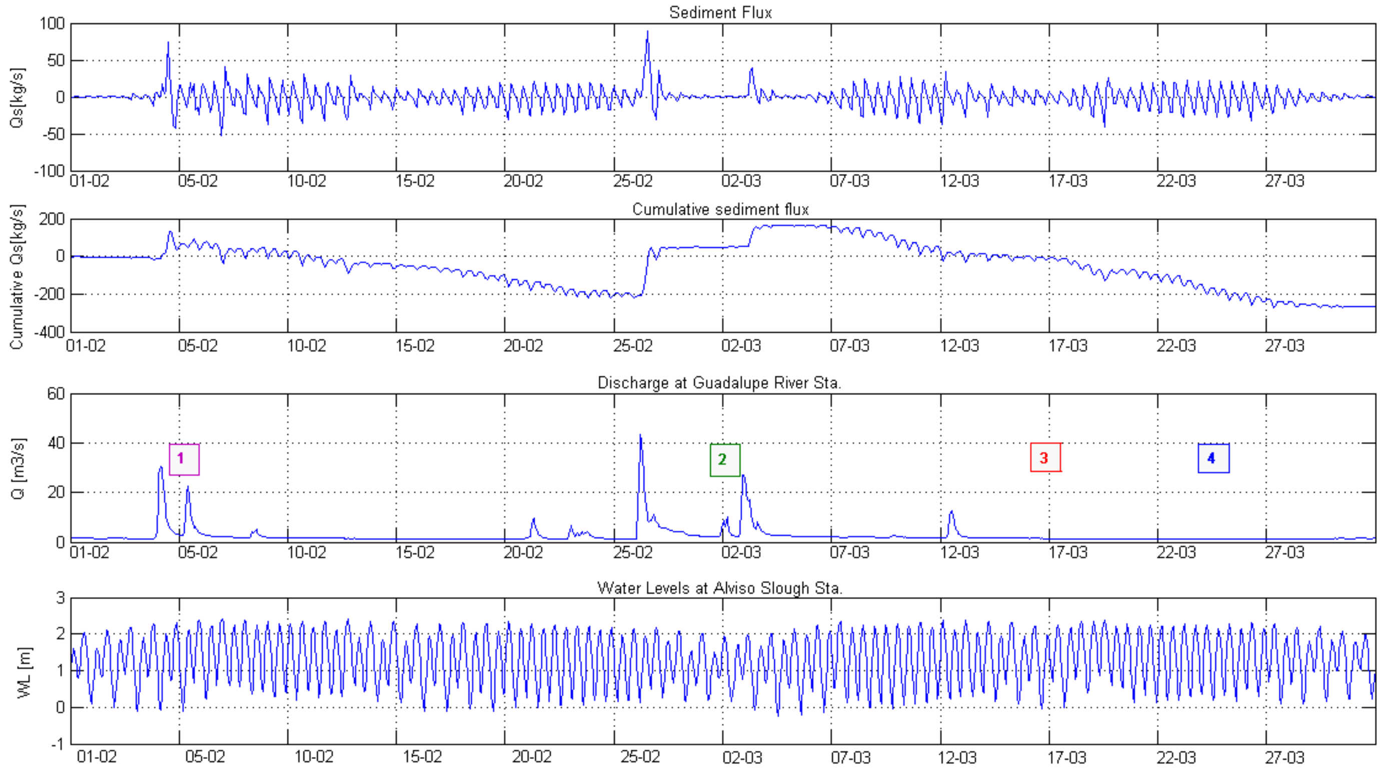

Figure 6-2. Sediment flux at Alviso Slough station - Scenario 1. Cumulative sediment flux: positive values towards bay or bayward (exporting sediments) and negative values towards upstream or landward (importing sediments). The events by order and colour square in the discharge subplot.

Figure 6-2 shows the impact of high river discharge in the sediment transport (event 2). At the beginning of neap tide (25/02) combined with high discharge, the trend of importing sediments changed from importing to exporting sediments. During neap tide the sediment flux is constant compared with spring tide. During spring tide the slough imports sediments.

This scenario had not breaches along the tidal channel. Hence, it allowed a better understanding of the sediment flux direction. Wherein, at the bayward side the slough exports sediments. In only one event at breach two with spring tide and low river flow, the slough was importing sediments (Figure 6-3).

Upstream from breach two, the sediment dynamic at Alviso Slough changes, from exporting sediments to importing sediments. Near A8 notch the slough stars exporting again. The reason of this last changed at the end of the slough, related with river discharge, instead of the tidal impact at area (Appendix C - Scenario 1).

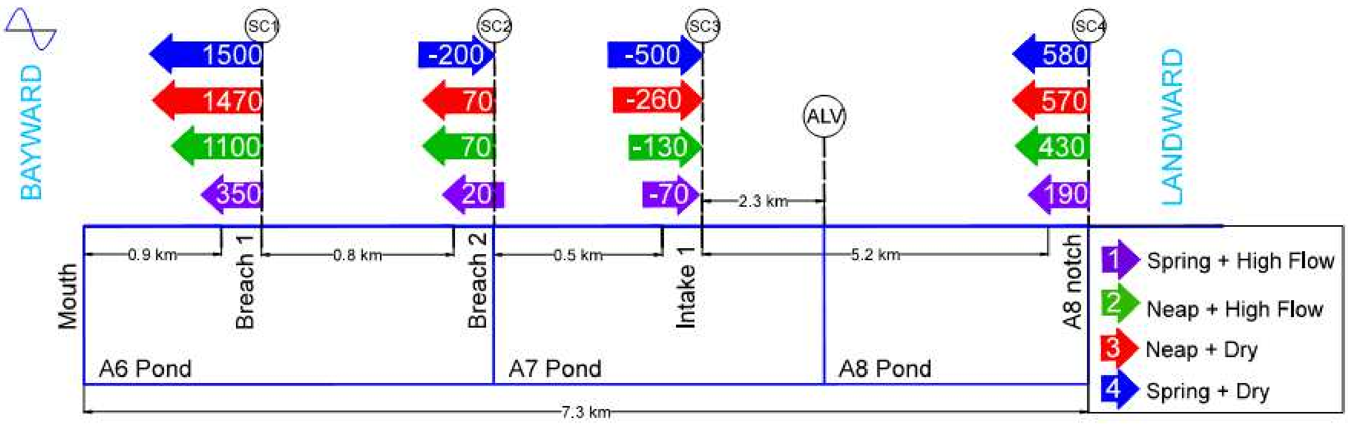

Figure 6-3. Cumulative sediment flux direction- Scenario 1. All values are in kilograms (kg) unless is defined. (Positive values are bayward and negative are landward)

The Figure 6-3 provides, the river flux impact area, where the reach nearby the mouth have the highest values in all events compare other sections. The difference is related with the direct impact of the tidal cycle.

Additionally the following figures allowed, to distinguish patterns of erosion and sedimentation.

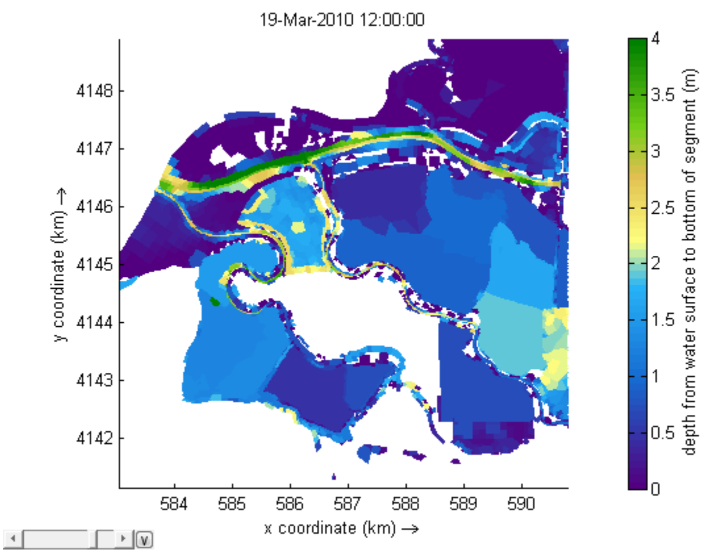

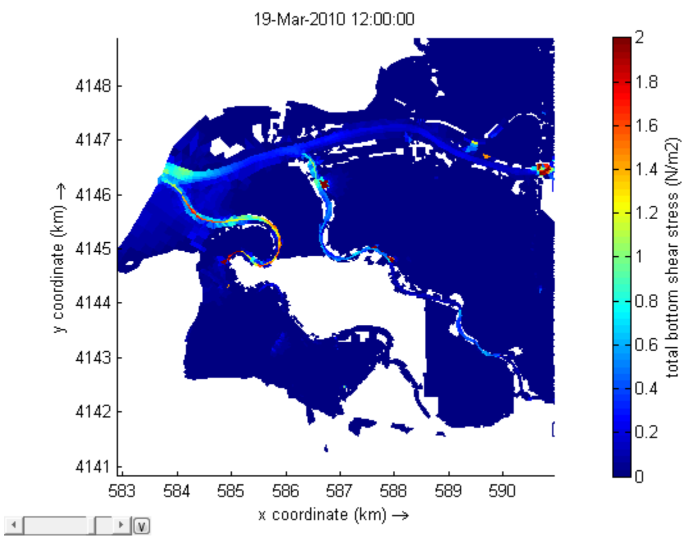

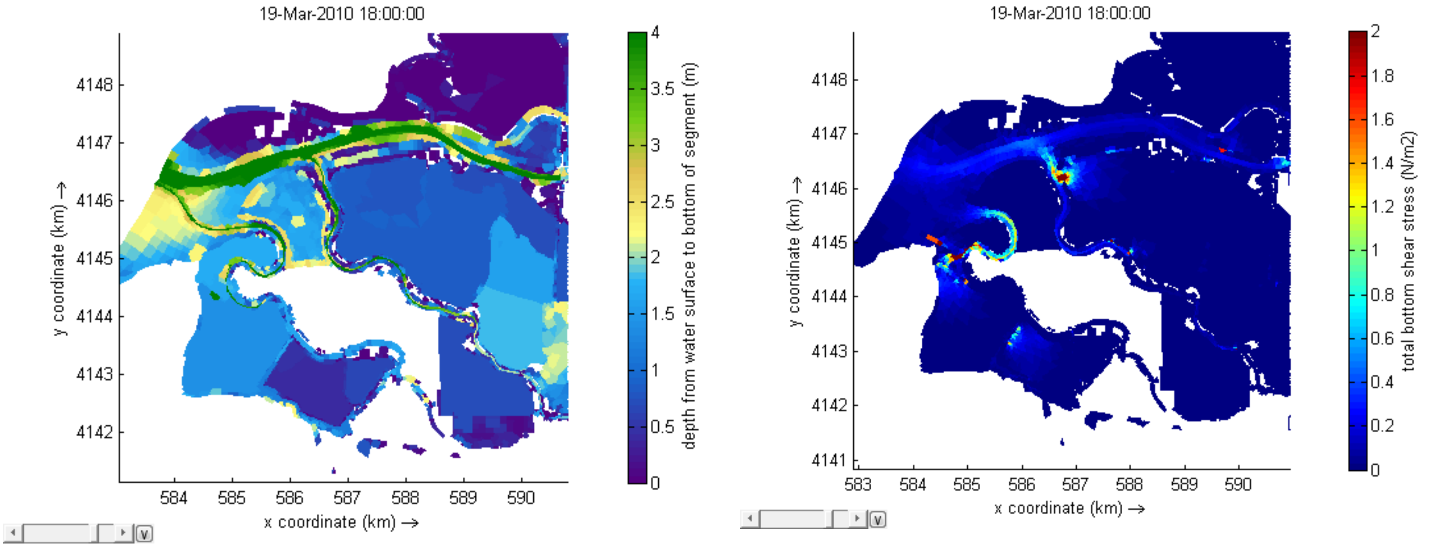

Figure 6-4 Total bottom shear stress during flood and ebb - Scenario 1. Water depth (left side) and Total bottom shear stress (right side)

During the flood the total bottom shear stress was lower than the ebb. In which, it can be distinguished the areas of higher sediment transport occurred. Figure 6-4 confirms the higher sediment transport at bayward side of the slough. In conclusion, most of the slough is deepening. Although, Figure 6-5confirmed what was said before, but also showed a deposition region in the middle of the Slough, which contributes to a better understanding of how the sediment dynamic in the tidal channel was variable, from importing to exporting sediments in between of intake 1 and A8 notch Figure 6-3.

The figure below showed the final plot after the simulation in terms of erosion and deposition. Also how the slough has been developed in terms of sediment dynamics and also in shape. In general, tidal channel is deepening, however in the middle of the slough deposition took place and also at the tidal marshes. That explains why the slough has contrast sediment flux in terms of exporting and importing sediments.

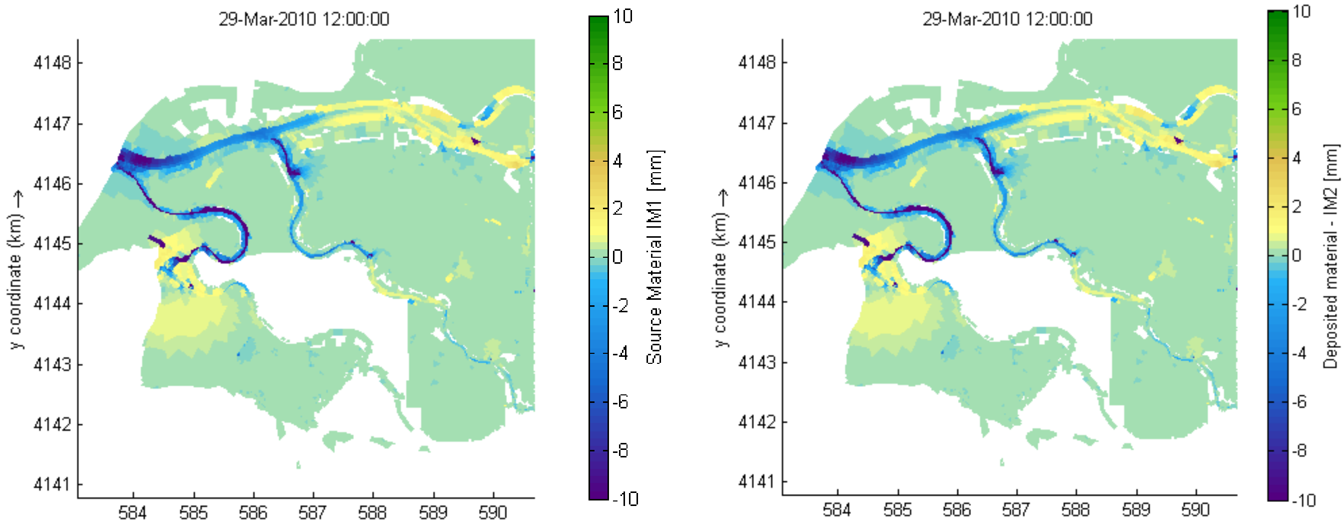

Figure 6-5. Erosion and deposition patterns - Scenario 1.
Bed source material (right) and bed deposited material (left).

Besides, these figures also showed that in terms of sediment transport both materials (bed composition defined by, deposited material and historical material) has the same behaviour, comparing in terms of sediment flux and cumulative sediment flux also had the same behaviour.

6.2. Scenario 2

The second scenario was based on 2010 data, both bathymetry and boundaries. In this scenario the A8 notch and breaches at A6 are open. It allows to identify the main impacts of the Alviso complex wetland restoration.

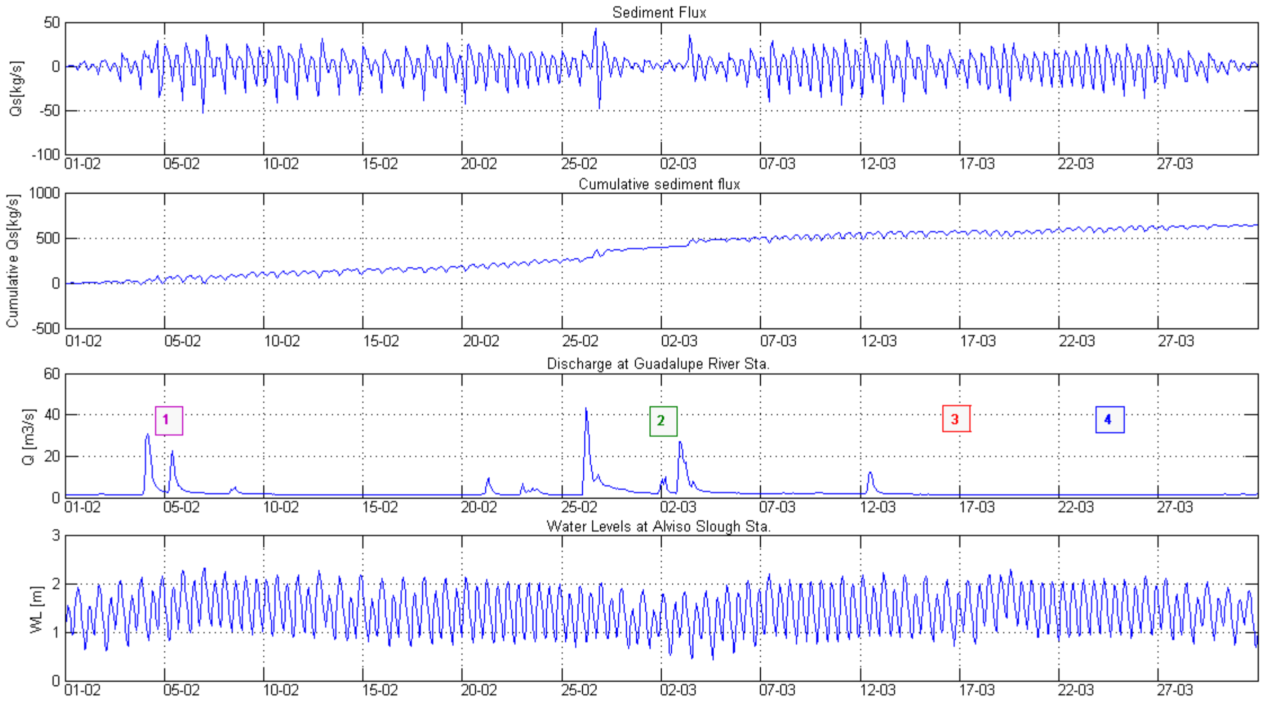

Figure 6-6. Sediment flux at Alviso Slough station - Scenario 2.

This scenario includes the same events as in scenario 1, to evaluate the sediment dynamic along the slough. As a comparison with the first scenario over the time of simulation, the slough was exporting at the station and the influence of river discharge had a lower impact at this observation point. Although, similar to first scenario the neap tide had lower variability compared with spring tidal event.

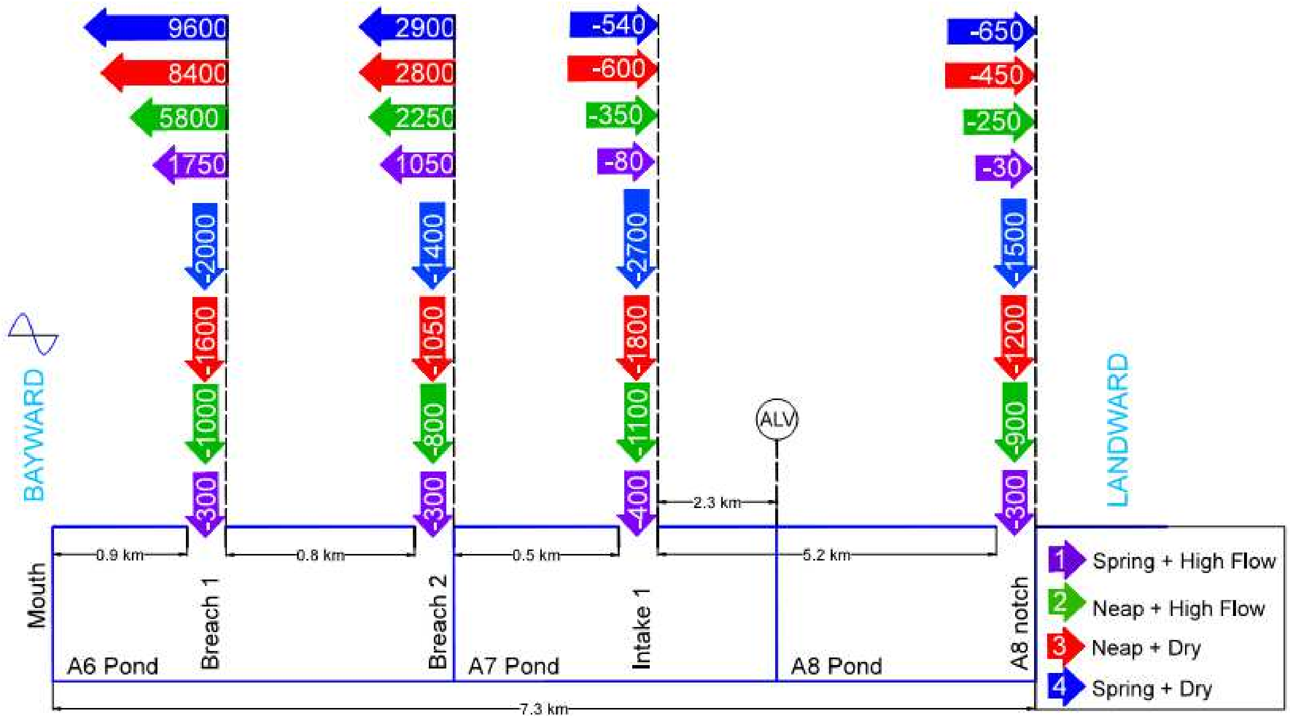

Figure 6-7. Cumulative sediment flux direction - Scenario 2. All values are in kilograms (kg) unless is defined.

However, it was clear that at the moment of the openings the Alviso slough dynamic changes dramatically, both, sediment flux magnitude, and erosion and deposition patterns. First of all, in terms of magnitude, the increasing of the sediment flux was huge comparing the first scenario, around 6 times more than scenario 1.

The first big change it was the transport of sediment towards the ponds in all the openings. Along the slough there were also some changes of sediment direction, compared with the first scenario. The first reach (from the mouth to breach 2), the slough was exporting sediment bayward and also at the ponds. In contrast, at the intake 1, the sediment transport direction changed. Where, the slough was importing material. The sediment import upstream continues all the way to A8 notch section.

Comparing ebb and flood there are difference as described in previous scenario, however Figure 6-8 presents higher shear stress compared with first scenario. This increasing confirms that salt ponds opening changed the dynamic and the magnitude of the sediment transport in the area. Figure 6-8 also provides information of higher shear stress areas like the openings and bayward reach slough. Additionally, it can be conclude that during both ebb and flood the highest velocities occurred, hence the remobilization of sediments. On the other hand, during slack tide deposition take place due to velocities equal to zero.

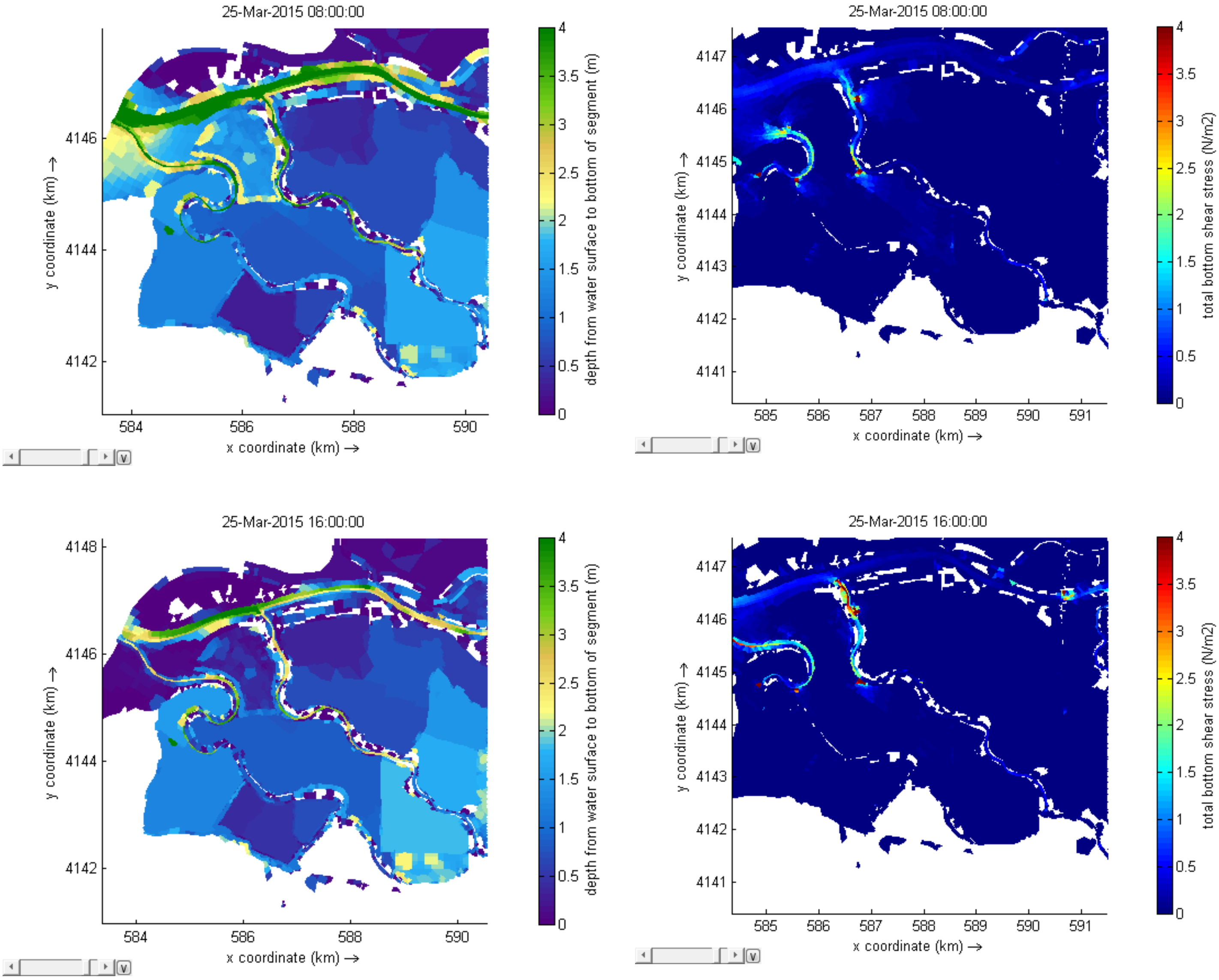

Figure 6-8. Total bottom shear stress during flood and ebb - Scenario2. Water depth (left side, flood - top and ebb - bottom) and Total bottom shear stress (right side).

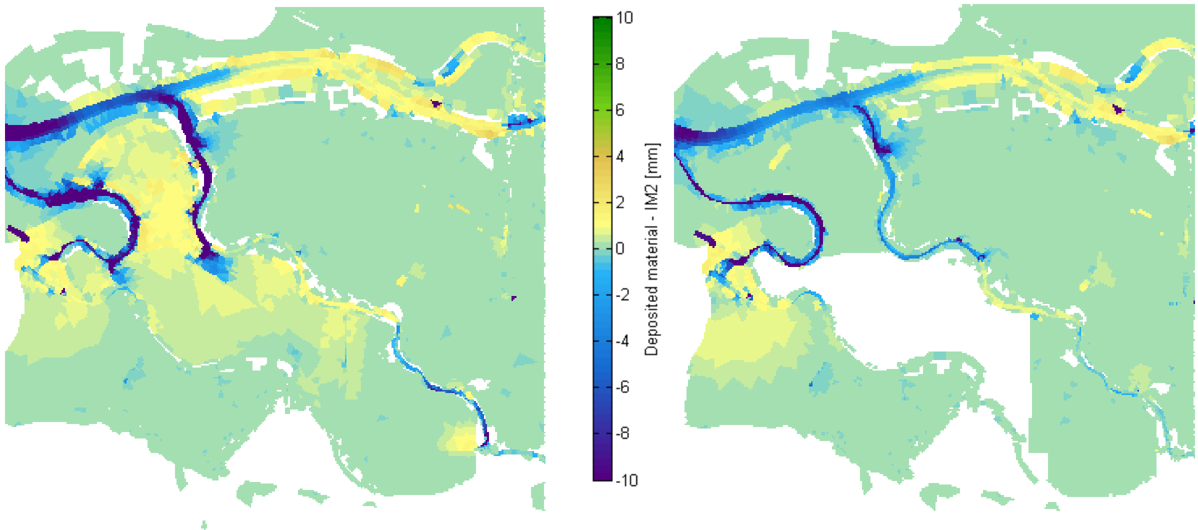

Figure 6-9. Erosion and deposition patterns - bed deposited material - Scenario 2 (left side) - Scenario 1 (right side).

The sediment transport in the slough increased with the opening of salt ponds. Despite the impact of the management in the slough, the patterns of erosion and deposition along the slough remained quite similar compared with last scenario. Figure 6-9 allowed to identify where the sediment were deposited. From landward to seaward into the ponds: at the A8 notch there is a patch of deposition near by the notch, pond A7 near the intake there is huge erosion but surround the pond there is a pattern of deposition, finally at A6 pond there is a huge deposition compare with other ponds, due to openings at Alviso Slough and Guadalupe slough (western side of Alviso complex).

Also, **Error! Reference source not found.** shows deposition pattern at the middle of the slough, which contrast with landward and bayward side of the slough. Hence, this result validated the impact of the A8 opening notch impact in the slough and changes of erosion patterns, besides the rapidly change of this patterns in the slough.

6.3. Scenario 3

This scenario was based on October 2012 bathymetry (The last bathymetry available, Table 3-3). The discharge and SSC boundary were set up with average of data from 2010 to 2014. The simulation results of this scenario are in the following figures:

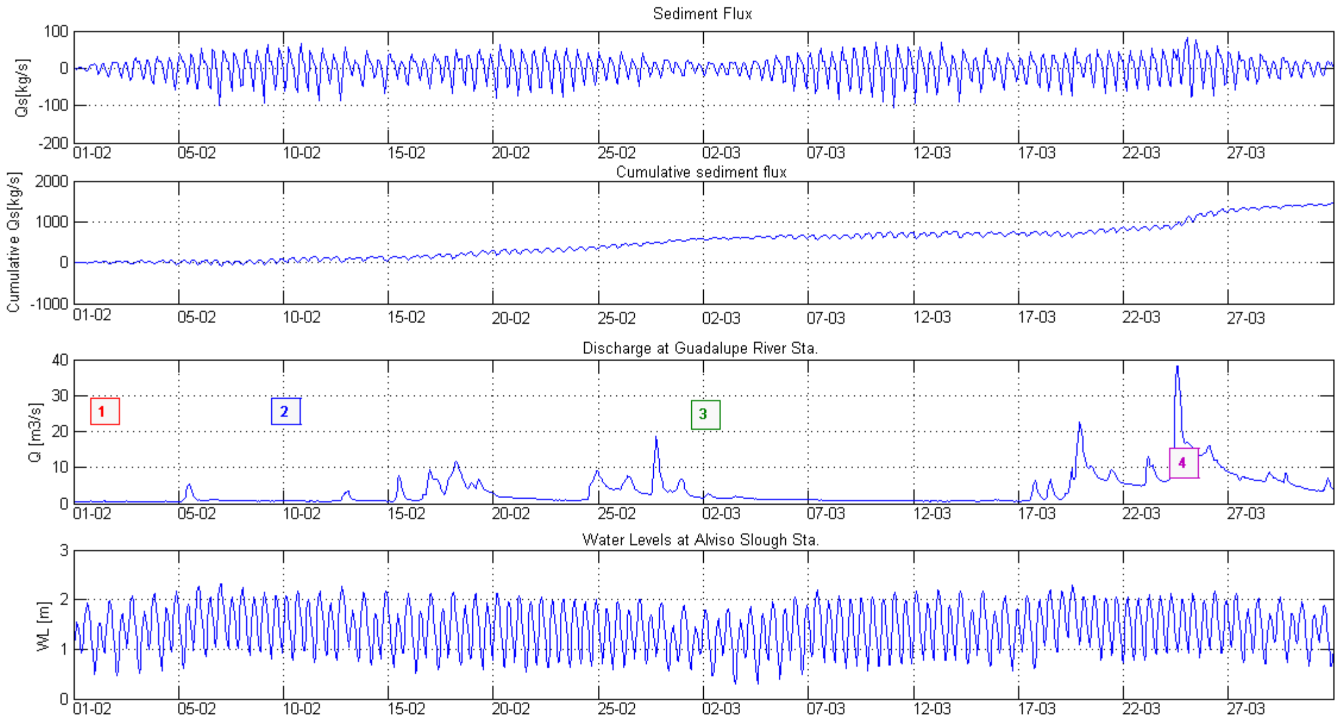

Figure 6-10 Sediment flux at Alviso Slough station - Scenario 3.

From the current scenario and further scenarios described in following chapters, the events were set up according with the most suitable time series, as follows:

1. Neap tidal cycle and low flow river discharge.
2. Spring tidal cycle and low flow river discharge.
3. Neap tidal cycle and high flow river discharge.
4. Spring tidal cycle and high flow river discharge.

Figure 6-10. shows at Alviso station it exports sediment not observed in scenario 2. It allows to identify sediment dynamic under the influences of tidal cycle, neap - spring. Moreover, during neap cycle the sediment transport is constant, while during the spring cycle the trend was slow rise, due to exporting sediments.

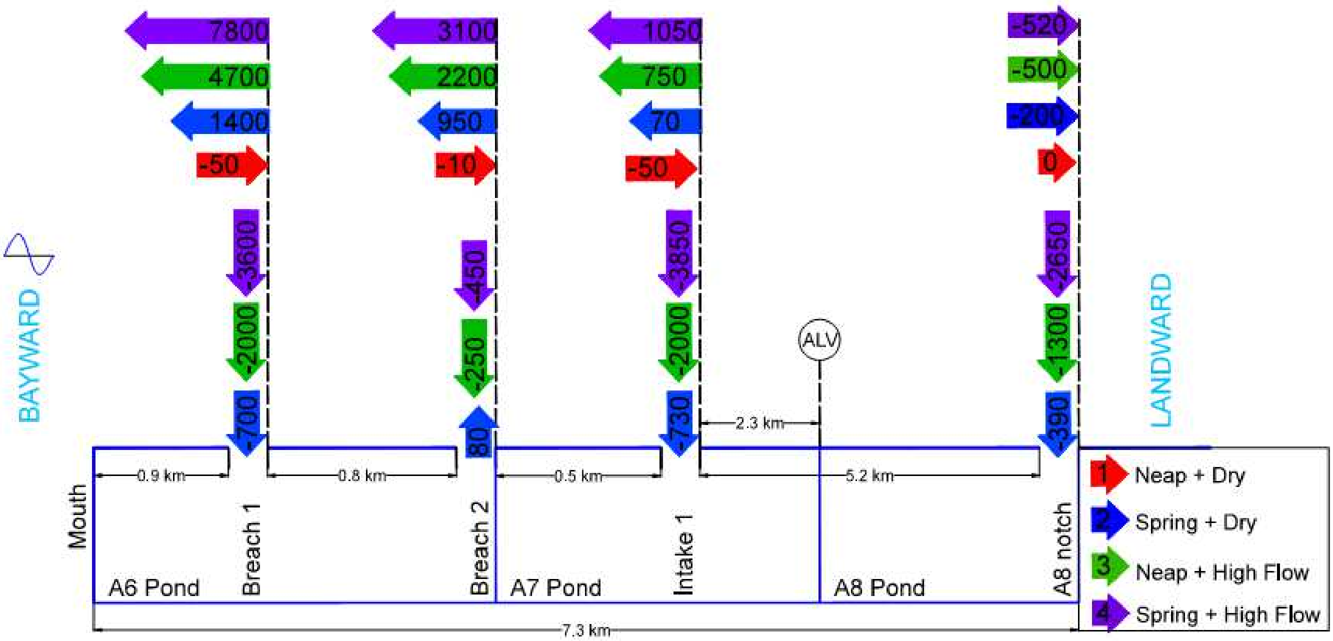

Figure 6-11. Cumulative sediment flux transport - Scenario 3. All values are in kilograms (kg) unless is defined.

During the dry periods both tidal cycles do not present high variability of sediment transport. The highest variation occurs during high river discharge, responsible for increasing the sediment flux, and specifically at neap tide near by the A8 notch. Over the simulated period, from the mouth until the intake, the tidal channel is exporting sediments. However, at the landward side the slough it is importing sediments. This means, that along the slough the sediment dynamics change from exporting to importing. Additionally, during all the events the sediment enters and deposits on the ponds. An exception took place, at breach 2 during lower discharge and spring tide.

From Figure 6-11 also can be determined the erosion patterns due to sediment trap. The highest erosion area occurred from intake 1 to breach 2. As well as, the reach between breaches 1 and 2, also presented and erosion pattern. In contrast, from intake to A8 notch it is not clear to identify, if there was erosion or sedimentation pattern, although there was change of the sediment transport due to shape, bathymetry and propagation of the tidal forcing and driven currents. As a complement to evaluate the sediment dynamic at Alviso Slough, the following figure provided another approached to evaluate it.

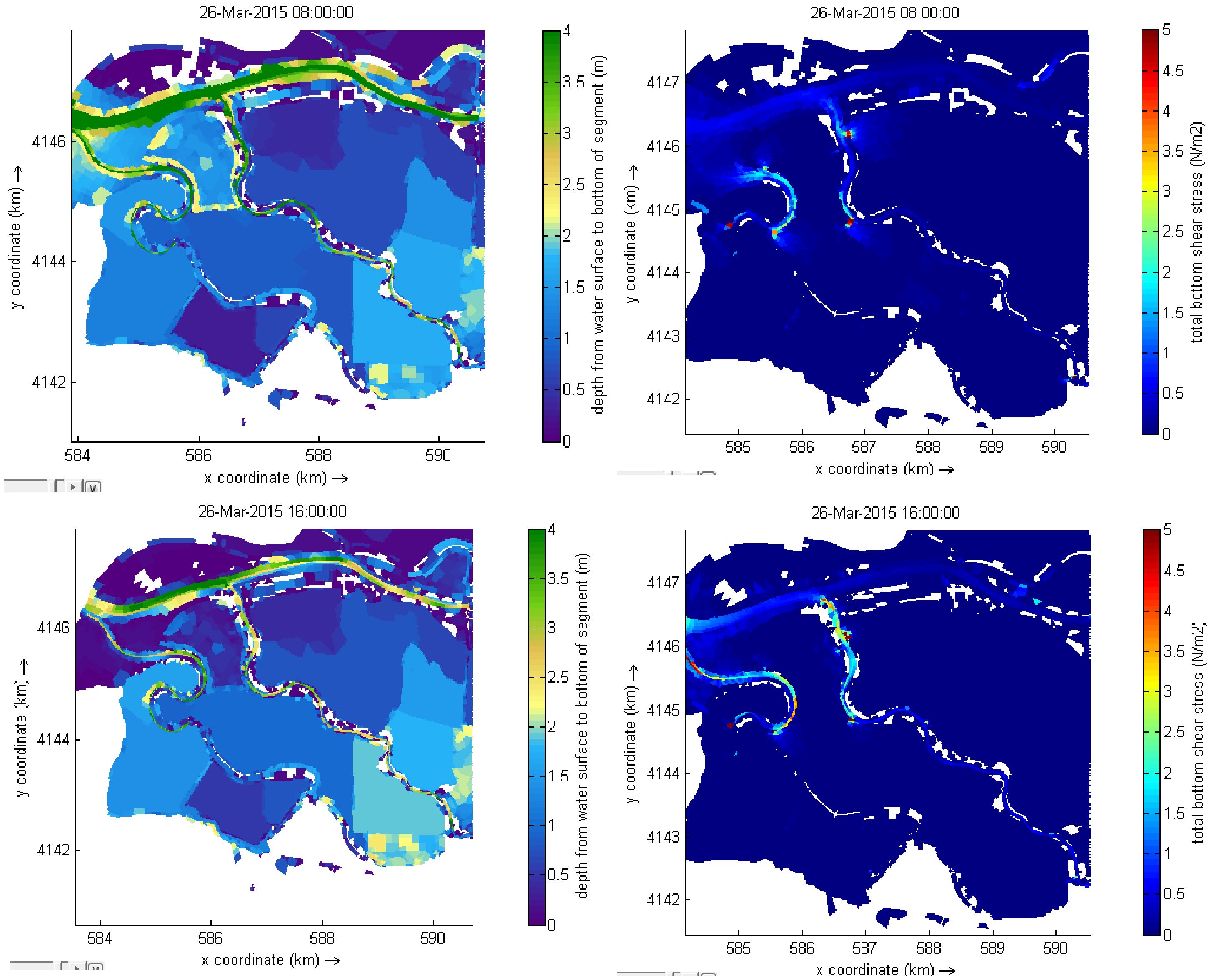

Figure 6-12 Total bottom shear stress during flood and ebb - Scenario 3. Water depth (left side, flood - top and ebb - bottom) and Total bottom shear stress (right side).

During flood and ebb the behaviour of the sediment dynamics at the water levels showed a variation in space and magnitude. Hence, it can be identified higher shear stress area. During flood the higher shear stress occurred at the breaches especially at breach 1 and also at the intake. During ebb occurred the higher dynamic, increasing the values along the seaward slough and nearby the openings.

The tidal channel in general it is deepening, although this pattern changes along the slough. In Figure 6-13 it can be observed these patterns. For the first 2 km (bayward to landward) higher erosion occurred when compared with the landward side from intake 1. In terms of deposition and remobilization of the sediment, the highest deposition took place at the pond especially at pond A6. The other ponds also presents a deposition patterns, like pond A8 nearby the notch. Where, it can be conclude from both, Figure 6-11 and Figure 6-13, that the material transported through the river during high peaks it is deposited at pond A8.

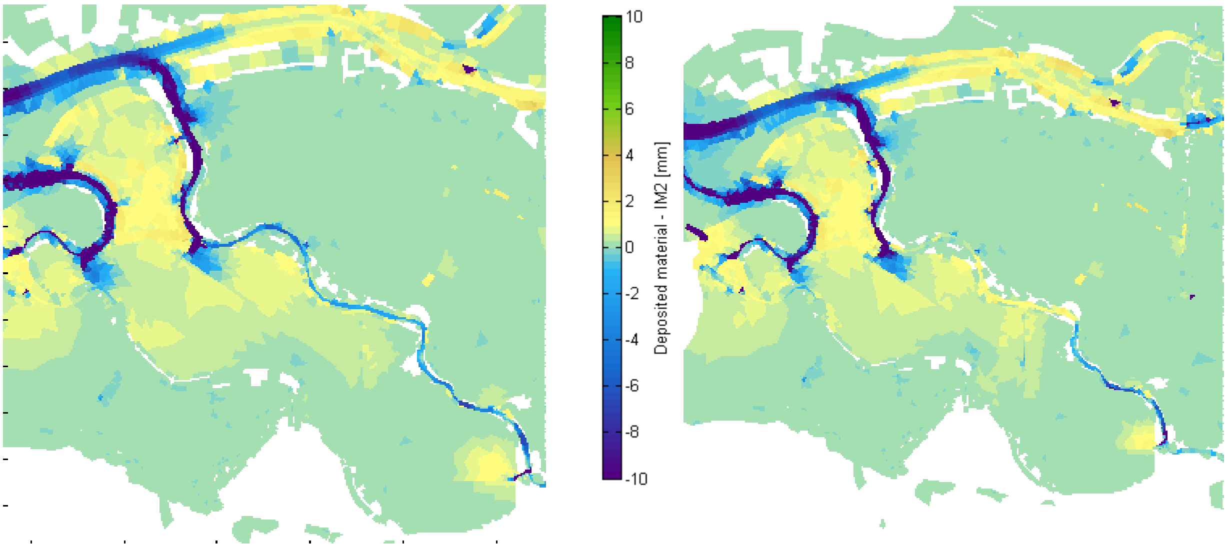

Figure 6-13. Erosion and deposition patterns - bed deposited material - Scenario 3 (left side) - Scenario 2 (right side).

Figure 6-13 also showed that erosion along the Slough is more predominant in this scenario compared with previous scenario, where the Slough had a small deposition pattern in the middle.

6.4. Scenario 4

This scenario is the same analyzed in third scenario. The difference is the opening at the A8 notch, in order to check the impact of the opening on the sediment dynamics.

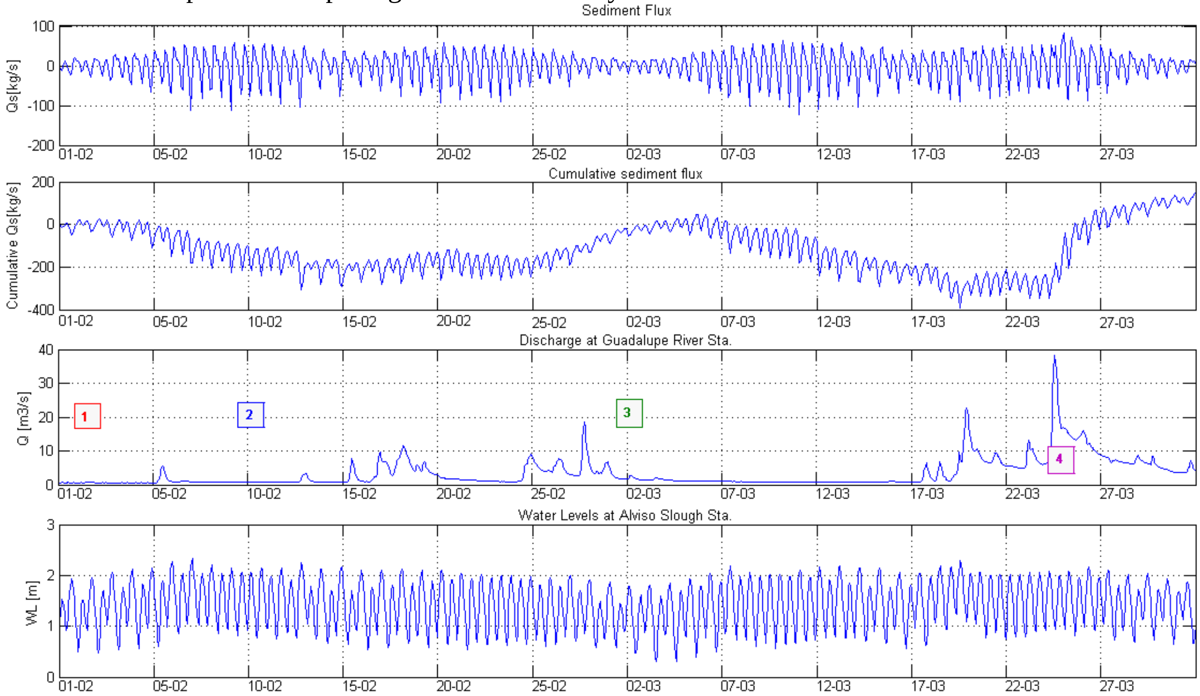

Figure 6-14 Sediment flux at Alviso Slough station - Scenario 4.

This scenario shows a slightly increasing of the sediment flux toward the pond, comparing with scenario 3. At A8 notch section, it was expected significance differences, but only a slight increasing of the sediments delivered to A8 pond took place.

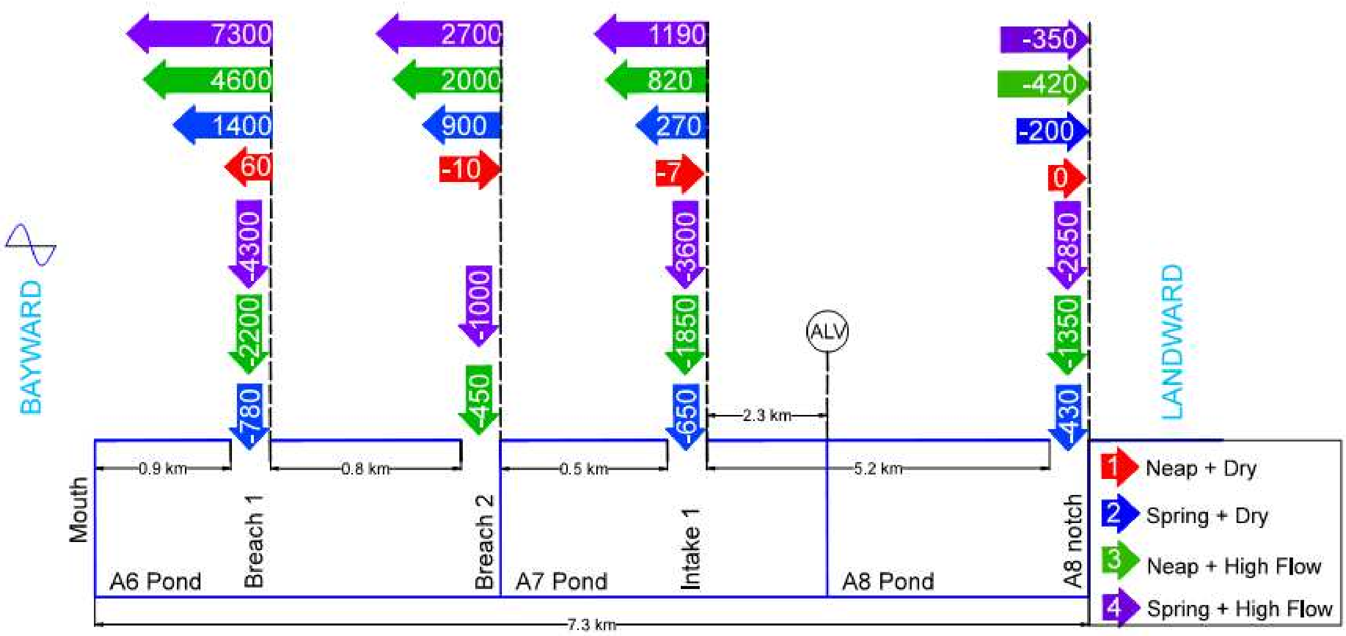

Figure 6-15. Cumulative sediment flux transport - Scenario 4. All values are in kilograms (kg) unless is defined.

Taking into account, the only difference between scenario 3and 4., it is the A8 notch width. The wider opening (current scenario) allowed more sediment through the pond A8, compared with narrow opened notch (scenario 3). Also, the patterns of sedimentation and erosion are similar, but with some changes along the slough. To get a better understanding Figure 6-16 provides additional information about the sediment transport.

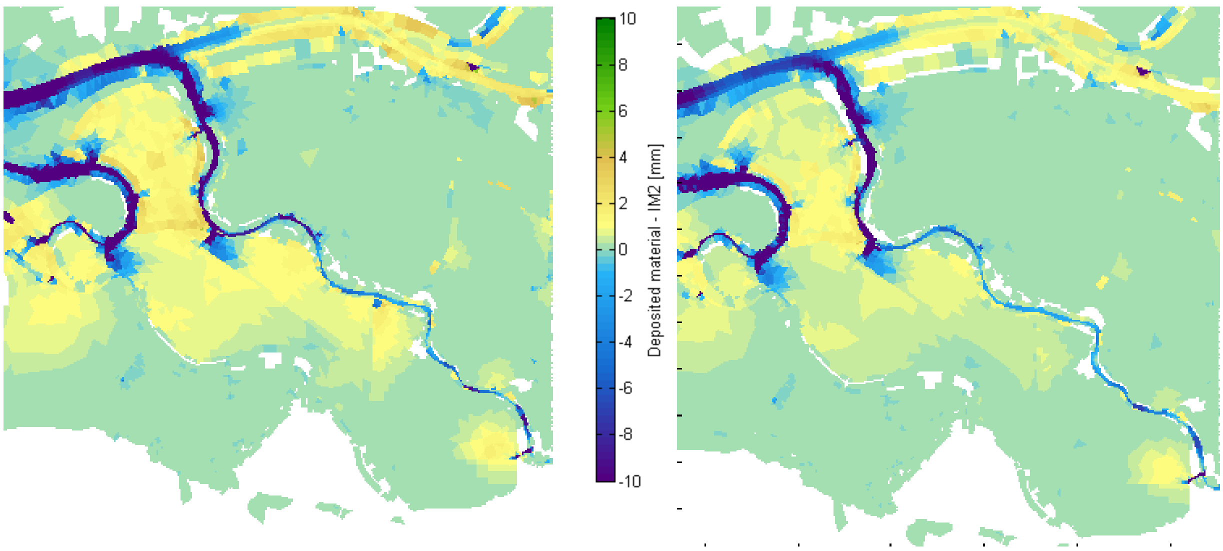

Figure 6-16. Erosion and deposition patterns - bed deposited material - Scenario 4 (left side) - Scenario 3 (right side).

Despite the similarity between the scenarios, the wider notch presents the following changes: 1. increasing the deposition into the ponds and tidal marshes, increasing erosion of the landward channel (From intake 1 to A8 notch), and same pattern of erosion at the breaches and intake.

The last three scenarios had shown a similarity trend, due to deposition at the ponds of Alviso Complex. Where, the A6 pond has the highest deposition in all the cases named, at the other ponds A5, A7 and A8, the influences of the A8 notch change the sediment dynamic into the ponds. A wider notch results in higher deposition at the pond and higher erosion at the slough.

6.5. Scenario 5

The final scenario has the same layout and conditions of the fourth scenario, but also including a hypothetical breach near the station at the north east side of the A8 pond (Figure 6-17).

Figure 6-17 Set up of scenario 5

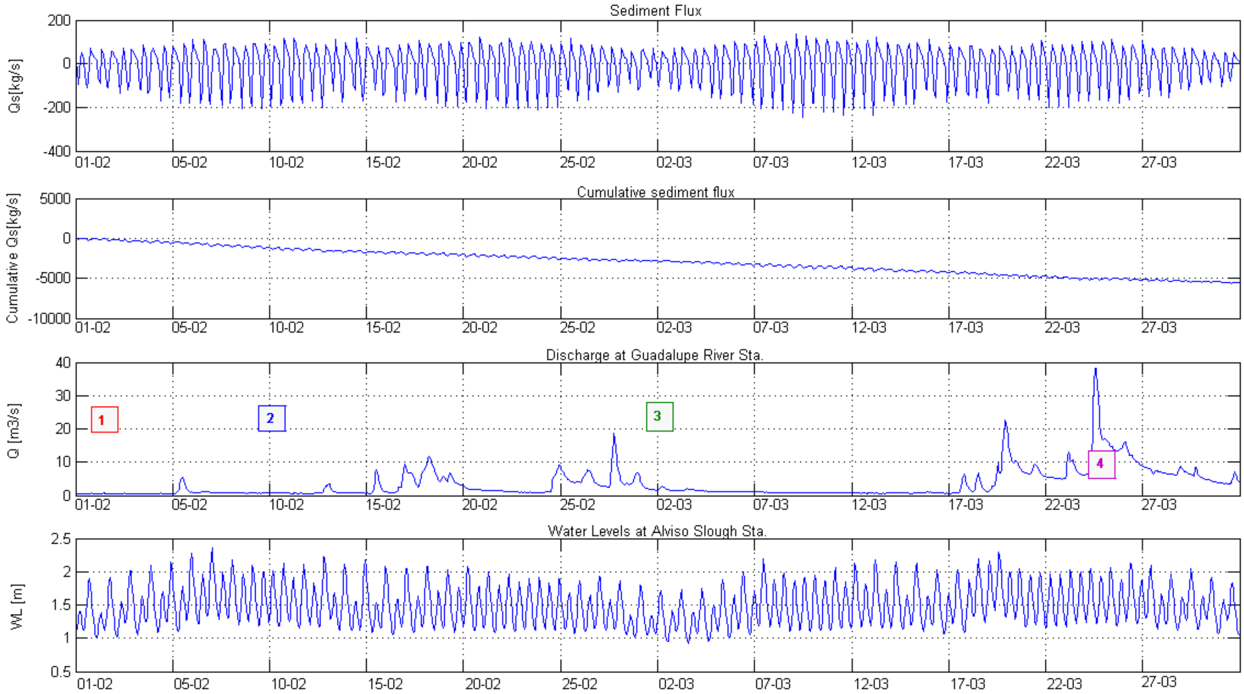

Figure 6-18. Sediment flux at Alviso Slough station - Scenario 5.

The fact of opening nearby the station might affect the sediment transport, and for instance the comparison with other scenarios. Nevertheless, it allows to forecast further impact at sediment dynamics of management operation at Alviso.

Figure 6-18 showed a slow fell of the cumulative sediment flux, due to importing sediment towards upstream. The influence of both discharge and tidal cycle cannot be clearly determined. To get a better understanding of the sediment transport of this scenario, the following figures provided additional information.

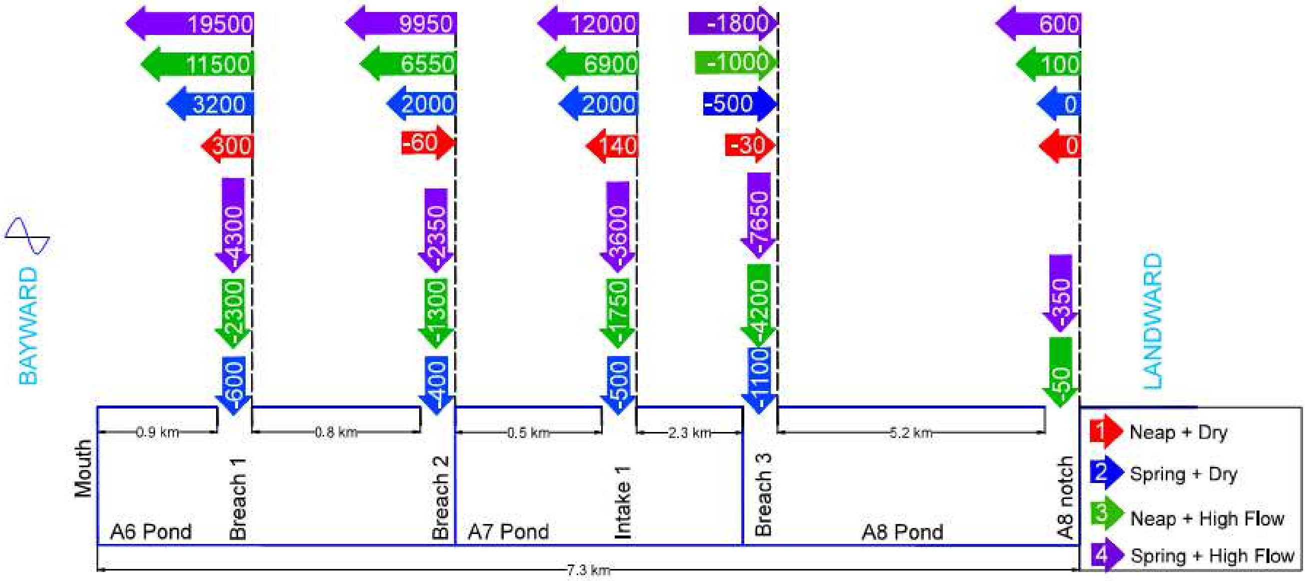

Figure 6-19. Cumulative sediment flux direction - Scenario 5. All values are in kilograms (kg) unless is defined.

Figure 6-19 shows a dramatic increase of sediment transport and sediment flux in almost all the events. This increase was even huge (Around 2 times than scenario 3 and 4) at the seaward side of the slough, comparing with other sections. Also, in terms of trend of sediment track along the slough, from the new breach towards the bay the slough was exporting sediments and increasing of erosion at the bottom took place. In contrast, the other side of the channel had opposite behaviour importing sediment towards upstream. The amount of sediment delivery into the pond is much bigger compared with other breaches and intake.

Despite the A8 notch had a wider opening there was not much sediment dynamic either at the pond or the slough. To clarify these analysis additional figures were done, as follows:

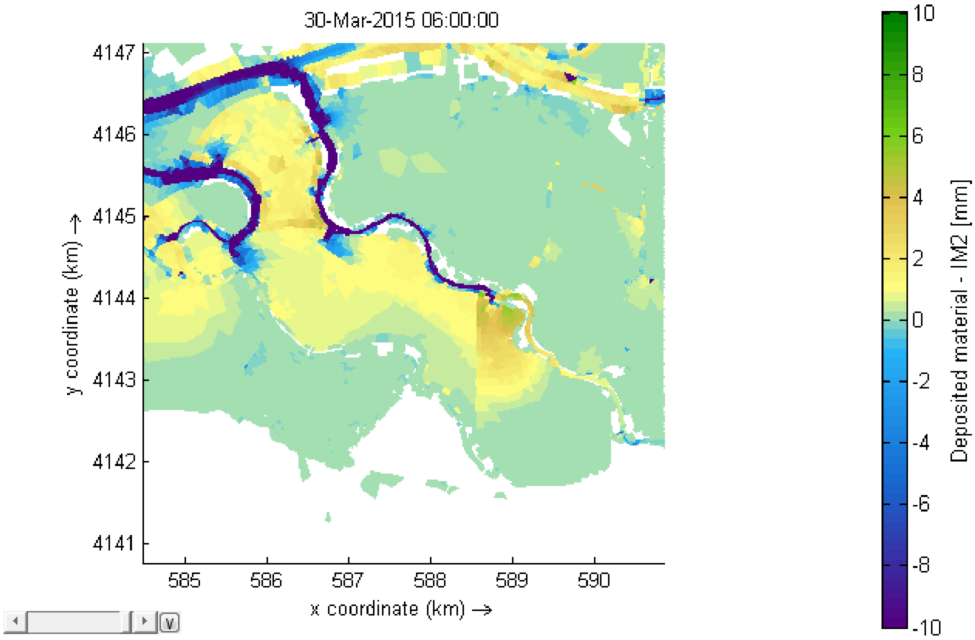

Figure 6-20. Erosion and deposition patterns - bed deposited material - Scenario 5.

Further ponds openings will changed the hydrodynamic and sediment transport of the complex. Figure 6-20 confirmed the huge delivery of the sediments into A8 pond at the new breach and shows the deposition pattern upstream the new breach. The patterns of deposition into the ponds increase slightly, however the erosion in slough increase compared with other scenarios.

6.6. Overall results

The scenario analysis show the sediment dynamic before and after the salt pond restoration took place at 2010. The Slough behaviour was described based on the most important events to sediment dynamic.
Figure 6-21 aims to highlight the most important analysis by compared net flux over the period simulated of each scenario along the Slough.

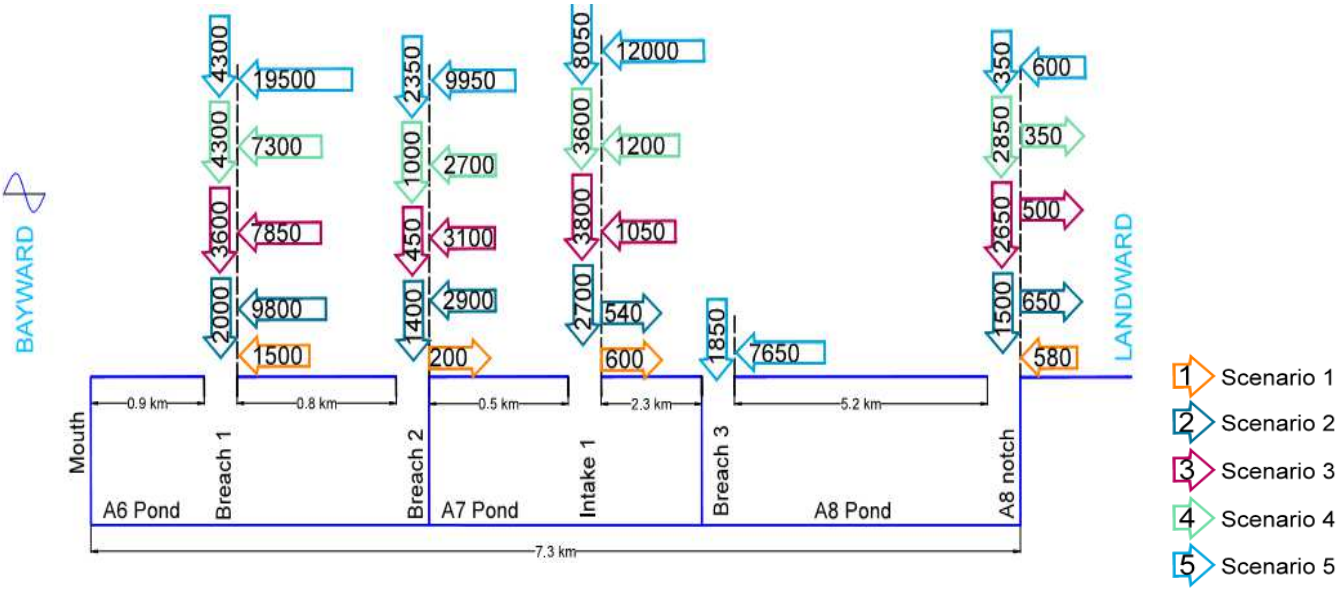

Figure 6-21. Overall net flux for all scenarios. All values are in kilograms (kg) unless is defined.

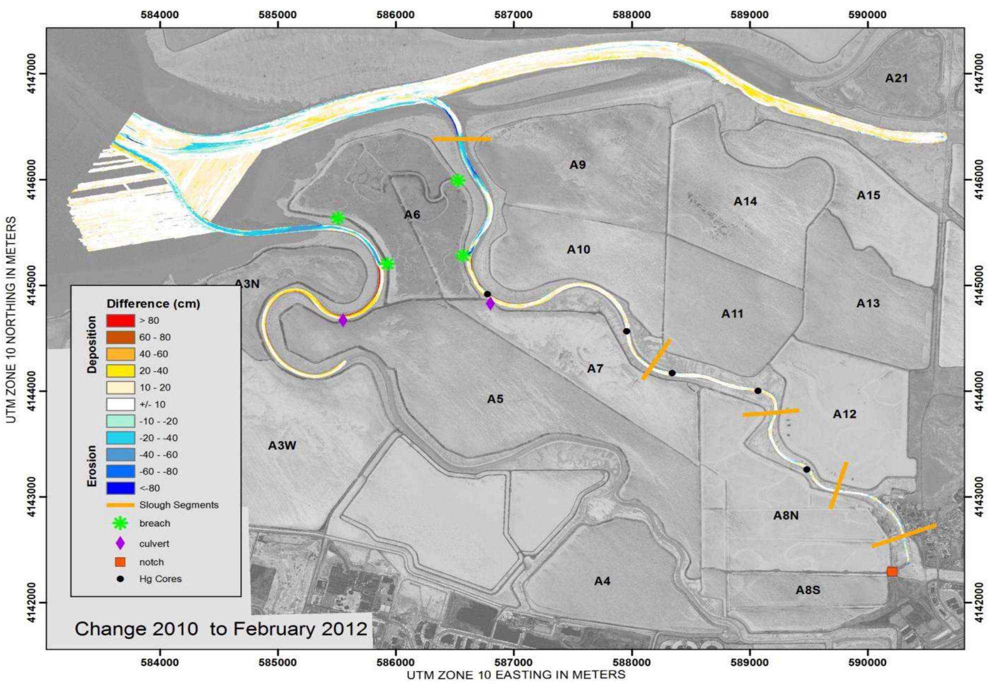

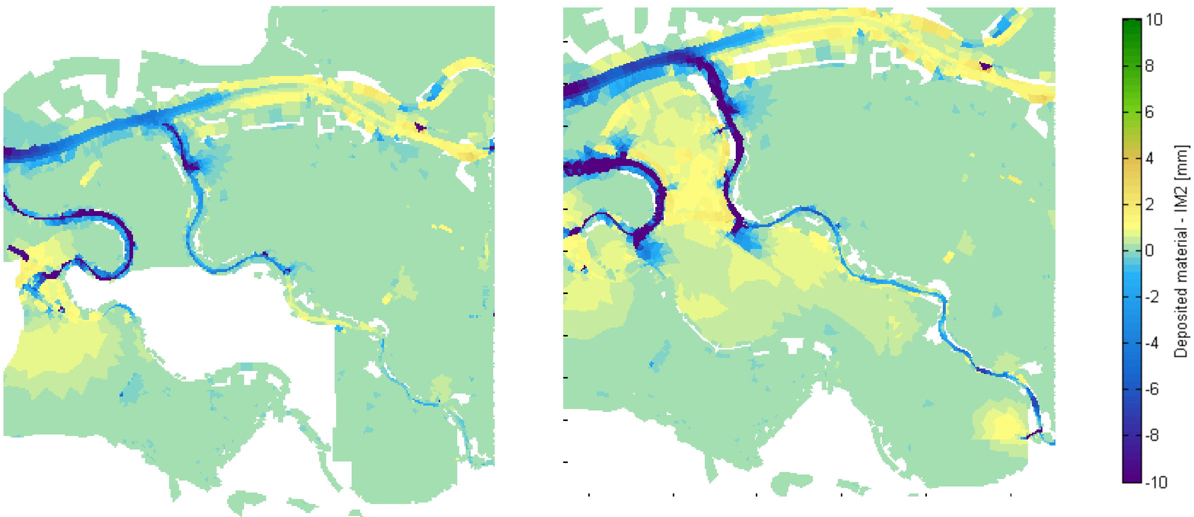

Figure 6-22. Differences of bathymetry 2010 to 2012 by Foxgrover, (2014) (top) and Erosion and deposition patterns - bed deposited material - Scenario 3 (left side) - Scenario 2 (right side) - (bottom)

Figure 6-21 and Figure 6-22 allows to determine the evolution of the sediment transport along the slough and the pond surround it, under different scenarios. As a result the following points describe this final analysis.

- Before the opening (scenario 1) the sediment dynamic along the Alviso Slough had a differential trend in terms of exported or imported sediment.
- The sand pond openings change the sediment transport of the area. It increases the sediment flux and the erosion in the slough allowing a sediment delivery deposition into the ponds.
- For all the scenarios with open ponds acts as sediment sink, most of the sediment transported and remobilized slough ends up in the ponds.
- In general, the most active stretch of the slough was the seaward side of the channel (between breach 2 and mouth), and it is the area which most suffer with erosion. Where, the highest values occurred at scenario 5 and follow by scenario 2, scenario 3 and finally scenario 4. The erosion at this reach of the slough impact the bathymetry as indicate the anomaly of bathymetry between 2010 and 2012 at this region the difference was about 60 cm (Figure 6-22).
- Scenarios 3 and 4 showed that a wider opening in A8 pond only increases the import of sediment by 10 to 20 percentages.
- The impact of the restoration management had developed a rapidly changed into the slough. Thus, It has shaped the slough, deepening the channel and remobilizing sediment, and most of it deposits upon the ponds.
- The events that most influences the sediment dynamics are spring tides and the combination of high runoff during neap tide.
- Finally, all those analysis has a clear influence with the mobilization of contaminated sediments. Therefore, if the sediment is transported from the source and bed composition, so contaminated sediment is transported too.

CHAPTER 7

CONCLUSION AND RECOMMENDATIONS

Firstly, the major impact due to sediment transport dynamics in Alviso Slough took place with the salt pond opening for wetland restoration. This impact increases the sediment transport along the Slough in direction and magnitude (around 6 times). The pond opening enhances the slough erosion which deposits in the pond. Moreover, it was found that any opening that connects the pond with the slough, it will may affect the whole system both hydrodynamic and sediment transport. Generating a rapidly impact that caused change in the sediment dynamics of the area.

Besides, the ponds are the areas with major deposition after the opening. However, the deposition pattern changed from pond to pond. A6 is the pond with major deposition, followed by A7, A5 and finally A8.

Due to the relationship of mercury remobilization and Alviso scouring, there is a clear pattern of erosion of the slough, directly related with the remobilization of the bed material. The bed sediment is a mixture of contaminated with no contaminated sediment, so erosion of the Slough allow to remobilized and transported contaminated sediment.

About the influences of A8 notch opening in the sediment dynamic in Alviso complex, it has been proved, that there is not importance influence due to entering of sediments through the pond A8. However, as wider the notch increases the sediments deposition upon the ponds around 20 percent, and also increases the erosion at the Slough border (bayward and landward side) around 5 percent. Moreover, at A8 we saw that the notch width does not plays a major role in sediment import through the A8 pond.

Finally, the numerical model developed provided an excellent tool to evaluate the hydrodynamic and sediment transport in the area. The model was calibrated and validated and it might be used to further scenarios and forecast. The numerical model also provides a complete overview of the area comparing with other studies approaches based on measurements in specific points at the Alviso Slough.

The recommendations of this research are:

- It is recommended to enhance the numerical model calibrated and validated with an updated bathymetry. In order hindcast future managements operations and identify the impacts.
- Development of a morphodynamic model. That will provided a great input in terms of bed level change at Alviso Slough but also the evolution of the wetland restoration.

References

Board CRWQC (2009) ORDER R2-2009-0061 - NPDES PERMIT NO. CA0037621.

Bricker J (2003) Bed drag coefficient variability under wind waves in a tidal estuary: field measurements and numerical modeling. PhD Thesis, Stanford University

Callaway JC, Parker VT, Schile LM, Herbert ER, Borgnis EL (2009) Dynamics of sediment accumulation in pond A21 at the island ponds. California State Coastal Conservancy.

Deltares (2011) Delft3D- WAQ, User Manual.

Deltares (2014) D-Flow Flexible Mesh.

Doody JP (2004) 'Coastal squeeze' - An historical perspective. J Coast Conserv 10: 129-138

Eertman RHM, Kornman BA, Stikvoort E, Verbeek H (2002) Restoration of the sieperda tidal marsh in the Scheldt estuary, The Netherlands. Restor Ecol 10: 438-449 DOI 10.1046/j.1526-100X.2002.01034.x

Foxgrover AC, Finlayson DP, Jaffe BE, Fregoso TA (2014) Bathymetry and Digital Elevation Models of Coyote Creek and Alviso Slough, South San Francisco Bay, California U.S. Department of the Interior U.S. Geological Survey.

Foxgrover BJA (2007) Sediment Deposition and Erosion in South San Francisco Bay,California from 1956 to 2005.

G. Arcement J, and V. Schneider (1989) Guide for Selecting Manning's Roughness Coefficients for Natural Channels and Flood Plains. United States Geological Survey Water-Supply Paper 2339

Ganju NK, D.H. Schoellhamer, M.C. Murrell, J.W. Gartner and S.A. Wright (2011) Constancy of the relation between floc size and density in San Francisco Bay

Gregory G. Shellenbarger MAD-KaDHS (2014) Suspended sedument dynamics in the tidal reach of a San Francisco Bay Triburary. Paper presented at the Proceeding of the 17th Physics of Estuaries and Coastal Seas (PECS) conference2014

H. T. Harvey & Associates, Philip Williams and Associates, Associates M, Staff of San Francisco Bay Conservation and Development Commision (1982) Guidelines for Enhancement and Restoration of Diked Historic Baylands Technical Report prepared for the San Francisco Bay Conservation and Development Commission, April 1982, pp. 100 plus appendices.

Inagaki S (2000) Effects of proposed San Francisco Airport runway extension on hydrodynamics and sediment transport in South San Francisco Bay. Engineers Thesis, Stanford University

Jaffe B, Foxgrover A (2006) A History of Intertidal Flat Area in South San Francisco Bay,California: 1858 to 2005 U.S. Department of the Interior, U.S. Geological Survey, pp. 32.

Jolliff K, Kindle John C , Shulman Igor, Penta Bradley, Friedrichs Marjorie A. M, A. R (2009) Summary diagrams for coupled hydrodynamic-ecosystem model skill assessment. Journal of Marine Systems 76: 64-82 DOI http://dx.doi.org/10.1016/j.jmarsys.2008.05.014

Josh Ackerman MM-D, Darrell Slotton, Mark Herzog, and Collin Eagles Smith. (2010) The Effects of Wetland Restoration on Mercury Bioaccumulation in the South Bay Salt Pond Restoration Project: Using the Biosentinel Toolbos to Monitor Changes Across Multiple Habitats and Spatial Scales Resources Legacy Fund, State Coastal Conservancy, South Bay Ponds Restoration Program.

Josh T. Ackeman MM-D, Darell Slotton, Collin A. Eagles-Smith, Mark P. Herzog, Alex Hartman, Jennifer L. Agree and haun Ayres (2013) The South Bay Mercury Project: Using Biosentinels to Monitor Effects of Wetland Restoration for the South Bay Salt Pond Restoration Project U.S. Department of the Interior U.S. Geological Survey.

Korschgen CE, Dahlgren, R. B. (1992) Human disturbances of waterfowl: causes, effects, and management U.S. Fish and Wildlife Service, pp. 1-8.

Krone RB (1962) Flume studies of the transport of sediment in estuarial shoaling processes UC Berkeley, Berkeley, CA.

Life Science (2003) South Bay Salt Ponds Initial Stewardship Plan Prepared for U.S. Fish and Wildlife Service and California Department of Fish and Game.

MacBroom JG (2000) Tidal marsh restorationOceans 2000 IEEE, Piscataway, NJ, United States Providence, RI, USA, pp. 1925-1928.

Manning AJ, Schoellhamer DH (2013) Factors controlling floc settling velocity along a longitudinal estuarine transect. Marine Geology 345: 266-280 DOI http://dx.doi.org/10.1016/j.margeo.2013.06.018

Marvin-DiPasquale M, Cox MH (2007) Legacy Mercury in Alviso Slough, South San Francisco Bay, California: Concentration, Speciation and Mobility U.S. Department on the Interior U.S. Geological Survey.

McDonald E, Cheng R (1996) A numerical model of sediment transport applied to San Francisco Bay, CA. Journal of Marine Environmental Engineering 4: 1-41

Moffatt & Nichol Engineers (2005b) Hydrodynamic modeling tools and techniques, South Bay Salt Pond Restoration Project California State Coastal Conservancy.

Montalto FA, Steenhuis TS (2004) The link between hydrology and restoration of tidal marshes in the New York/New Jersey Estuary. Wetlands 24: 414-425

Partheniades E (1962) A study of erosion and deposition of cohesive soils in salt water. University of California

Philip Williams & Associates L (2005) Hydrodynamics and Sediment Dynamics, Existing Conditions Report California State Coastal Conservancy U.S. Fish & Wildlife Service California Department of Fish and Game.

Reynolds CS (1984) The ecology of freshwater phytoplankton Cambridge University Press

Rijn LCv (2007) Unified View of Sediment Transport by Currents and Waves. I: Initiation of Motion, Bed Roughness, and Bed-Load Transport

Scherrer P (2006) Le Havre – Port 2000: a move towards the environmental restoration of the Seine Estuary: Part 1

Shellenbarger GG, Schoellhamer DH, Lionberger MA (2004) A South San Francisco Bay Sediment Budget: Wetland Restoration and Potential Effects on Phytoplankton BloomsASLO-TOS 2004 Ocean Research Conference.

Stenzel LE, Hickey CM, Kjelmyr JE, Page G (2002) Abundance and distribution of shorebirds in the San Francisco Bay area. Western Birds 33: 69-98

Uncles RJ, Peterson DH (1995) A computer model of long-term salinity in San Francisco Bay: sensitivity to mixing and inflows. Environmental International 21: 647-656

Walters RA (1982) Low-Frequency Variations in Sea Level and Currents in South San Francisco Bay. Journal of Physical Oceanography 12: p658-668

Williams P, Faber PM (2004) Design guidelines for tidal wetland restoration in San Francisco bay Prepared for The Bay Institu.

Yang Z, Wang T (2012) Hydrodynamic modeling analysis of tidal wetland restoration in Snohomish River, Washington12th International Conference on Estuarine and Coastal Modeling 2011, St. Augustine, FL, pp. 139-155.

Appendices

Appendix A D-FLOW - FM detailed set up and remarks

Network

This methodology was based on the manual of D Flow (Deltares, 2014).The advantage of use D Flow unstructured mesh is the capacity to generate a mesh adaptable to complex geometry environment system, such as this area of study.

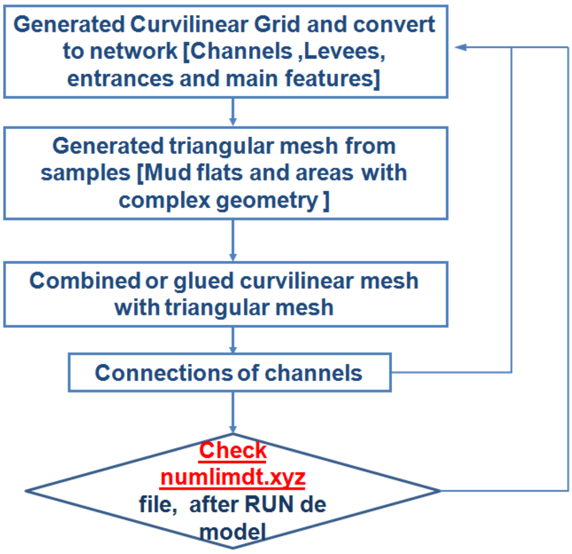

Figure 7-1 Network methodology diagram

The following steps are a detailed explanation of the diagram above:

1.1. At the area of importance, such as, channel (this case tidal channels), levees or dikes, and entrance tributary flows, create a rectangular grid.

1.2. To create a rectangular grid: from splines follow the bathymetry and shape of the feature (channel or levee) create a network with the splines.

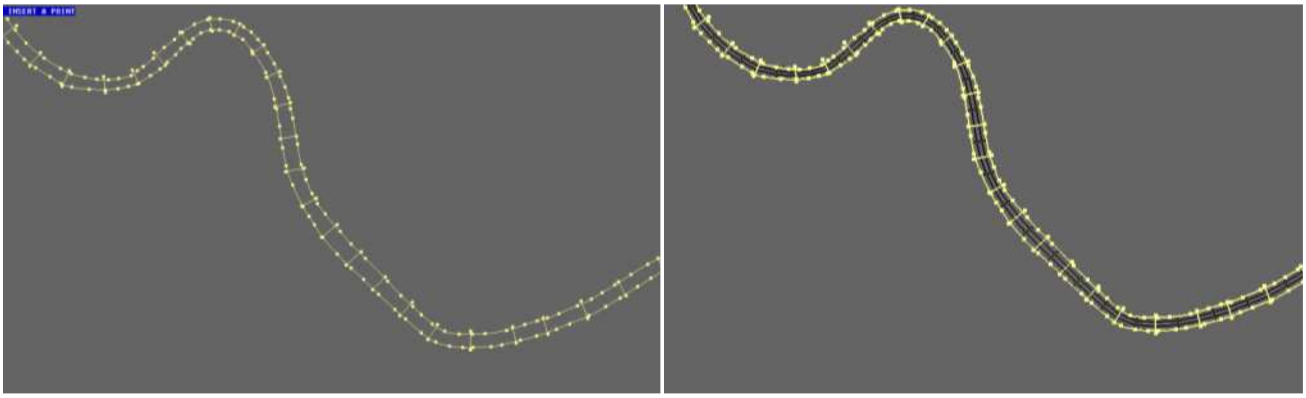

Figure 7-2 Generation of curvilinear grid form splines.

Remark or Advice: In the case of the main channel defined a grid with at least 3 cells per width. For other cases like tributary flows, generate at least 2 cells per width between levees or bank to bank.

1.3. Once the rectangular grid is generated, convert it to a network and checking the orthogonality. Remember that as defined a rectangular mesh you will have a detailed and better approach. That is the reason to define these features first, to get a good quality mesh at this area (Tidal channel and levees)

Remark or Advice: It is recommended at the moment of checking and improving the orthogonality, the values should be start from 0.90, then 0.93, till 0.99. Until have good quality orthogonality mesh error around of 0.5%.

1.4. With this networks generated, the empty area in between (for instance, levees and channel) can be glued together, by a triangular mesh. To generate this triangular mesh, it is recommended to do it by patches, according with the geometry or shape complexity of the area. First, insert the polygon of the area to fill up, you can either to create samples in polygon or do it manually. It is recommended do it manually to have more control of your mesh. Then glued the network and checked the orthogonality of the triangular mesh. At the moment of checked this area, tried to do not affect the orthogonality of area around it

1.5.

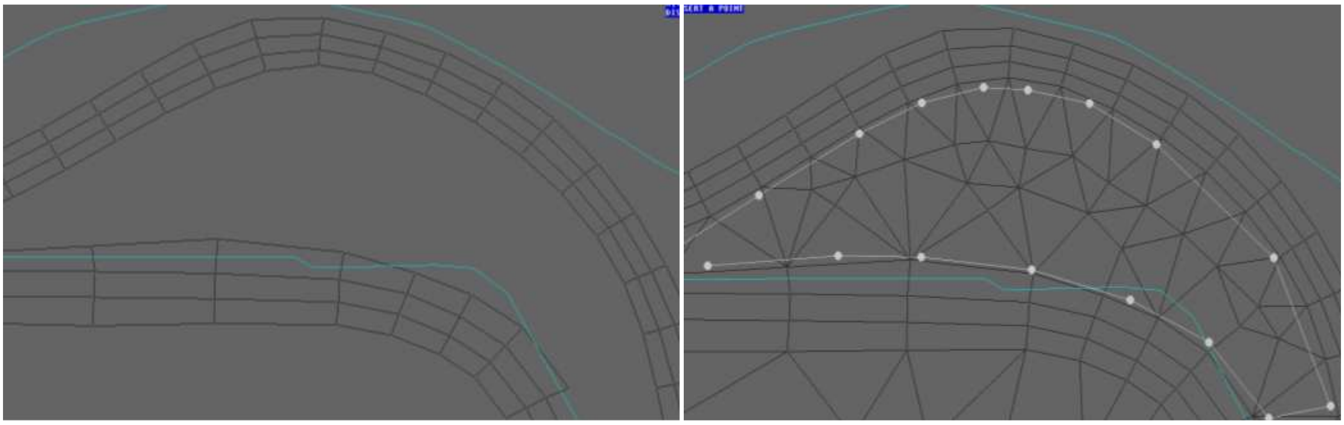

Figure 7-3 Generation of triangular mesh from samples in polygon

1.6. The last part, to have an accurate mesh, it is to generate the connections, like tributary flows with main channels or gates. Be sure that these connections are generated by rectangular grid, using all editing networks tools and of course the orthogonality.

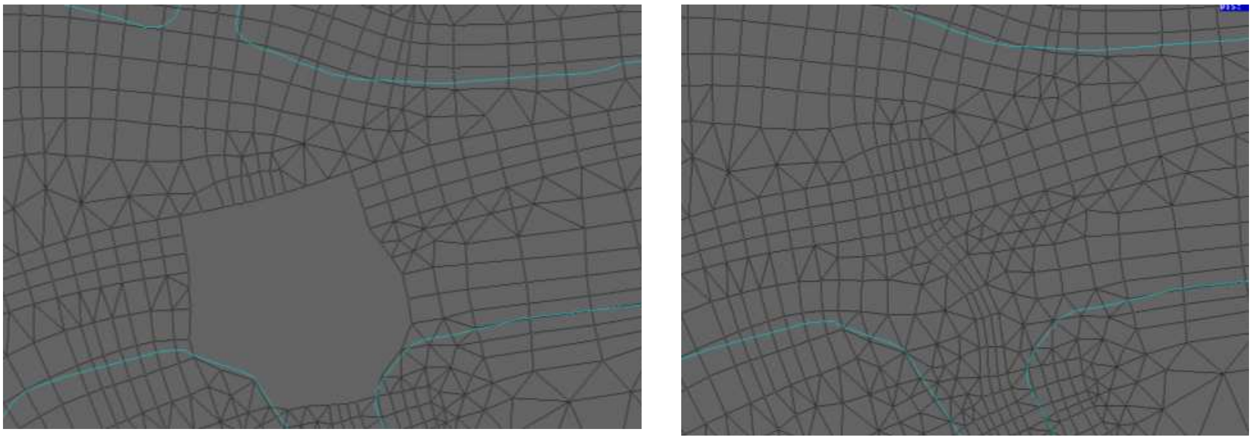

Figure 7-4 Connections of main features.

The mesh generated for the study area has accomplished as follows: At the seaward side downwards Dumbarton bridge, at the landward side or upstream at the northern side of San Jose California.

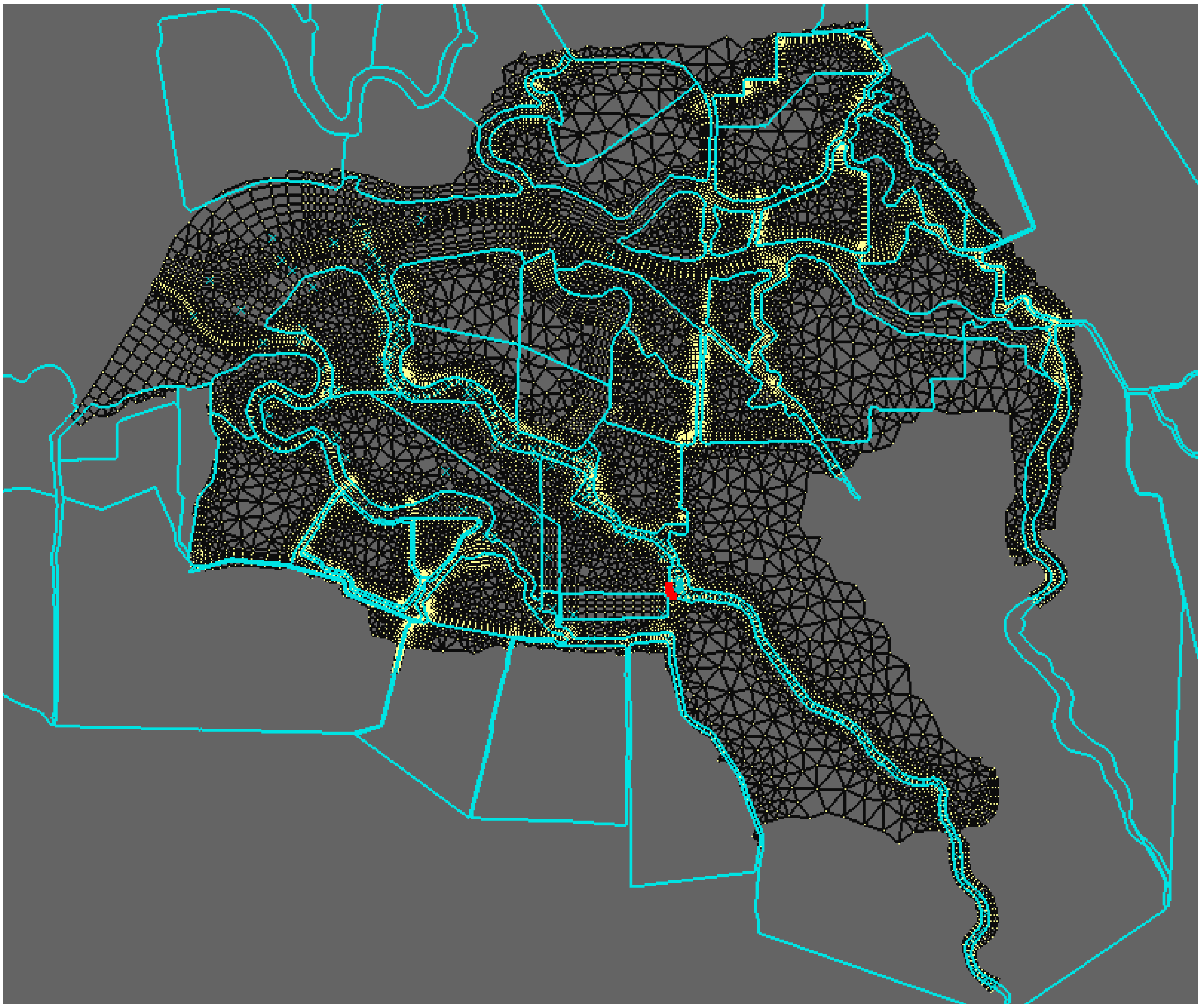

Figure 7-5 Unstructured mesh of Alviso Complex

Finally, make a run of the model and check the "numldt.xyz" file, in which you can find the cell where it generates the major interpolation, and for instance the errors of the mesh due to orthogonality and multiple connections. Improving those cells connections, enhanced the model to do a better performance.

Bathymetry

Create or generate the interpolation between the network and the samples (*.xyz file) from the bathymetry run the model for a considerable time and check the bathymetry. It is recommended to not flowing cells or spots and features like, bridges, gates and others.

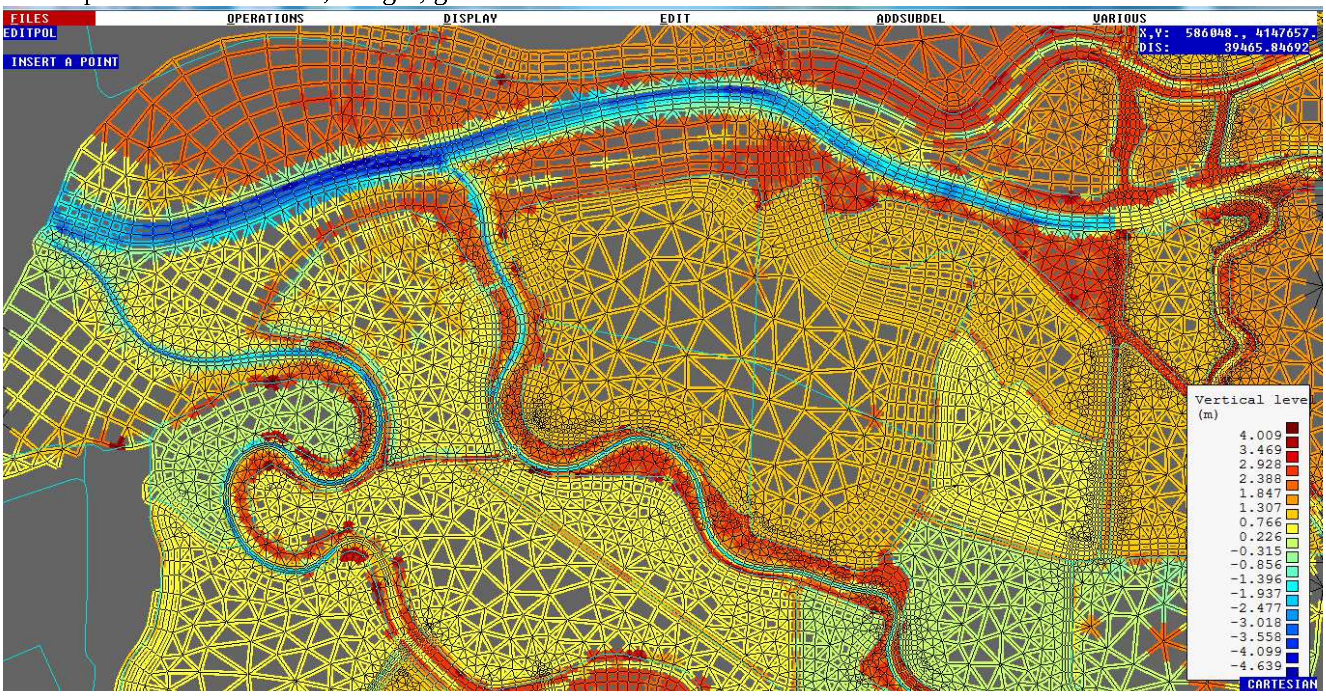

Figure 7-6 Interpolated network with bathymetry.

Master definition Unstruc (MDU)

The Master Definition Unstructured file (MDU-file) is the input of D-Flow FM that contains all the parameters and data required to define the model and the running simulation. (Deltares, 2014). This file will determine the conditions and needs of the model. Although, it defines if the simulation it will be run by 2D or 3D model.

The following table provided an overview of the scheme used for a 3D model, most of the values assign in this table were used it.

Table 7-1 3D model MDU file.

Parameter	Value or File	Observation
NetFile	alviso_net.nc	*_net.nc
BathymetryFile		*.xyb
ThinDamFile	1_thd.pli	# *_thd.pli, Polyline(s) for tracing thin dams
FixedWeirFile	SBlevees_tdk.pli	# *_fxw.pliz, Polyline(s) x,y,z, z = fixed weir top levels (formerly

		fixed weir)
WaterLevIni	Variable	# Initial water level
Conveyance2D	3	-1:R=HU,0:R=H, 1:R=A/P, 2:K=analytic-1D conv, 3:K=analytic-2D conv
Kmx	10	# Max nr of vertical layers
CFLMax	0.7	# Max. Courant nr.
AdvecType	3	# Adv type, 0=no, 1= Wenneker, qu-udzt, 2=1, q(uio-u), 3=Perot q(uio-u), 4=Perot q(ui-u), 5=Perot q(ui-u) without itself
TimeStepType	2	# 0=only transport, 1=transport + velocity update, 2=full implicit step_reduce, 3=step_jacobi, 4=explicit
Limtypmom	4	# Limiter type for cell center advection velocity, 0=no, 1=minmod,2=vanLeer,3=Kooren,4=Monotone Central
Limtypsa	4	# Limiter type for salinity transport, 0=no,1=minmod,2=vanLeer,3=Kooren,4=Monotone Central
Vertadvtypsal	6	# Vertical advection type for salinity, 0=No, 1=UpwexpL, 2=Centralexpl, 3=UpwimpL, 4=CentraLimpL, 5=4 but 3 for neg. stratif., 6=higher order expl, no forester
Icgsolver	4	# Solver type , 1 = sobekGS_OMP, 2 = sobekGS_OMPthreadsafe, 3 = sobekGS, 4 = sobekGS + Saadilud, 5 = parallel/global Saad, 6 = parallel/Petsc, 7 = parallel/GS
FixedWeirScheme	6	# 0 = no, 1 = compact stencil, 2 = whole tile lifted, full subgrid weir + factor
FixedWeirContraction	1	# flow width = flow width*FixedWeirContraction
UnifFrictCoef	3.d-2	# Uniform friction coefficient, 0=no friction
UnifFrictType	1	# 0=Chezy, 1=Manning, 2=White Colebrook, 3=idem, WAQUA style
Vicouv	1	# Uniform horizontal eddy viscosity (m2/s)
Dicouv	1	# Uniform horizontal eddy diffusivity (m2/s)
Vicoww	5.d-5	# Uniform vertical eddy viscosity (m2/s)
Dicoww	5.d-5	# Uniform vertical eddy diffusivity (m2/s)
Rhomean	1000	# Average water density (kg/m3)
Ag	9.81	# Gravitational acceleration
TidalForcing	1	# Tidal forcing (0=no, 1=yes) (only for jsferic == 1)
Salinity	1	# Include salinity, (0=no, 1=yes)
InitialSalinity	15	# Inital salinity concentration (ppt)
Temperature	1	# Include temperature, (0=no, 1=only transport, 5=heat flux model (5) of D3D), 3=excess model of D3D
InitialTemperature	10	# Inital temperature (degC)
RefDate	Variable	# Reference date (yyyymmdd)
Tzone	0	# Data Sources in GMT are interrogated with time in minutes since refdat-Tzone*60
Tunit	S	# Time units in MDU (H, M or S)
DtUser	80	# User timestep in seconds (interval for external forcing update & his/map output)

DtMax	30	# Max timestep in seconds
DtInit	1	# Initial timestep in seconds
AutoTimestep	5	# Use CFL timestep limiter or not (1/0)
TStart	Variable	# Start time w.r.t. RefDate (in TUnit)
TStop	Variable	# Stop time w.r.t. RefDate (in TUnit)
RestartFile		# Restart file, only from netcdf-file, hence: either *_rst.nc or *_map.nc
RestartDateTime		= yyyymmdd_HHMMSS # Restart time (YYYYMMDDHHMMSS), only relevant in case of restart from *_map.nc
ExtForceFile	alvisocomplex.ext	# *.ext
ObsFile	OBS_obs.xyn	# *.xyn Coords+name of observation stations
CrsFile	sections_crs.pli	# *_crs.pli Polyline(s) definining cross section(s)
HisInterval	3600	# History output, given as "interval" "start period" "end period" (s)
MapInterval	86400	# Map file output, given as "interval" "start period" "end period" (s)
MapFormat	1	# Map file format, 1: netCDF, 2: Tecplot, 3: netCFD and Tecplot
RstInterval	Variable	# Restart file output, given as "interval" "start period" "end period" (s)
WaqInterval	3600	# Interval (Reynolds) between Delwaq file outputs

Appendix B Sediment transport calibration figures

The first comparison was 2D model against 3D model; it showed a bad performance of the 2D model, comparing with 3D model

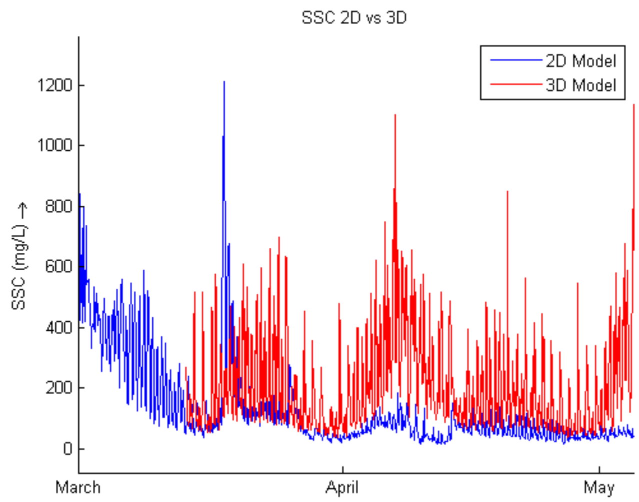

Figure 7-7 Suspended solids sediments of 2D model and 3D model.

The output of sensitivity model performance are:

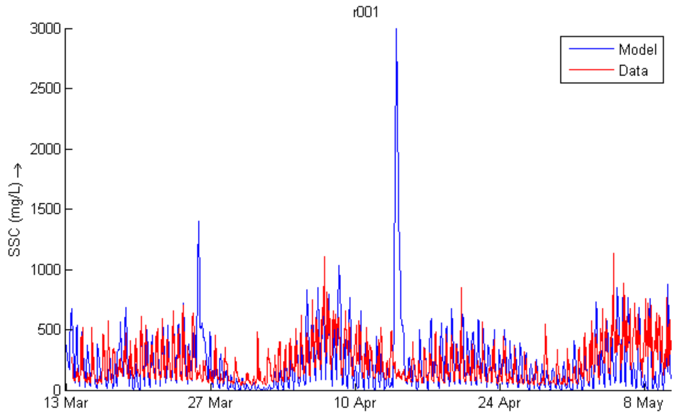
r001
Model
Data
SSC (mg/L) →
3000
2500
2000
1500
1000
500
0
13 Mar
27 Mar
10 Apr
24 Apr
8 May

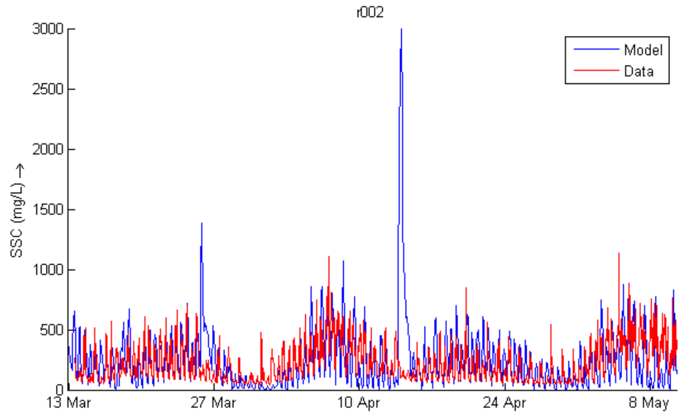
r002
Model
Data
SSC (mg/L) →
3000
2500
2000
1500
1000
500
0
13 Mar
27 Mar
10 Apr
24 Apr
8 May

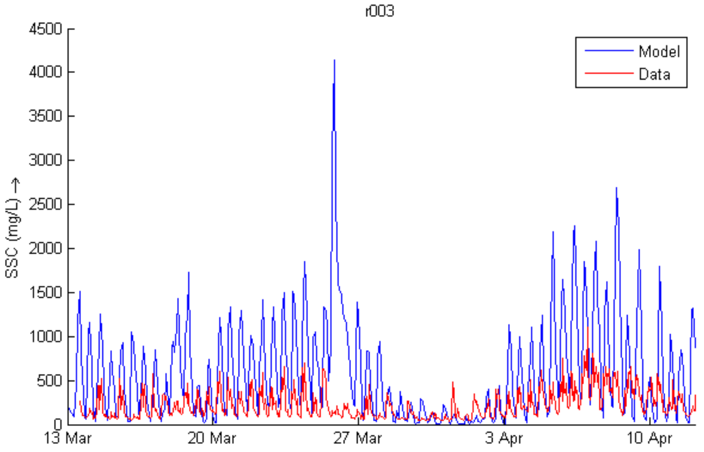
r003
Model
Data
SSC (mg/L) →
4500
4000
3500
3000
2500
2000
1500
1000
500
0
13 Mar
20 Mar
27 Mar
3 Apr
10 Apr

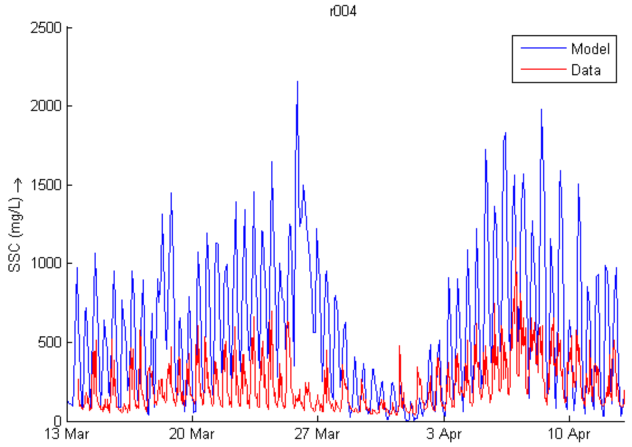
r004
Model
Data
SSC (mg/L) →
2500
2000
1500
1000
500
0
13 Mar
20 Mar
27 Mar
3 Apr
10 Apr

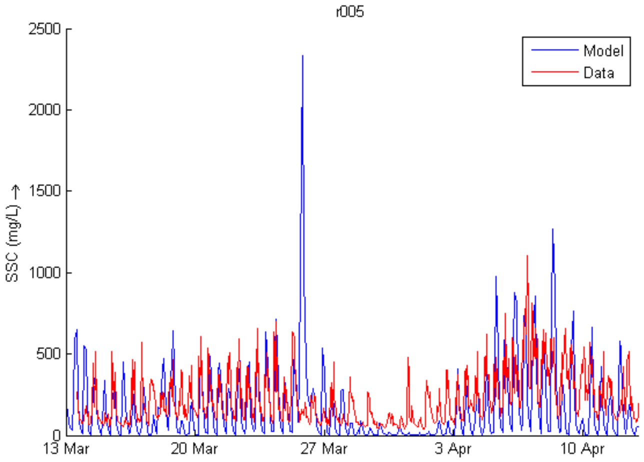
r005
Model
Data
SSC (mg/L) →
2500
2000
1500
1000
500
0
13 Mar
20 Mar
27 Mar
3 Apr
10 Apr

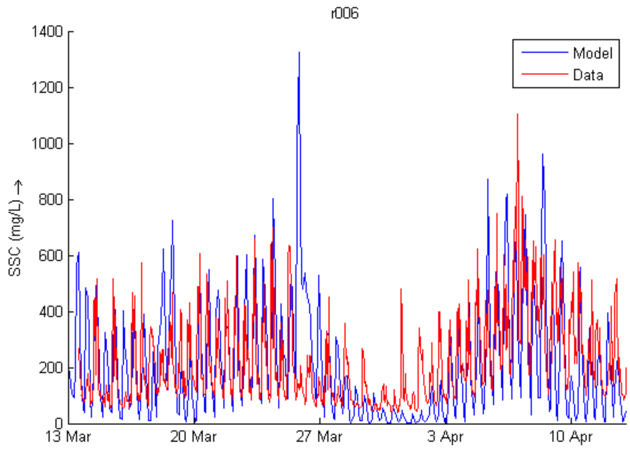
r006
Model
Data
SSC (mg/L) →
1400
1200
1000
800
600
400
200
0
13 Mar
20 Mar
27 Mar
3 Apr
10 Apr

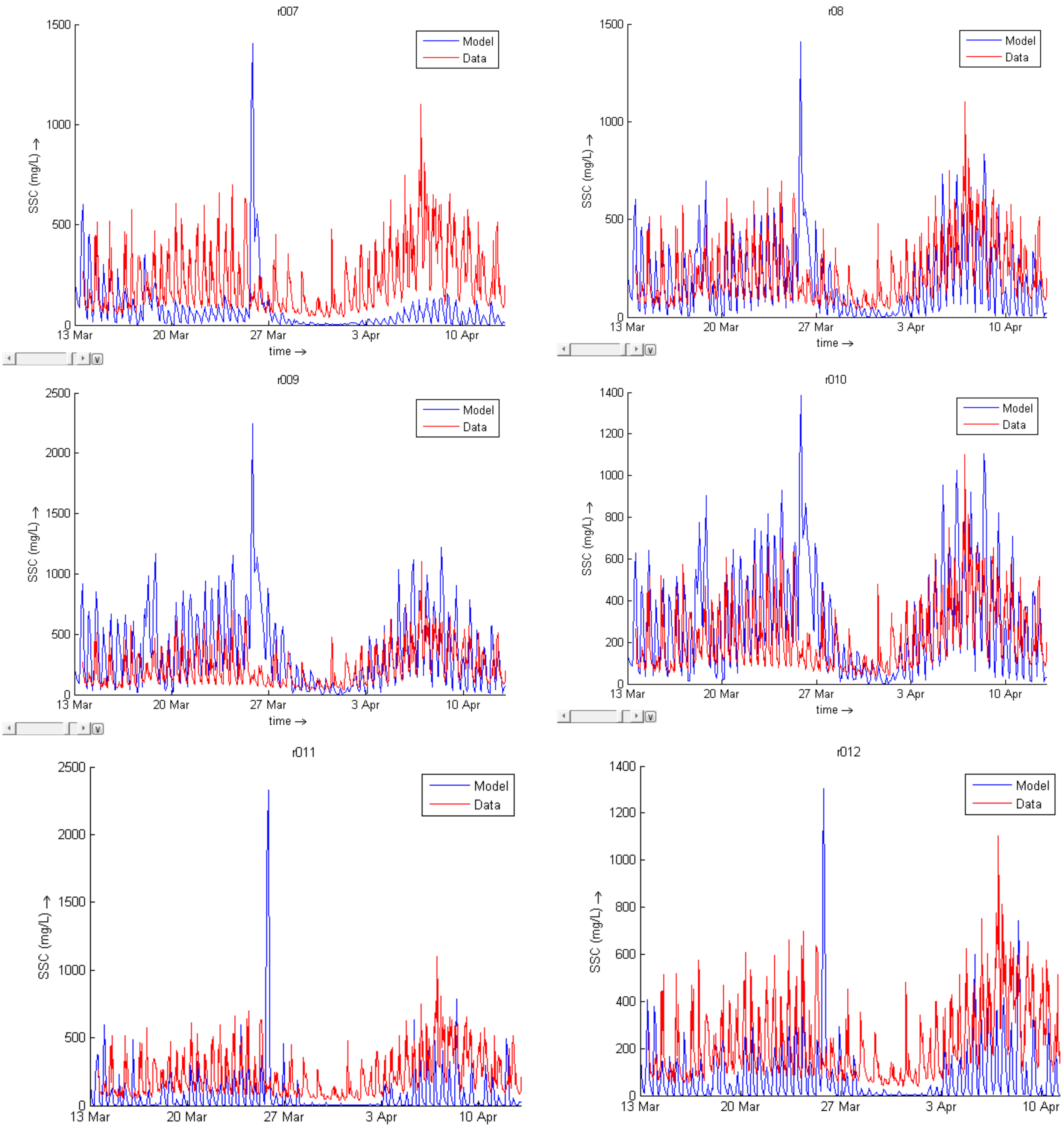

Figure 7-8 Suspended solids concentration, Model vs Data at Alviso Slough Sta.

Appendix C Cumulative Sediment flux Scenarios

The figure bellow sketch Alviso Slough shown the sections along the channel. This sketch provided a general overview of all the figures that is presented in this appendix. Taking into account, that this figures are the result of the sediment direction sketch in Scenario evaluation chapter:

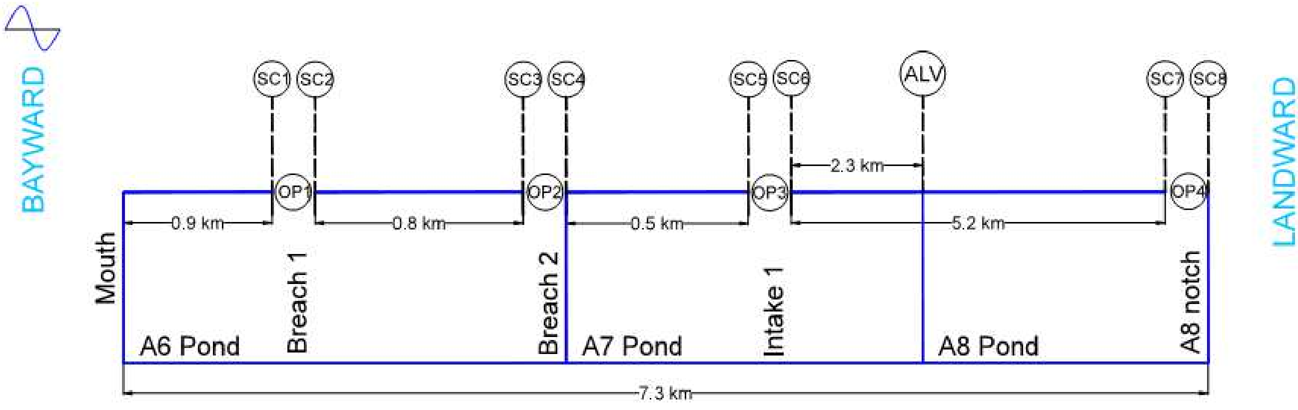

Figure 7-9 Alviso Slough sketch and sections location.

Scenario 1

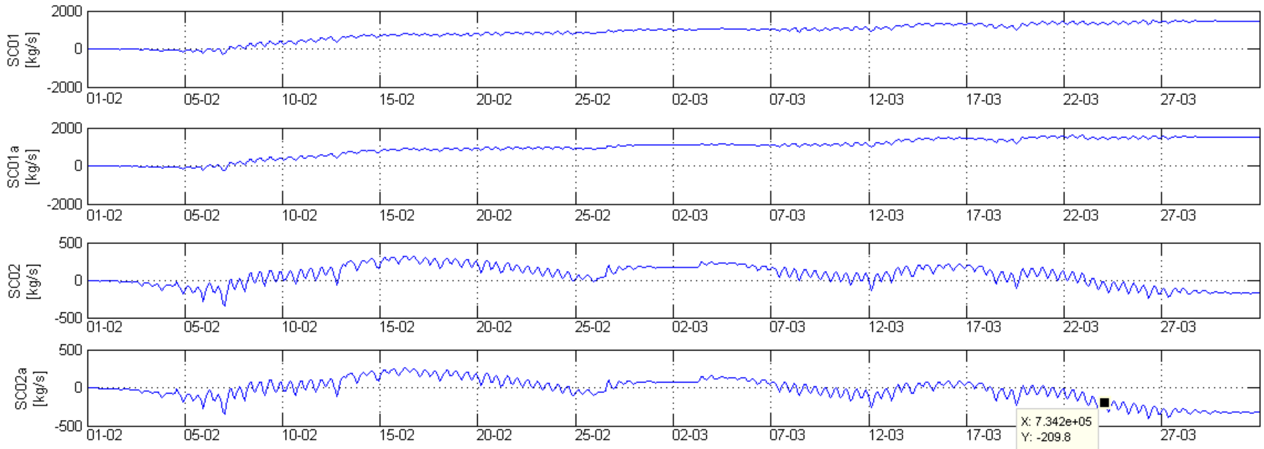

Figure 7-10 Cumulative time series flux - Scenario 1 - Sec 01 to Sec 02a

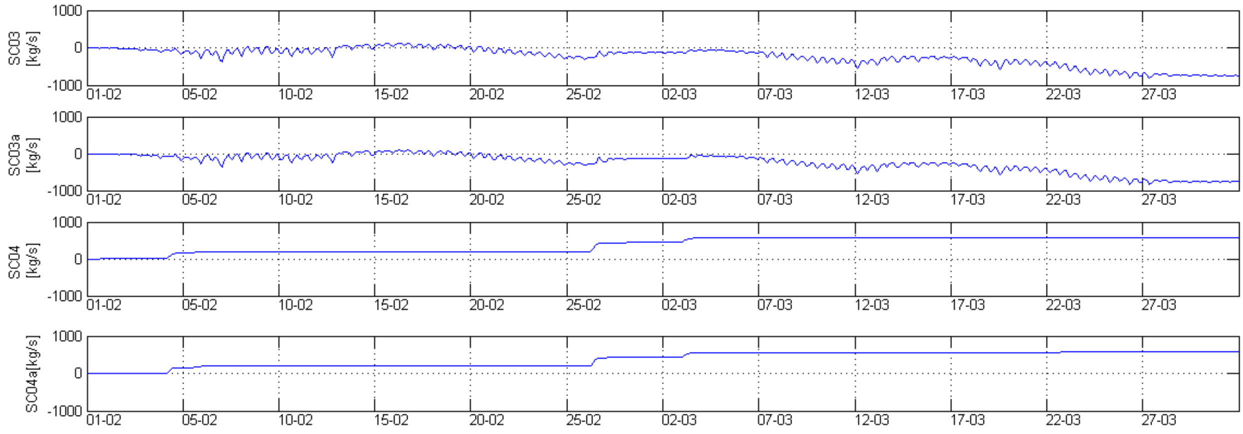

Figure 7-11 Cumulative time series flux - Scenario 2- Sec 03 to Sec 04a

Scenario 2

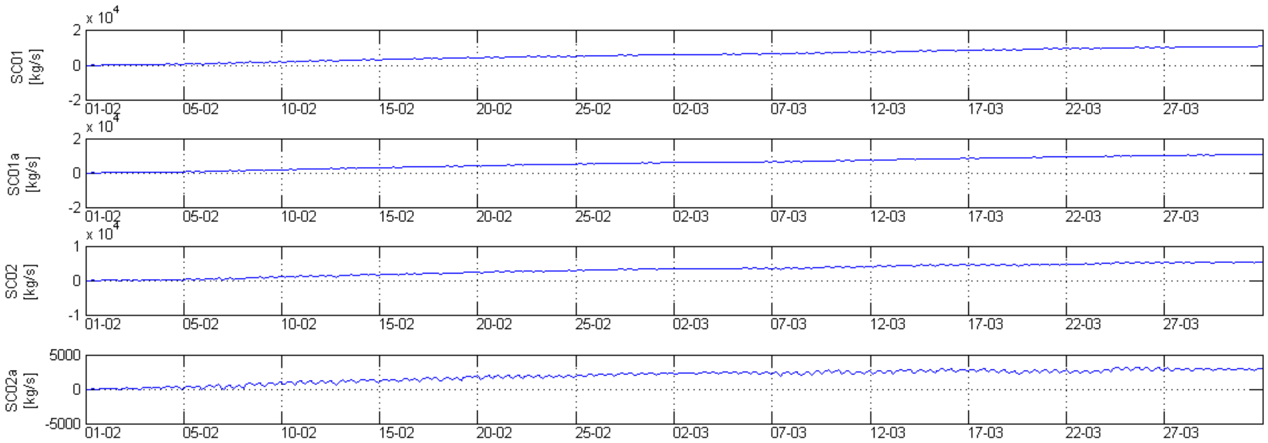

Figure 7-12 Cumulative time series flux - Scenario 2 - Sec 01 to Sec 02a

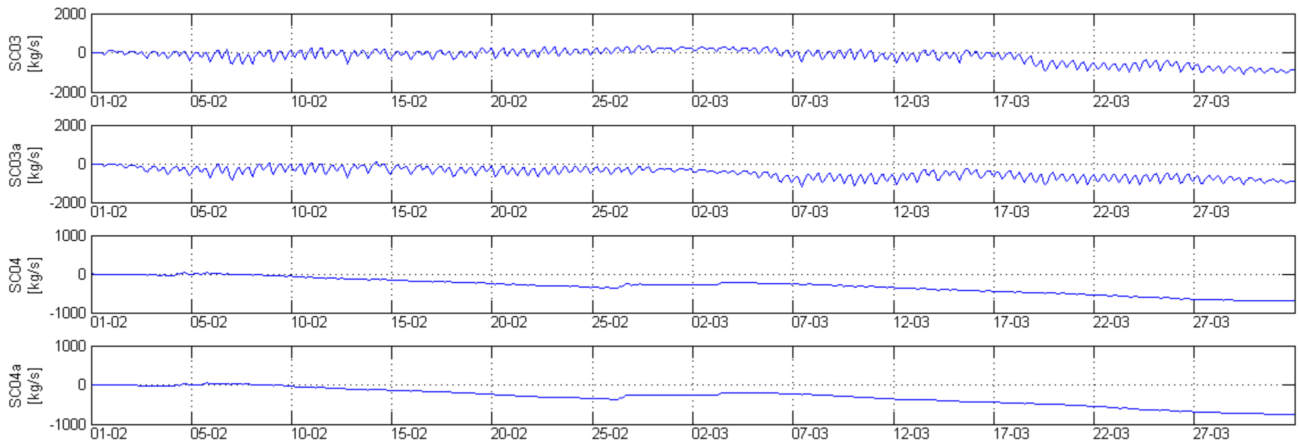

Figure 7-13 Cumulative time series flux - Scenario 2 - Sec 03 to Sec 04a

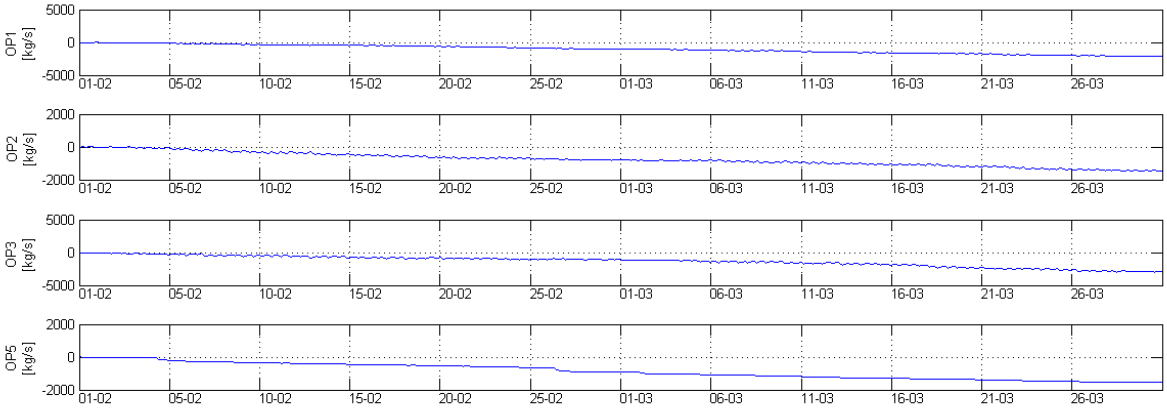

Figure 7-14 Cumulative time series flux - Scenario 2 - Openings

Scenario 3

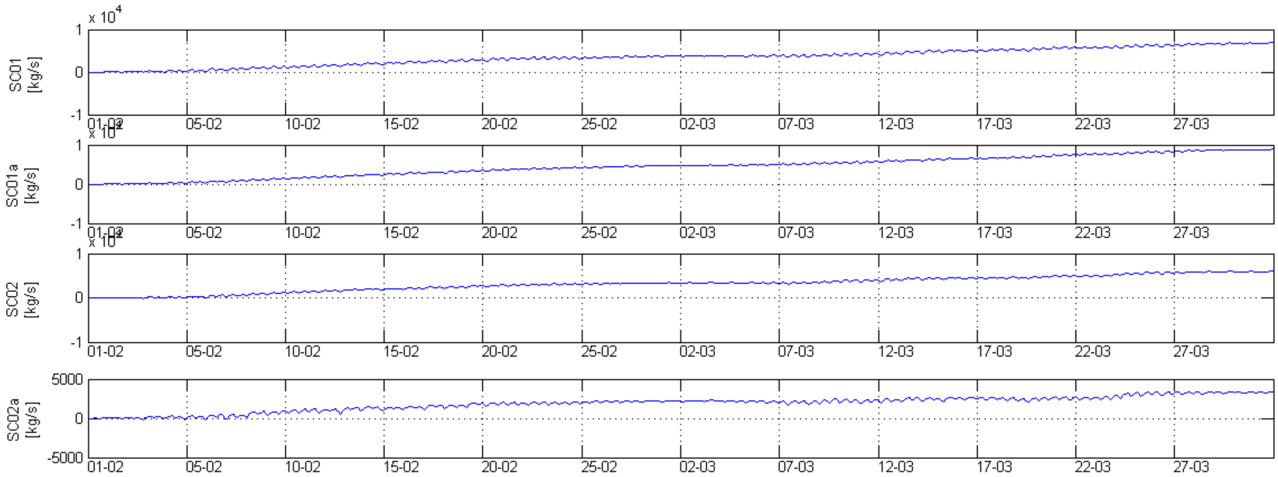

Figure 7-15 Cumulative time series flux - Scenario 3 - Sec 01 to Sec 02a

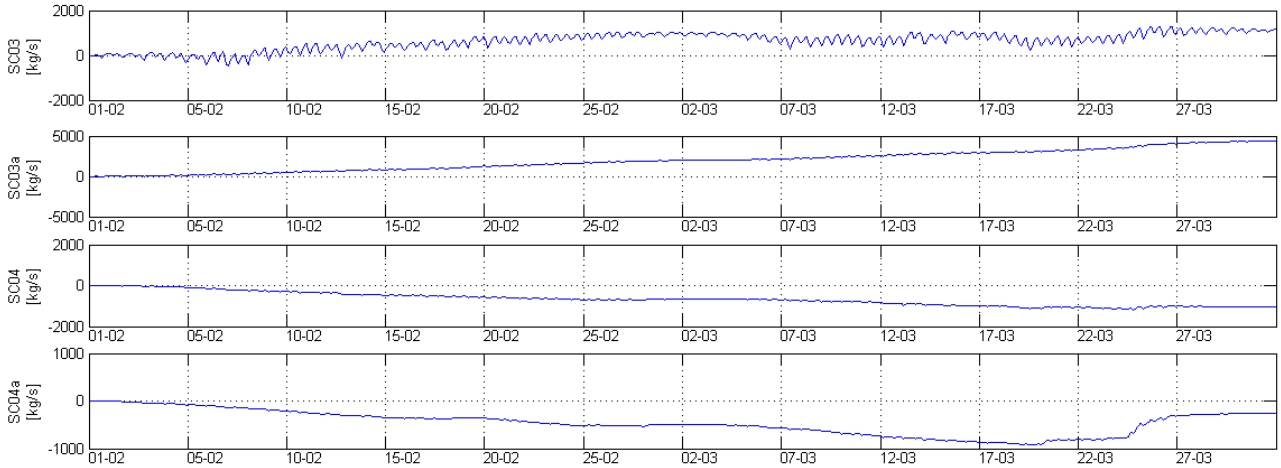

Figure 7-16 Cumulative time series flux - Scenario 3 - Sec 03 to Sec 04a

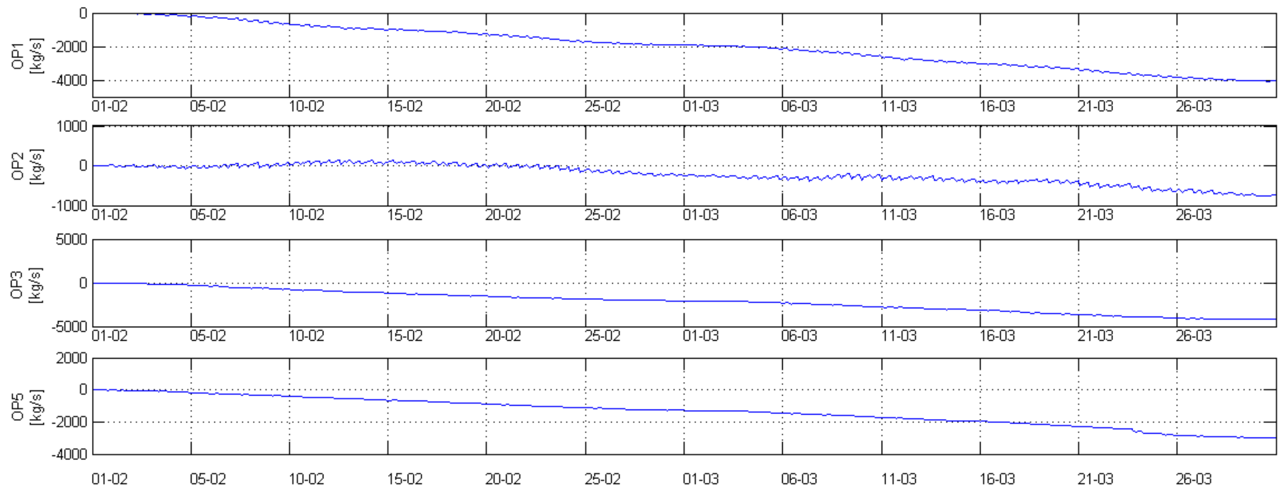

Figure 7-17 Cumulative time series flux - Scenario 3 - Openings

Scenario 4

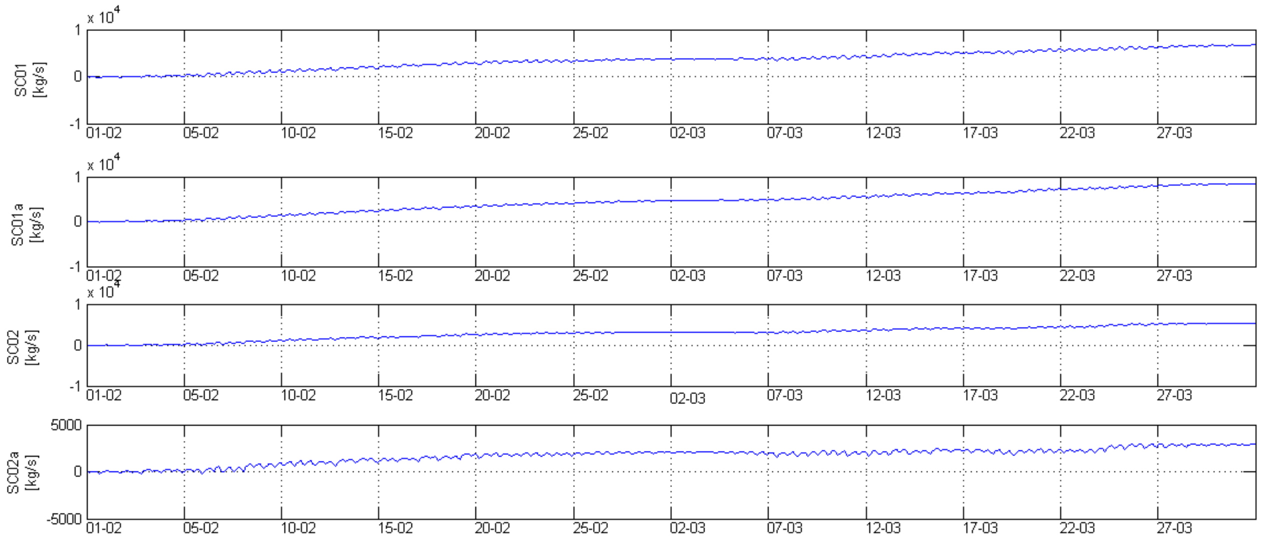

Figure 7-18 Cumulative time series flux - Scenario 4 - Sec 01 to Sec 02a

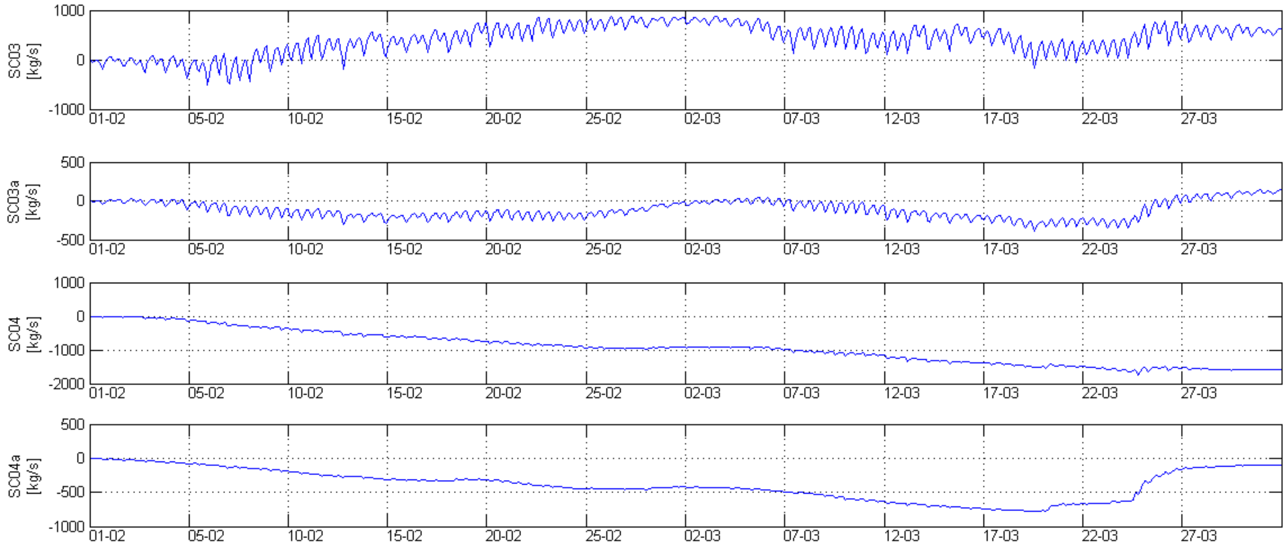

Figure 7-19 Cumulative time series flux - Scenario 4 - Sec 03 to Sec 04a

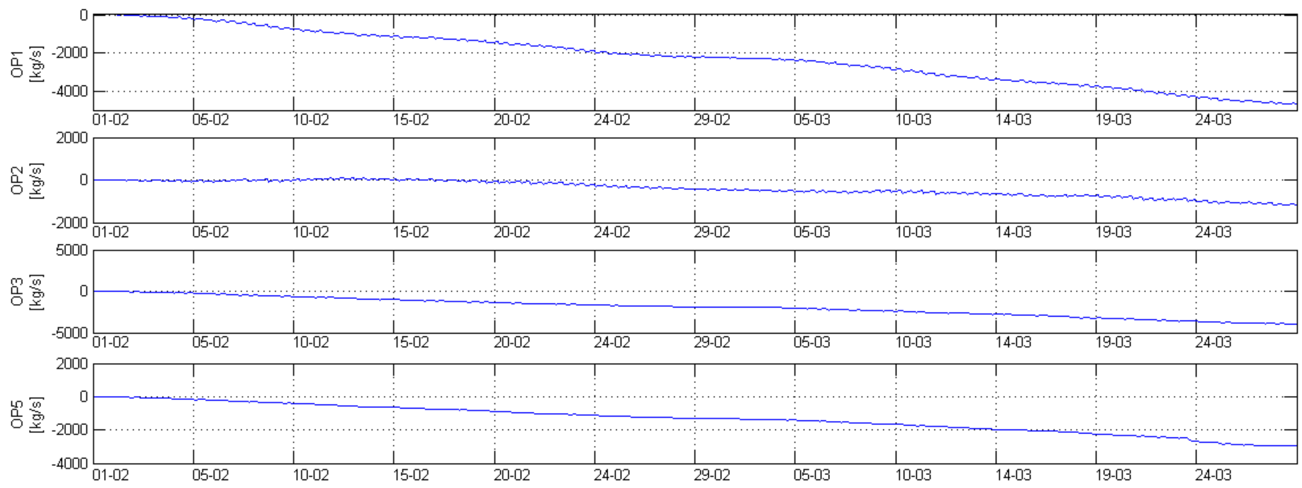

Figure 7-20 Cumulative time series flux - Scenario 4 - Openings

Scenario 5

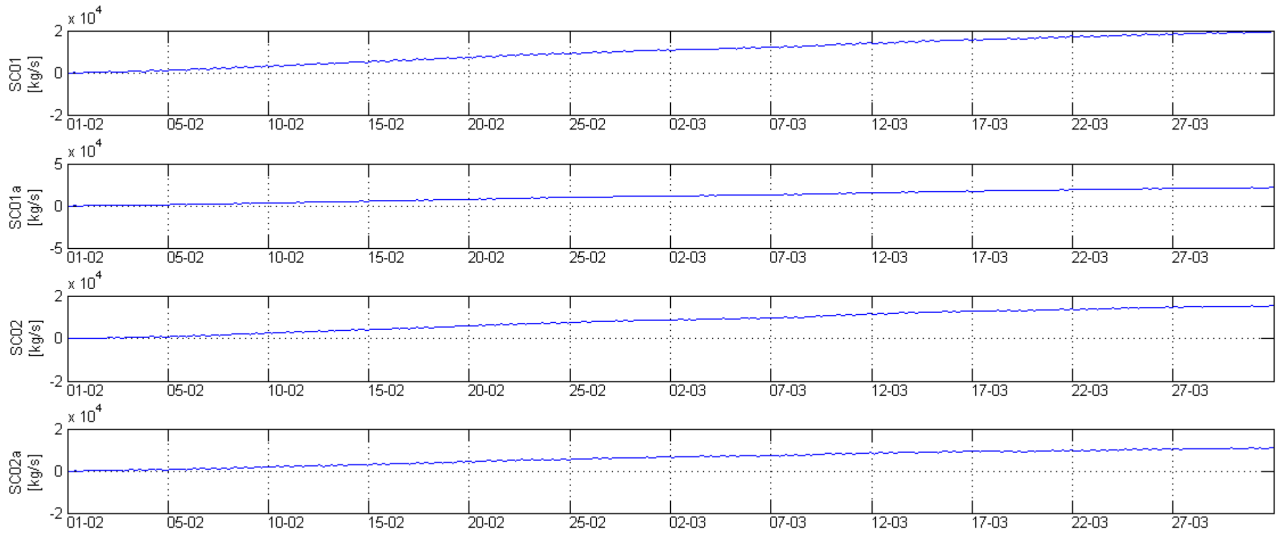

Figure 7-21 Cumulative time series flux - Scenario 5 - Sec 01 to Sec 02a

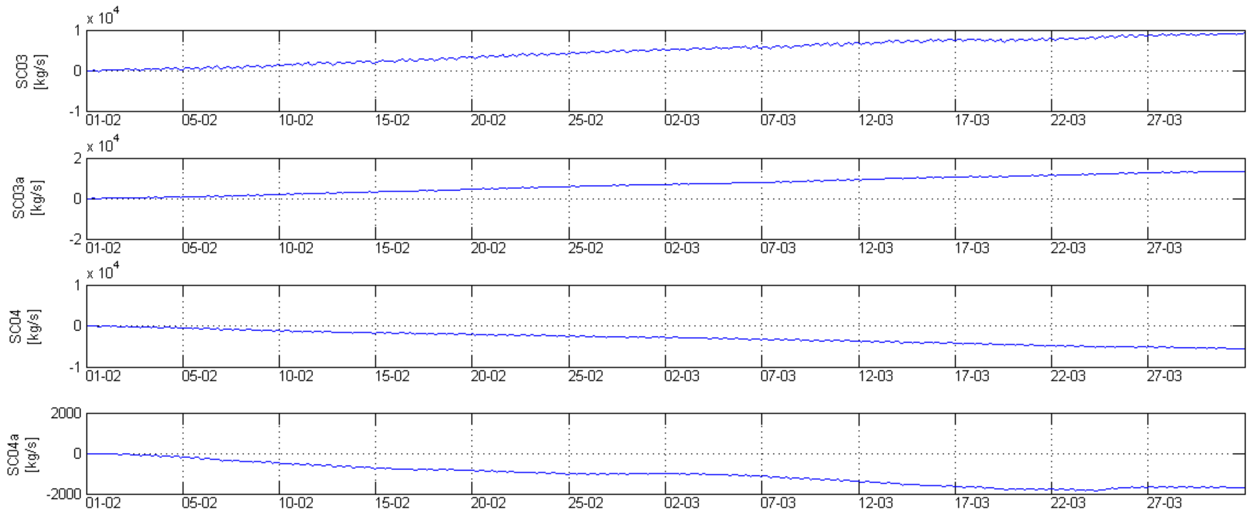

Figure 7-22 Cumulative time series flux - Scenario 5 - Sec 03 to Sec 04a

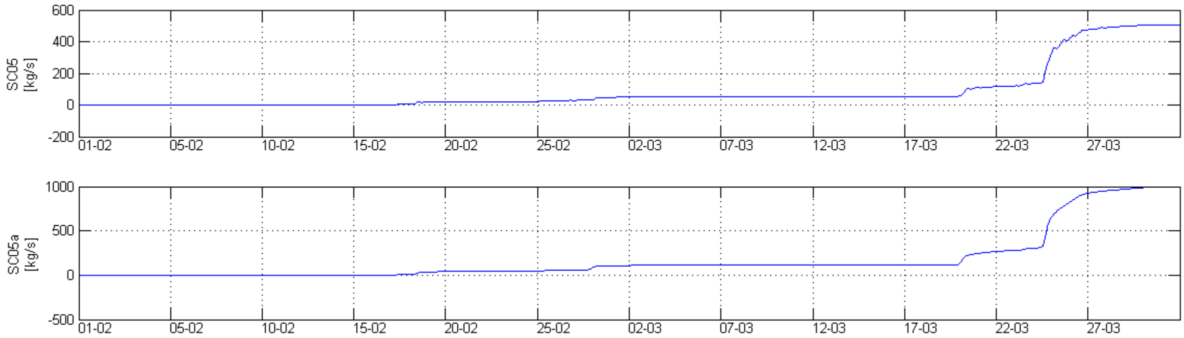

Figure 7-23 Cumulative time series flux - Scenario 5 - Sec 05 to Sec 05a

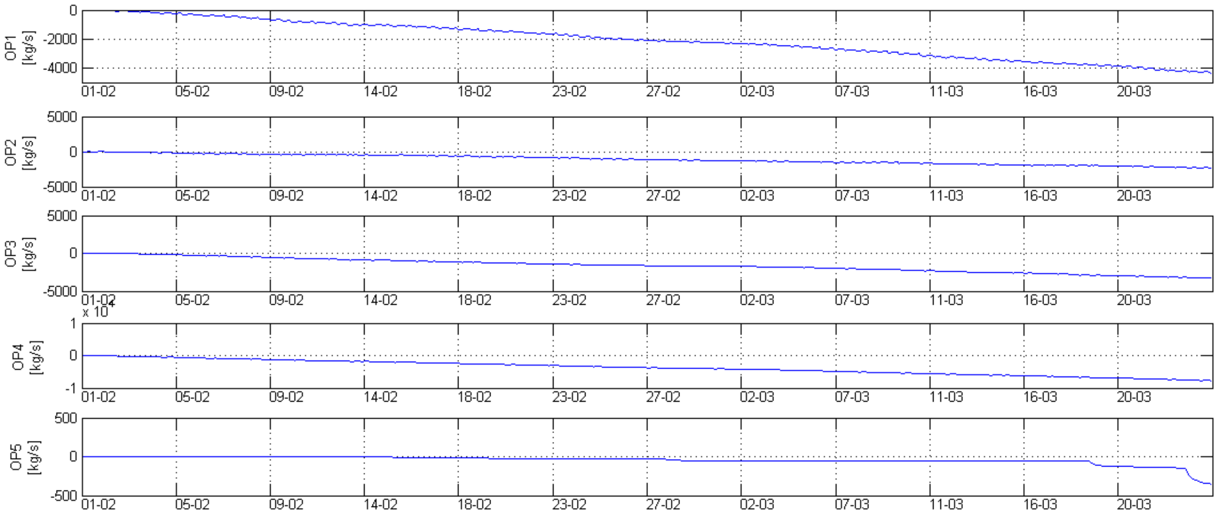

Figure 7-24 Cumulative time series flux - Scenario 5 - Openings